



CENTER FOR INFRASTRUCTURE ENGINEERING STUDIES

In-Plane and Out-of-Plane Behavior of Masonry Walls Strengthened with FRP Systems

by

J. Gustavo Tumialan

Antonio Nanni

Department of Civil Engineering

University of Missouri - Rolla

May 2001

**CIES
01-24**

Disclaimer

The contents of this report reflect the views of the author(s), who are responsible for the facts and the accuracy of information presented herein. This document is disseminated under the sponsorship of the Center for Infrastructure Engineering Studies (CIES), University of Missouri -Rolla, in the interest of information exchange. CIES assumes no liability for the contents or use thereof.

The mission of CIES is to provide leadership in research and education for solving society's problems affecting the nation's infrastructure systems. CIES is the primary conduit for communication among those on the UMR campus interested in infrastructure studies and provides coordination for collaborative efforts. CIES activities include interdisciplinary research and development with projects tailored to address needs of federal agencies, state agencies, and private industry as well as technology transfer and continuing/distance education to the engineering community and industry.

Center for Infrastructure Engineering Studies (CIES)
University of Missouri-Rolla
223 Engineering Research Laboratory
1870 Miner Circle
Rolla, MO 65409-070
Tel: (573) 341-6223; fax -6215
E-mail: cies@umr.edu
www.cies.umr.edu

**In-Plane and Out-of-Plane Behavior of Masonry Walls
Strengthened with FRP Systems**

by

J. Gustavo Tumialan

Antonio Nanni

Department of Civil Engineering

University of Missouri - Rolla

Report No. CIES 01-24

Center for Infrastructure Engineering Studies

University of Missouri - Rolla

ABSTRACT

The worldwide engineering community has identified failures of URM walls as one of the major causes of material damage and loss of human life due to seismic events. Therefore, the development of effective and affordable retrofitting techniques for masonry members is an urgent need. Fiber Reinforced Polymer (FRP) composites provide solutions for the strengthening of URM walls subjected to in-plane and out-of-plane overstresses caused by high wind pressures or earthquake loads. Three series of walls strengthened with FRP composite materials were tested for this research study. Part of the experimental phase was conducted on masonry walls belonging to a decommissioned building. The first two series studied the behavior of masonry walls under in-plane loads; whereas, the third series of walls investigated the out-of-plane behavior. FRP composites in the form of laminates and rods were used as strengthening materials. The results showed that both shear and flexural capacities of masonry walls can be notably increased by strengthening with FRP composites. The tests performed in the field made possible to identify modes of failure not commonly observed in a laboratory environment. A strengthening method denominated “FRP structural repointing” demonstrated that besides increasing the wall capacity it can preserve its aesthetics. Analytical models to predict the behavior of strengthened walls, as well as provisional guidelines to design the FRP strengthening for shear and flexure are also presented. A financial justification for strengthening of masonry elements with FRP materials is also discussed. Finally, conclusions are provided and future research needs on the area of masonry strengthening with FRP systems are outlined.

TABLE OF CONTENTS

	Page
ABSTRACT.....	ii
LIST OF ILLUSTRATIONS.....	vi
LIST OF TABLES.....	xiii
SECTION	
1. INTRODUCTION.....	1
1.1. BACKGROUND.....	1
1.2. SCOPE AND OBJECTIVES.....	4
1.3. DISSERTATION LAYOUT.....	4
2. LITERATURE REVIEW.....	6
2.1. MASONRY THROUGHOUT THE UNITED STATES.....	6
2.1.1. General Overview.....	6
2.1.2. Masonry Units in Backup Walls.....	8
2.2. RETROFITTING OF MASONRY WALLS.....	10
2.2.1. Conventional Strengthening Methods.....	10
2.2.1.1. External Reinforcing Overlay.....	10
2.2.1.2. Internal Steel Reinforcing.....	11
2.2.1.3. External Steel Plate Reinforcing.....	14
2.2.2. Strengthening with FRP Composites.....	15
2.2.2.1. Strengthening with FRP Laminates.....	15
2.2.2.2. Strengthening with FRP Rods.....	20
2.2.3. Final Remarks.....	21
3. FRP COMPOSITE SYSTEMS.....	23
3.1. MECHANICAL PROPERTIES.....	23
3.2. INSTALLATION TECHNIQUES.....	24
3.2.1. Laminate Manual Lay-up.....	26
3.2.2. Near-Surface Mounted (NSM) Rods.....	29

4. WALLS SUBJECTED TO IN-PLANE LOADING.....	32
4.1. PROBLEM STATEMENT.....	32
4.2. SERIES IL.....	35
4.2.1. Test Specimens.....	35
4.2.2. Test Setup.....	36
4.2.3. Test Results.....	37
4.2.4. Mechanism of Failure.....	40
4.2.5. Analytical Study.....	40
4.3. SERIES IF.....	43
4.3.1. Test Specimens.....	43
4.3.2. Test Setup.....	45
4.3.3. Test Results.....	47
4.3.4. Analytical Study.....	49
5. WALLS SUBJECTED TO OUT-OF-PLANE LOADING.....	51
5.1. PROBLEM STATEMENT.....	51
5.2. SERIES OF.....	51
5.2.1. Test Specimens.....	51
5.2.2. Test Setup.....	54
5.2.3. Test Results.....	57
5.2.4. Mechanism of Failure.....	70
5.2.5. Analytical Study.....	72
5.2.5.1. Analytical Derivations for URM Wall.....	72
5.2.5.2. Analytical Derivations for Strengthened Wall.....	75
5.2.5.3. Validation of the Analytical Model.....	77
6. PROVISIONAL DESIGN APPROACHES.....	82
6.1. SHEAR STRENGTHENING WITH FRP RODS.....	82
6.1.1. Protocol.....	82
6.1.2. Design Example.....	85
6.2. FLEXURAL STRENGTHENING WITH FRP LAMINATES.....	87
6.2.1. Protocol.....	93
6.2.2. Design Example.....	95

7. FINANCIAL JUSTIFICATION.....	98
7.1. BACKGROUND.....	98
7.2. RETROFITTING ALTERNATIVES.....	98
7.2.1. Conventional Strengthening Methods.....	98
7.2.2. Strengthening with FRP Composite Materials.....	99
7.3. FINANCIAL ANALYSIS.....	100
7.3.1. The “no action” Alternative.....	100
7.3.2. Demolition and Reconstruction.....	101
7.3.3. Structural Retrofitting.....	101
7.3.4. Comparison of Alternatives.....	101
7.3.3.1. Direct Costs.....	103
7.3.3.2. Indirect Costs.....	105
7.4. MATERIAL AND CONSTRUCTION COST OF FRP RETROFITTING.....	107
7.4.1. Strengthening Scheme A.....	107
7.4.2. Strengthening Scheme B.....	108
7.5. SUMMARY.....	109
8. CONCLUSIONS AND FUTURE WORK.....	110
8.1. WALLS UNDER IN-PLANE LOADING.....	110
8.2. WALLS UNDER OUT-OF-PLANE LOADING.....	111
8.3. FUTURE WORK.....	112
APPENDICES	
A. SERIES IL.....	114
B. SERIES IF.....	130
C. SERIES OF.....	142
BIBLIOGRAPHY.....	183

LIST OF ILLUSTRATIONS

Figure	Page
1.1. Failure of URM Walls (Turkey, 1999).....	1
1.2. Collapse of URM Walls – Turkey (1999).....	2
2.1. Monadnock Building, Chicago.....	6
2.2. Production of Clay Tile in the 20 th Century.....	9
2.3. Test Results – External Reinforcing Overlay.....	11
2.4. Location of Horizontal Reinforcement – Internal Steel Reinforcing.....	12
2.5. Test Results – Internal Steel Reinforcing.....	12
2.6. Internal Reinforcement.....	13
2.7. Steel Plate Reinforcing.....	14
2.8. Test Results – External Steel Reinforcing.....	15
2.9. Strengthened Wall – Schwegler.....	16
2.10. Test Results – Schwegler.....	16
2.11. Test Results – Laursen.....	17
2.12. Test Results – Ehsani.....	18
2.13. Debonding of FRP Laminate.....	19
2.14. Test Results – Velasquez.....	20
2.15. Test Results – Ahmid.....	21
3.1. City Hospital Complex – St. Louis, Missouri.....	25
3.2. FRP Systems.....	26
3.3. Aggregates Exposure.....	27
3.4. Installation of FRP Laminates.....	28
3.5. Surface Preparation in Bare Walls.....	29
3.6. Installation of NSM Rods.....	29
3.7. FRP Structural Repointing.....	30
3.8. Strengthening with FRP Structural Repointing.....	31
4.1. Diagonal Compression Strut.....	33
4.2. Diagonal Tension Failure (Turkey, 1999).....	33
4.3. Crushing of Infill Corners (Turkey, 1999).....	34

4.4. Joint-Slip Failure.....	34
4.5. Potential Failures in Walls with No Axial Load.....	35
4.6. Test Setup for Series IL.....	37
4.7. Envelopes of Load vs. Crack Opening.....	38
4.8. Specimens after Failure – Series IL.....	39
4.9. Strengthened Wall after Failure.....	39
4.10. Mechanism of Failure – Series IL.....	40
4.11. Controlling Areas to Estimate V_F	41
4.12. Cross Section – Series IF.....	44
4.13. Steel Distribution – Series IF.....	45
4.14. Test Setup – Series IF.....	46
4.15. In-Plane Test Setup.....	47
4.16. Flexural Crack at the Bottom of Walls.....	48
4.17. Lateral Load vs. Top Displacement – Series IF.....	49
5.1. Vertical Cross Section of Typical Wall.....	52
5.2. Plates on the External Face of the Wall.....	55
5.3. Test Setup – Series OF.....	55
5.4. View of Test Setup for Series OF.....	56
5.5. Hoist and Metallic Frame.....	56
5.6. Test Instrumentation – Series OF.....	57
5.7. Horizontal Crack in Wall OF1.....	58
5.8. Load vs. Mid-Height Net Deflection Curve – Wall OF1.....	58
5.9. Load vs. Mid-Height Net Deflection Curve – Wall OF2.....	59
5.10. Load vs. Mid-Height Net Deflection Curve – Wall OF3.....	60
5.11. Fracture of Tile Unit.....	60
5.12. Load vs. Mid-Height Net Deflection Curve – Wall OF4.....	61
5.13. Load vs. Mid-Height Net Deflection Curve – Wall OF5.....	61
5.14. Cracking in Wall OF5.....	62
5.15. Load vs. Mid-Height Net Deflection Curve – Wall OF6.....	62
5.16. Fracture of Units at the Bottom of Wall OF6.....	63
5.17. Load vs. Mid-Height Net Deflection Curve – Wall OF7.....	63

5.18. Plaster Delamination.....	64
5.19. Load vs. Mid-Height Net Deflection Curve – Wall OF8.....	64
5.20. Horizontal Crack in Wall OF9.....	65
5.21. Load vs. Mid-Height Net Deflection Curve – Wall OF9.....	65
5.22. Load vs. Mid-Height Net Deflection Curve – Wall OF10.....	66
5.23. Behavior Comparison of Walls OF1, OF2, OF3 and OF4.....	67
5.24. Strain Comparison for Walls OF3 and OF4.....	67
5.25. Behavior Comparison of Walls OF3, OF5 and OF8.....	68
5.26. Behavior Comparison of Walls OF9 and OF10.....	69
5.27. Behavior Comparison of Walls OF1, OF3, OF6 and OF7.....	69
5.28. Rotations in Wall OF7.....	70
5.29. Out-of-Plane Mechanism of Failure.....	71
5.30. Behavior of Infill URM Wall.....	72
5.31. Free-Body Diagram of Upper Part of URM Wall.....	73
5.32. Computation of Δ_0	74
5.33. Free-body Diagram of Upper Part of Strengthened Wall.....	75
5.34. Relation between Δ_1 and Δ_2	76
5.35. Experimental and Predicted Values – URM Wall.....	79
5.36. Wall Strip for Analysis.....	80
5.37. Experimental and Predicted Values – Strengthened Wall.....	81
6.1. Equivalent Bracing Action of Infill Panel.....	83
6.2. Influence of Amount of FRP Reinforcement.....	88
6.3. Strain and Stress Distribution.....	89
6.4. Strain and Stress Distribution in Cracked Transformed Section.....	90
6.5. Correlation between Experimental and Analytical Values.....	91
6.6. Anchorage Systems.....	92
6.7. Anchorage with NSM Rods.....	93
6.8. Strengthening Layout.....	97
7.1. Strengthening Scheme A.....	107
7.2. Strengthening Scheme B.....	108
A.1-1. Control Specimens – Walls IL1-a and IL-b.....	115

A.1-2. Strengthening Scheme for Wall IL2.....	115
A.1-3. Strengthening Scheme for Wall IL3.....	116
A.1-4. Strengthening Scheme for Wall IL4.....	116
A.2-1. In-Plane Load vs. Deformation – Wall IL1-a (Front).....	117
A.2-2. In-Plane Load vs. Deformation – Wall IL1-a (Back).....	117
A.2-3. In-Plane Load vs. Deformation – Wall IL1-b (Front).....	118
A.2-4. In-Plane Load vs. Deformation – Wall IL1-b (Back).....	118
A.2-5. In-Plane Load vs. Deformation – Wall IL2 (Front).....	119
A.2-6. In-Plane Load vs. Deformation – Wall IL2 (Back).....	119
A.2-7. In-Plane Load vs. Deformation – Wall IL3 (Front).....	120
A.2-8. In-Plane Load vs. Deformation – Wall IL3 (Back).....	120
A.2-9. In-Plane Load vs. Deformation – Wall IL4 (Front).....	121
A.2-10. In-Plane Load vs. Deformation – Wall IL4 (Back).....	121
A.3-1. Cracking Pattern – Wall IL1-a.....	122
A.3-2. Cracking Pattern – Wall IL1-b.....	122
A.3-3. Cracking Pattern – Wall IL2 (Front).....	123
A.3-4. Cracking Pattern – Wall IL2 (Back).....	123
A.3-5. Cracking Pattern – Wall IL3 (Front).....	124
A.3-6. Cracking Pattern – Wall IL3 (Back).....	124
A.3-7. Cracking Pattern – Wall IL4 (Front).....	125
A.3-8. Cracking Pattern – Wall IL4 (Back).....	125
A.4-1. Overall View of Test Specimens.....	126
A.4-2. View of Test Setup.....	126
A.4-3. View of Hydraulic Jacks.....	127
A.4-4. Wall IL1-b after collapsing.....	127
A.4-5. Crack on front side – Wall IL2.....	128
A.4-6. Crack on back side – Wall IL2.....	128
A.4-7. Crack on front side – Wall IL3.....	129
A.4-8. Crack on back side – Wall IL3.....	129
B.1-1. Strengthening Scheme for Walls IF2 and IF3.....	131
B.1-2. #3 GFRP rods in one toe region of Wall IF3.....	132

B.2-1. Lateral Load vs. Top Displacement Wall IF2.....	133
B.2-2. Lateral Load vs. Top Displacement Wall IF1.....	133
B.2-3. Lateral Load vs. Top Displacement Wall IF1.....	134
B.4-1. Installation of GFRP Laminates.....	139
B.4-2. Installation of GFRP Rods.....	139
B.4-3. Preparation of Test Setup.....	140
B.4-4. Reaction Beam.....	140
B.4-5. View of the unstrengthened sides.....	141
B.4-6. Rocking of Wall.....	141
C.1-1. Strengthening Scheme for Walls OF3, OF4, OF6 and OF7.....	143
C.1-2. Strengthening Scheme for Wall OF5.....	143
C.1-3. Strengthening Scheme for Wall OF8.....	144
C.1-4. Strengthening Scheme for Walls OF9 and OF10.....	145
C.2-1. Two-way Action – Wall OF1.....	146
C.2-2. Out-of-Plane Load vs. Rotation – Wall OF1.....	146
C.2-3. Height vs. Deflection – Wall OF1.....	147
C.2-4. Two-way Action – Wall OF2.....	148
C.2-5. Out-of-Plane Load vs. Rotation – Wall OF2.....	148
C.2-6. Height vs. Deflection – Wall OF2.....	149
C.2-7. Two-way Action – Wall OF3.....	150
C.2-8. Out-of-Plane Load vs. Rotation – Wall OF3.....	150
C.2-9. Height vs. Deflection – Wall OF3.....	151
C.2-10. Out-of-Plane Load vs. Strains – Wall OF3.....	152
C.2-11. Two-way Action – Wall OF4.....	152
C.2-12. Out-of-Plane Load vs. Rotation – Wall OF4.....	153
C.2-13. Height vs. Deflection – Wall OF4.....	154
C.2-14. Out-of-Plane Load vs. Strains – Wall OF4.....	155
C.2-15. Two-way Action – Wall OF5.....	155
C.2-16. Out-of-Plane Load vs. Rotation – Wall OF5.....	156
C.2-17. Height vs. Deflection – Wall OF5.....	157
C.2-18. Out-of-Plane Load vs. Strains – Wall OF5.....	158

C.2-19. Two-way Action – Wall OF6.....	158
C.2-20. Out-of-Plane Load vs. Rotation – Wall OF6.....	159
C.2-21. Height vs. Deflection – Wall OF6.....	160
C.2-22. Out-of-Plane Load vs. Strains – Wall OF6.....	161
C.2-23. Two-way Action – Wall OF7.....	161
C.2-24. Out-of-Plane Load vs. Rotation – Wall OF7.....	162
C.2-25. Height vs. Deflection – Wall OF7.....	163
C.2-26. Out-of-Plane Load vs. Strains – Wall OF7.....	164
C.2-27. Two-way Action – Wall OF8.....	165
C.2-28. Out-of-Plane Load vs. Rotation – Wall OF8.....	165
C.2-29. Height vs. Deflection – Wall OF8.....	166
C.2-30. Out-of-Plane Load vs. Strains – Wall OF8.....	167
C.2-31. Two-way Action – Wall OF9.....	167
C.2-32. Out-of-Plane Load vs. Rotation – Wall OF9.....	168
C.2-33. Height vs. Deflection – Wall OF9.....	169
C.2-34. Out-of-Plane Load vs. Strains – Wall OF9.....	170
C.2-35. Two-way Action – Wall OF10.....	170
C.2-36. Out-of-Plane Load vs. Rotation – Wall OF10.....	171
C.2-37. Height vs. Deflection – Wall OF10.....	172
C.2-38. Out-of-Plane Load vs. Strains – Wall OF10.....	173
C.4-1. Malcolm Bliss Hospital.....	176
C.4-2. Removal of Plaster Layer.....	176
C.4-3. Leveling of Masonry Surface.....	177
C.4-4. Cutting of Fiber Sheets.....	177
C.4-5. Use of Impregnating Resin as a Primer.....	178
C.4-6. Installation of Fiber Sheets.....	178
C.4-7. NSM Rod used as Flexural Reinforcement.....	179
C.4-8. Drilling of Holes for testing of Walls.....	179
C.4-9. Overall View of Test Setup.....	180
C.4-10. Plates used to apply the loads.....	180
C.4-11. View of Hydraulic Jacks and Reaction Beam.....	181

C.4-12. Beam on the Reaction Side.....	181
C.4-13. Wall being tested.....	182
C.4-14. Delamination of Plaster.....	182

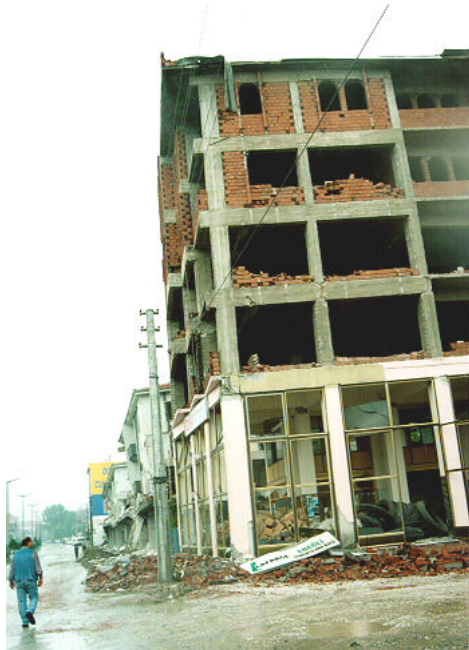
LIST OF TABLES

Table	Page
3.1. Resin Properties in Tension.....	23
3.2. Engineering Properties for FRP Sheets and GFRP Rods.....	24
4.1. Test Matrix for Series IL.....	36
4.2. Experimental and Analytical Values –Series IL.....	43
4.3. Experimental and Analytical Values –Series IF.....	50
5.1. Test Matrix for Series OF.....	54
5.2. Compressive Strengths of Clay Tile Prisms.....	78
6.1. C_E Factor for Various Fibers and Exposure Conditions.....	85
7.1. Comparative Costs of Alternatives.....	102
7.2. Cost Comparison.....	109

1. INTRODUCTION

1.1. BACKGROUND

Structural weakness or overloading, dynamic vibrations, settlement, and in-plane and out-of-plane deformations can cause failure of masonry structures. Unreinforced masonry (URM) buildings represent a large portion of the buildings around the world. As a matter of fact, many of the existing buildings in the United States consists of URM buildings, especially in the Eastern part of the country. URM buildings have features that can threaten lives, which include unbraced parapets, inadequate connections to the roof, and the brittle nature of the URM elements themselves. Organizations such as The Masonry Society (TMS) and the Federal Emergency Management Agency (FEMA), have identified that failures of URM walls result in most of the material damage and loss of human life. This was evident from the post-earthquake observations in Northridge, California (1994) and Turkey (1999). Figure 1.1 illustrates the collapse of URM walls due to out-of-plane and in-plane loads after the earthquake in Turkey in 1999. Note the debris at the bottom, which during an earthquake is a potential threat to bystanders.



(a) Out-of-Plane Failure



(b) In-Plane Failure

Figure 1.1. Failure of URM Walls (Turkey, 1999)

Under the URM Building Law of California, passed in 1986, approximately 25,500 URM buildings were inventoried throughout the state. Even though, this number is a relatively small percentage of the building inventory in California, it includes many cultural icons and historical resources. The building evaluation showed that 96% of the buildings needed to be retrofitted, which would result in approximately \$4 billion in retrofit expenditures. To date, it has been estimated that only half of the owners have taken remedial actions, which may attributed to high retrofitting costs. Thereby, the development of effective and affordable retrofitting techniques for masonry elements is an urgent need.

URM walls are commonly used as interior partitions or exterior walls bound by steel or concrete frames forming the building envelope. Depending on design considerations, these walls can resist lateral and/or gravity loads. Due to weak anchorage to adjacent concrete members, or to absence of anchorage, URM walls may crack, tear and collapse under the combined effects of out-of-plane and in-plane loads generated by seismic forces, as illustrated in Figure 1.2.



Figure 1.2. Collapse of URM Walls (Turkey, 1999)

Conventional retrofitting techniques can be classified according to the problem to be addressed: damage repair or structure upgrading. For damage repair in the form of cracks, the following methods can be used:

- Filling of cracks and voids by injecting epoxy or grout.

- Stitching of large cracks and weak areas with metallic or brick elements.

For strengthening or upgrading, the following procedures are available:

- Grout injection of hollow masonry units with non-shrink portland cement grout or epoxy grout to strengthen or stiffen the wall.
- Construction of an additional wythe to increase the axial and flexural strength.
- Post-tensioning of an existing construction.
- External reinforcement with steel plates and angles.
- Surface coating with reinforced cement paste or shotcrete, such as a welded mesh.

Fiber Reinforced Polymer (FRP) composites provide solutions for the strengthening of URM walls subjected to in-plane and out-of-plane over stresses caused by high wind pressures or earthquake loads. Even though most of the research on FRP composites has focused on reinforced concrete (RC), available literature on masonry shows that each potential failure cause of URM walls can be prevented and/or lessened by using FRP composites. Some of the previous researches on masonry strengthening are described in Section 2. Investigations on masonry walls strengthened with FRP composites have included variables such as types of loading, strengthening schemes, as well as anchorage systems.

The most important characteristics of a strengthening work are the predominance of labor and shutdown costs as opposed to material costs, time, site constraints and long-term durability. In addition to their outstanding mechanical properties, the advantages of FRP composites versus conventional materials for strengthening of structural and non-structural elements include lower installation costs, improved corrosion resistance, on-site flexibility of use, and minimum changes in the member size after repair. In addition, disturbance to the occupants of the facility being retrofitted is minimized and there is minimal loss of usable space during the strengthening work. Furthermore, from the structural point of view, the dynamic properties of the structure remain unchanged because there is little addition of weight and stiffness. Any alteration to the aforementioned properties would result in an increase in seismic forces.

1.2. SCOPE AND OBJECTIVES

Previous works on URM and reinforced masonry walls strengthened with FRP laminates have shown remarkable increases in capacity and ductility. During a seismic event, walls located at the lower stories of the building may be overstressed because the shear forces at that level are larger than at any other story. On the other hand, walls located at the upper stories are susceptible to failure under out-of-plane loading because the maximum seismic accelerations occur at those levels. Three series of walls strengthened with FRP composite materials were tested as part of this research. The first two series of walls dealt with the behavior of members subjected to in-plane loading. The walls were tested in a laboratory environment and in-situ. The latter specimens corresponded to walls of a decommissioned building. The second series of walls was tested in the field under out-of-plane loading. It is known that in the laboratory restraint conditions, in most cases, are not representative of those found in the field. In this context, the field tests offered the opportunity for performing more realistic experimentation. Parameters such as the type of composite system and FRP installation methods were evaluated.

The main objectives of this research are to evaluate the effectiveness of different types of commercially available and experimental forms of fiber reinforced polymer (FRP) composite systems to increase flexural and shear capacities of masonry elements, and to develop provisional design guidelines. Static load tests to failure were carried out to evaluate the behavior of the walls. The goal of the static load test evaluation is to assess the performance of structural and non-structural members before and after strengthening with composite systems. The load testing procedure involved applying concentrated loads to the walls, which response was monitored and used for their evaluation.

1.3. DISSERTATION LAYOUT

This dissertation is organized according to the stages followed for the development of the investigation. Thus, Section One introduces the significance of the strengthening of masonry elements, which led to setting the objectives of the research. There is a great diversity of masonry systems around the world. Masonry differs from

region to region. Furthermore, it can be said that in addition to architectural and structural requirements, the construction practice of a region or country plays a role in selecting a determined typology. In that context Section Two provides a brief description of the masonry walls typologies used throughout the United States. Also, strengthening methods using “conventional” and FRP materials are presented.

In Section Three, the properties of the FRP materials as well as the constituent materials are presented. The techniques used for the installation of FRP laminates and rods for the experimental programs conducted in this investigation are described. The behavior of masonry walls subjected to in-plane and out-of-plane loads is discussed in Section Four and Section Five, respectively. The walls were strengthened with different composite systems such as Carbon FRP (CFRP), Aramid FRP (AFRP) and Glass FRP (GFRP) laminates. In addition, considering that masonry buildings may have visual and architectural significance and that the retrofit work should be executed with the least possible irrevocable alteration to the architectural finishes, the behavior of masonry walls strengthened with GFRP rods was studied. The specimens, test setups, and test procedures are thoroughly described. The test results are interpreted and mechanisms of failure are identified. Assumptions and expressions used for the development of analytical models are presented. The analytical values were confronted with the experimental values.

With the premise that further research needs to be conducted, Section 6 presents provisional design guidelines for shear and flexural strengthening of URM walls with FRP composites. Section Seven describes factors to be considered for financial justification of retrofitting of masonry elements with FRP materials.

Finally, Section Eight provides conclusions and recommendations for future work in the area of masonry strengthening with FRP composites.

2. LITERATURE REVIEW

2.1. MASONRY THROUGHOUT THE UNITED STATES

2.1.1. General Overview. Masonry constitutes approximately 70% of the existing building inventory in the United States. Most of these buildings are made of unreinforced masonry, particularly to the east of the Rocky Mountains. During the formation of the United States as a new nation, bearing unreinforced masonry walls were a very common form of construction. These walls had a thickness ranging from 12 to 40 inches, and were multi-wythe walls, where sometimes rubble was used for the interior wythes. The walls were commonly built with hand-made and fired clay units, bonded by sand-lime mortar. A good example of this kind of construction is the Monadnock Building in Chicago (see Figure 2.1). This 16-story building completed in 1891 has 6 foot-thick walls at the base, decreasing 4 inches in thickness per floor, to a minimum thickness of 12 inches at the top. The thick walls occupy a valuable floor space and impose a heavy load on the foundations; that is why that by 1940, the building had settled 20 inches in the soft clay soil.



Figure 2.1. Monadnock Building, Chicago

The transition from traditional to modern methods was a consequence of the severe damage to URM walls due to the earthquake of 1933 in Long Beach, California. This seismic event forced to take preventive actions for future earthquakes. Through the

California's Field Act, the use of masonry was prohibited in all the public buildings throughout the state of California. In the late 1940's and early 1950's, masonry construction was revitalized in California. It was required that new masonry edification comply with the newly developed Uniform Building Code, which was based on the reinforced concrete design practice of the time. Those provisions required that minimum seismic lateral forces be considered in the design of masonry elements, that tensile stresses in masonry be resisted by steel reinforcement, and that at least a minimum percentage of horizontal and vertical reinforcement be used.

In contemporary North American commercial construction, masonry walls include panel, curtain, and bearing walls, which can be unreinforced or reinforced (Klingner, 1994). Panel walls are single-story walls meant to primarily resist out-of-plane loads generated by either earthquakes or wind; and vertical loads primarily due to self-weight. Panel walls are a common façade element in buildings conformed by frames of steel or reinforced concrete. This kind of walls may consist of two wythes separated by at least 2-inch air space, commonly referred to as cavity walls. Panel walls may also consist of single wythe or multiple wythes in contact with each other. In the latter case, they are denominated composite walls. When built within steel or RC frames, these walls are called infill walls, and are commonly found forming the envelope of the building to protect the interior from the external environment; for this reason they are also called "barrier walls". Infill walls can be subjected to in-plane loads caused by their interaction with the surrounding frame. Due to vertical spans of 12 feet or less, panel walls can satisfactorily resist out-of-plane loading and are generally unreinforced.

Curtain walls are multi-story walls that also resist out-of-plane loads due to earthquakes or wind. If a single wythe is used, horizontal steel, in the form of welded reinforcement, is placed in the mortar joints to increase resistance. This kind of construction is commonly referred to as "partially reinforced". Bearing walls are arranged at a fairly uniform spacing to resist out-of-plane loads, in-plane loads (traditionally called "shear walls" when having this function); and vertical loads from self-weight and upper tributary floor areas. Cavity and composite walls can also lie on this category. Depending on the load solicitations, bearing walls can be unreinforced or reinforced.

In the United States, differences of masonry systems can be categorized according to the geographical region. Thus, in contrast to the eastern United States, masonry in the western United States has been primarily developed for earthquake resistance criteria, and secondarily for architectural and fire resistance criteria. Because of the seismic considerations, the majority of the masonry construction in that part of the country consists of reinforced and fully grouted walls built with concrete masonry units (CMU), which are meant to act as shear and bearing elements.

2.1.2. Masonry Units in Backup Walls. Two different masonry units are commonly found in backup or inner walls, clay tiles and concrete units. Structural clay tile has been first manufactured in the United States approximately since 1875. A clay tile is a hollow unit, which is characterized by possessing parallel cores and thin webs and faceshells. In the beginning, structural tile was used in building floors and as a fireproofing material for steel frame construction. Owing to its lightweight, large unit size and ease of handling during construction, the use of clay tiles was extended to load-bearing walls, wall facings, silos, columns, etc. In the early 1900's, structural clay tiles were used in infill walls throughout the United States. Some notable structures where it is possible to observe this kind of construction are the New York Chrysler Building (New York), Los Angeles City Hall Building (California), and the Oakland City Hall Building (California), which is considered a historic structure.

Figure 2.2 illustrates information made available by the U.S. Department of Commerce Census of Manufacturers, on the production of clay tile in the 20th century. As can be observed, the production of clay tiles was peaked in the 1920's. As a consequence of the Great Depression, production then suffered a dramatic decrease. As World War II began, the economy was revitalized and large public works were performed. Some of military facilities built primarily with clay tiles included Fort Benning in Georgia, and the Women's Army Auxiliary Corps Barracks in Iowa. From Figure 2.2, it is observed that the production of clay tiles decreased during the 1960's, when concrete units began to be widely used.

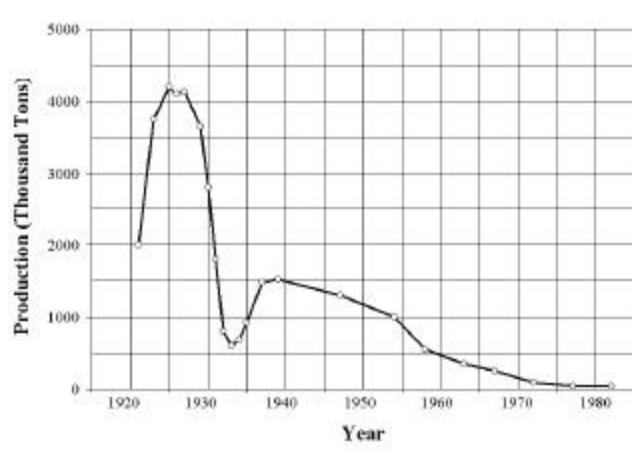


Figure 2.2. Production of Clay Tile during the 20th Century

It is important to point out that the use of concrete units was not new in the United States. Concrete blocks were first manufactured in the United States at about the turn of the 20th century in small one-at-a-time machines that could be operated by hand and purchased from Sears and Roebuck catalogs. Using this kind of machines, the production was limited to 10 blocks per man-hour. Due to manufacturing and aesthetic limitations, and because the architects preferred the integrity of natural stone, the use of concrete units was limited. Concrete blocks were not widely used until the 1920's when the manufacturing processes were improved; however due to the recession many plants had to close or merge. It was not until the 1960's that the market started to change. This change is attributed to the automation of plant equipment, which increased the production capability of concrete blocks. The increase in production capability led to low unit cost and increased available quantity. In addition, the manufacturing process of concrete units allowed a better quality control of the products. For instance, concrete units show more uniformity since they are not fired during their fabrication. Also, the brittle characteristics of clay tiles when being handled and transported, made the demand of concrete units increase. In addition, the Environmental Protection Agency (EPA) made efforts to reduce the environmental effects associated with the manufacture of clay masonry units. This led to the closing of many old plants where the kilns generated emissions above the allowable standard.

2.2. RETROFITTING OF MASONRY WALLS

Existing masonry buildings around the world, many of which are of historical and architectural value, may not have adequate resistance against seismic and wind loads. In the following sections some studies on masonry walls retrofitted with conventional methods and with FRP composites are briefly described.

2.2.1. Conventional Strengthening Methods.

2.2.1.1. External Reinforcing Overlay. Prawel et al. (1985) conducted an investigation on masonry panels retrofitted with ferrocement overlays. Ferrocement is an orthotropic composite material, which consists of a high-strength cement mortar matrix and layers of fine steel wires configured in the form of a mesh. The overall thickness usually varies between 0.5 and 1-in. The tensile strength of the ferrocement layer ranges from 500 to 2000 psi, and it is dependable on mesh type, and the amount and orientation of the reinforcement. These overlays are used to increase in-plane and out-of-plane resistance. This study focused on masonry specimens subjected to in-plane loading. The specimens consisted of 25.5 by 25.5-in. brick panels laid in a stack bond pattern, having a thickness of 8-in. A 0.5-in.-wide layer of ferrocement, with different amounts of reinforcement, was attached to both sides of the masonry to increase the shear strength.

The specimens were subjected to diagonal in-plane loading. Two modes of failure were observed, a ductile one caused by yielding of the steel wire and a brittle failure caused by debonding of the ferrocement overlay from the masonry surface. The experimental results indicated that the strength and ductility were almost doubled in the coated walls compared to the unstrengthened wall. Figure 2.3 illustrates the test results of three specimens. In the testing of panel 2, which had a 0.5-in. mesh wire spacing, it was observed that the layer of ferrocement debonded from masonry after substantial cracking. In contrast, in panel 3, with a mesh wire spacing of 0.125-in., complete yielding and tensile failure of the mesh was observed.

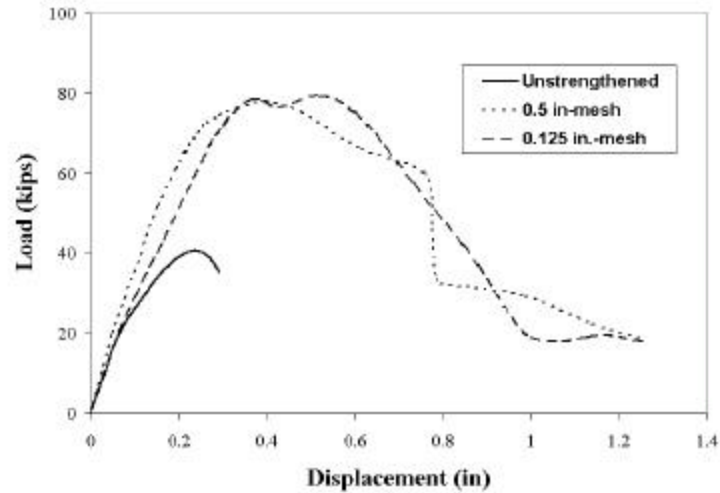


Figure 2.3. Test Results-External Reinforcing Overlay

2.2.1.2. Internal Steel Reinforcing. Manzouri et.al. (1996) evaluated the efficiency of repairing URM walls by grout injection in combination with horizontal and vertical steel reinforcement. URM walls were built in three whites with clay bricks for an overall dimension of 8.5 by 5-ft. The walls were tested under in-plane loading. First, the behavior of the walls in their original condition was investigated. Then, the walls were retrofitted to be tested once again. All the retrofitted walls were injected with grout. The severely damaged areas were repaired by replacement with similar materials. Crack widths larger than 0.06 in were injected with a coarse aggregate; whereas, crack widths ranging between 0.008 to 0.06-in. were injected with a fine grout. Steel ties for use as dry-fix remedial anchor were placed as vertical reinforcement used for the pinning of the wythes in the toe area, and horizontal reinforcement (see Figure 2.4). The ties were made of Type 304 stainless steel with a helical design, similar to a self-tapping screw, which cuts a spiral groove as it is tapped into a pilot hole. The installation procedure included cutting of certain bed joints to a depth of 3-in. followed by placement of the tie in the slot and sealing with mortar.

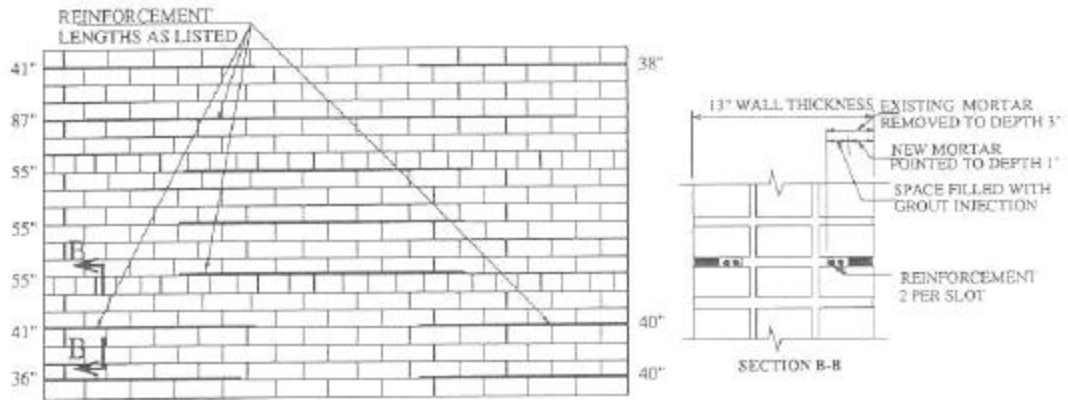


Figure 2.4. Location of Horizontal Reinforcement-Internal Steel Reinforcing

The test results demonstrated that the injection of grout accompanied by repair of localized damaged areas can restore the original strength and stiffness of retrofitted walls. The introduction of horizontal reinforcement increased the strength and ductility of the wall system, since shear failure was prevented. It was also observed that the vertical reinforcement increased the lateral resistance and ductility. Figure 2.5 illustrates the test results for a wall before and after being strengthened.

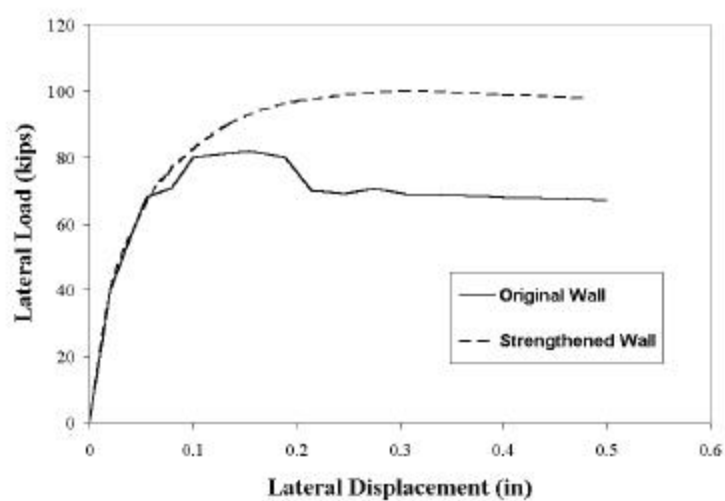


Figure 2.5. Test Results-Internal Steel Reinforcing

In old structures, load bearing masonry elements are prone to vertical cracking due to the combined effect of the gravitational sustained load and cyclic loads. This phenomenon has been observed in masonry towers and pillars throughout Europe, and can eventually lead to the collapse of the structure. Binda et.al (1999) investigated a technique to repair and strengthen masonry elements subjected to the aforementioned mechanism. This technique consisted of grooving the bed joints, placing of mortar along with the steel reinforcement (bars or plates) as shown in Figure 2.6. 10x20x 44-in. panels were built for this research program. Initially, the specimens were pre-cracked by compressive loads representing the 80% of their capacity. After this, the specimens were repaired by placing two bars with a diameter of 0.25 inch every third bed joint. The depth of the grooves was 2.5 inches. The test results of the repaired specimens showed that the strength was not improved. However, significant results in terms of deformation were attained, which was evident from the reduced cracking observed. In the repaired walls, reductions in the strains ranging between 40% to 50% were recorded. It was concluded that the structural degradation process of a masonry element can be detained; especially if the overall conditions are improved by other strengthening techniques such as injections and replacement of damaged sections.

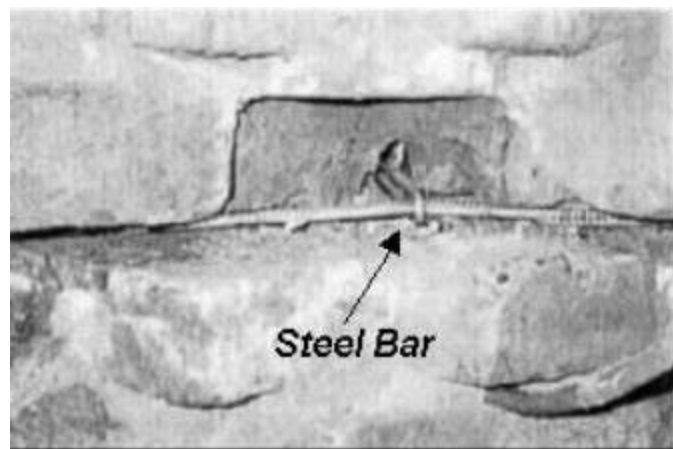


Figure 2.6. Internal Reinforcement

2.2.1.3. External Steel Plate Reinforcing. Taghdi et al. (2000) proposed a strengthening method which consisted of placing diagonal and vertical steel strips on both sides of lightly reinforced masonry walls, as illustrated in Figure 2.7.

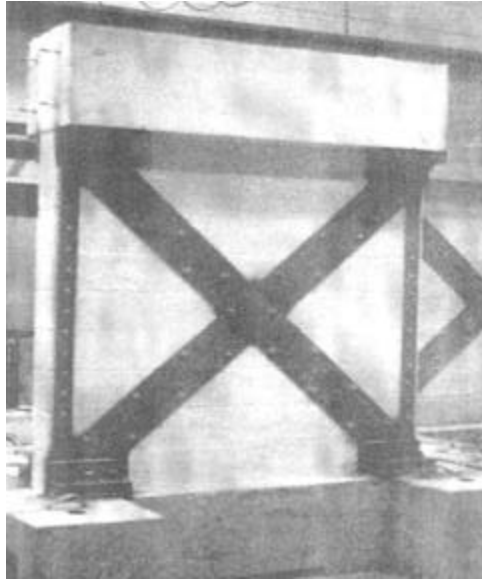


Figure 2.7. Steel Plate Reinforcing

The walls were built with standard concrete masonry units, being their overall dimensions 6 by 6-ft. The walls were internally reinforced with No.8 gauge ladder reinforcement every 2 courses, and Canadian M15 vertical steel placed at the edges and at the center of the wall. The retrofitting strategy consisted of two 9-in wide diagonal steel strips with a thickness of 0.15-in. The diagonal steel strips were welded at the intersection. Structural steel bolts were used to fasten the steel strips to the walls. Also, steel angles and high strength anchors connected the strips to the floor to prevent sliding of the walls. Figure 2.8 illustrates the test results of an unstrengthened wall and a wall strengthened with the described method. Although the primary objective of this experimental program was to study the in-plane behavior of strengthened walls, it was suggested that the proposed technique could also be effective for walls subjected to out-of-plane loading. A shear failure with crushing of the masonry diagonal struts was

observed in the unstrengthened wall. In the strengthened wall, the diagonal steel strips delayed the crushing of masonry until excessive yielding, which led to buckling in the strips, occurred. It was observed that the vertical strips provided a ductile flexural behavior to the walls, and the steel strip system prevented the development of rigid body rotation and allowed cracks to spread.

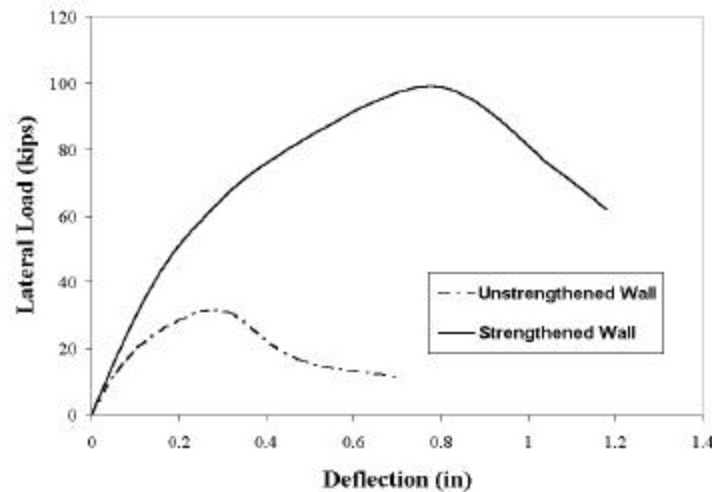


Figure 2.8. Test Results-External Steel Reinforcing

2.2.2. Strengthening with FRP Composites.

2.2.2.1. Strengthening with FRP Laminates. Schwegler (1995) investigated strengthening methods for masonry shear walls. The objectives of this study were to increase the system ductility, generate uniform crack distribution, and increase the load carrying capacity of the system. The dimensions of the walls were 12 by 6.5-ft. CFRP sheets were bonded diagonally to the masonry walls as shown in Figure 2.9, and mechanically anchored to the adjoining slabs.

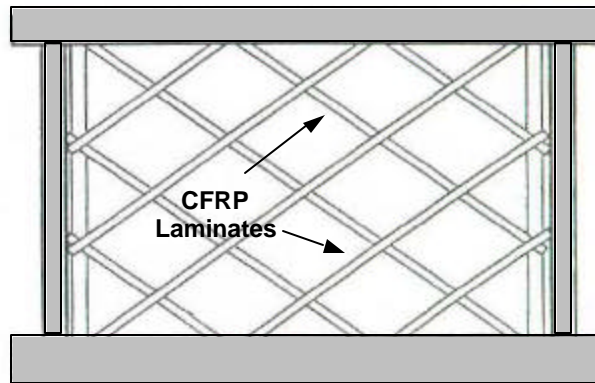


Figure 2.9. Strengthened Wall-Schwegler

As observed in Figure 2.10, the test results showed that the strengthened wall exhibited elastic behavior up to 70% of the maximum shear force. It was also observed that the carrying capacity decreased as a consequence of massive crack formation in the masonry. By comparing walls strengthened in one side and two sides, it was observed that if only one side of the masonry wall is strengthened, the capacity could be halved. In addition, the eccentricities caused by this strengthening scheme had a minimum effect on the shear carrying capacity. In all the strengthened walls fine cracks were observed perpendicular to the sheets. The crack separation was constant and the crack widths remained small.

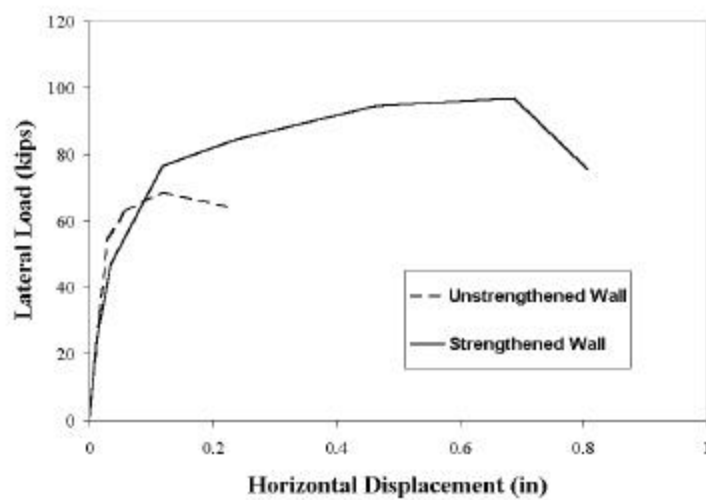


Figure 2.10. Test Results-Schwegler

Laursen et al. (1995) studied the shear behavior of masonry walls strengthened with CFRP laminates. The walls were built with concrete blocks; and fully grouted. The overall dimensions were 6 by 6-ft. The walls were internally reinforced; horizontally with a low shear reinforcement ratio of 0.14%, and vertically with a ratio of 0.54%. The “original” wall failed in shear. The specimen was re-tested after being repaired. The repair was performed by closing the large diagonal shear cracks with epoxy filler and epoxy injection, and repairing the crushed compression toes with epoxy mortar. The “repaired” wall was then strengthened with CFRP laminates, which covered the two sides of the wall; an additional layer was applied in the end regions as confinement. The amount of strengthening in the “retrofitted” wall was similar to the previous wall but applied to only one side of the wall.

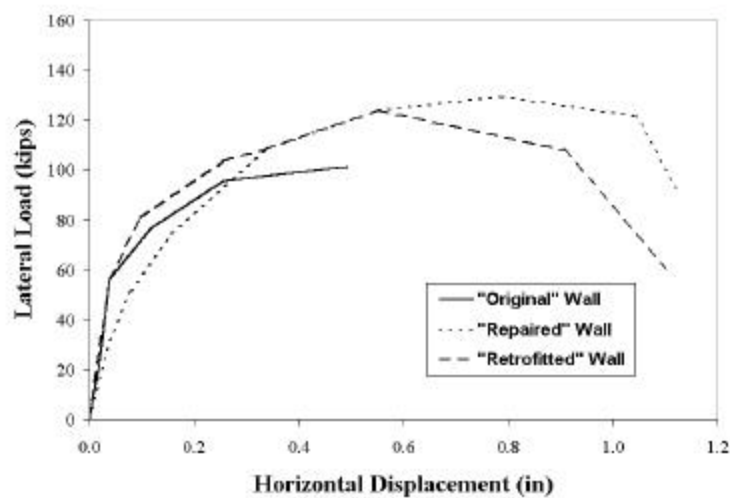


Figure 2.11. Test Results-Laursen

It was observed that the presence of the FRP laminates improved the wall performance by changing the failure from a shear-controlled failure to a flexural-controlled failure. This change caused an increase in the capability of deformation of approximately 100% by preventing a brittle failure mode. The test results of this wall, shown in Figure 2.11, also proved that even though the wall failed in shear, it could be repaired to restore the initial stiffness and strength compared to the standard of the “original” and “retrofitted” walls.

Ehsani et al. (1996) investigated the flexural behavior of URM walls strengthened with GFRP sheets. Their dimensions were 8.5-in. wide, 4-in. high, and 57-in. long. Two different kinds of mortar were used for their construction, type M with cement:lime:sand ratios of 1:1/4:3 and a compressive strength of 4.65 ksi; and type M* with ratios of 1:1/4:5 and a compressive strength of 4.1 ksi. The specimens were subjected to four-point bending. The primary failure was a tension failure, which was observed when low amount of strengthening was used. When the number of plies was increased, the masonry failed in compression. It was observed that the flexural capacity was increased up to 24 times compared to the control specimen. As observed in Figure 2.12, the effect of the mortar strength appeared to be negligible, both specimens failed by crushing of the masonry.

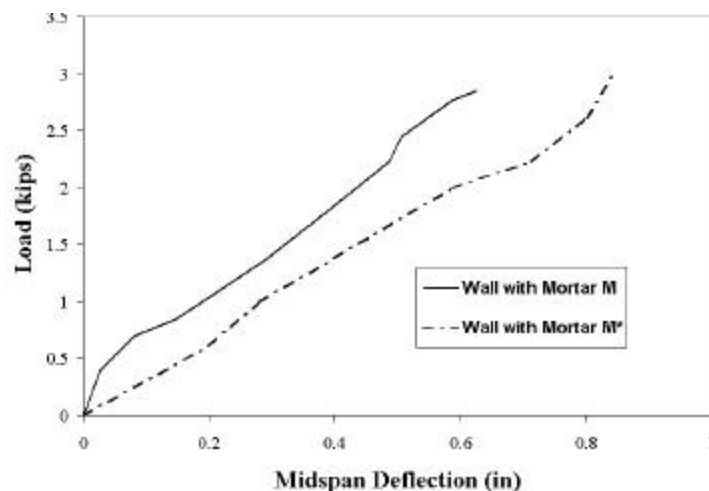


Figure 2.12. Test Results-Ehsani

Hamilton et al. (1999) investigated the flexural behavior of URM walls strengthened with different composite materials. The walls were built with standard concrete blocks, with an overall dimension of 2 by 6-ft. The use of high strength composite materials such as CFRP and AFRP led to undesirable modes of failure such as delamination and shear in the masonry. In order to use the material efficiently, two alternatives were recommended. The first one was to increase the spacing of the material until observing the rupture of the laminate. The second one was to use less expensive

materials such as GFRP. Four modes of failure were identified: debonding, laminate rupture, shear, and face shell pull out. It was reported that debonding from the masonry substrate caused the failure of most of the test specimens (see Figure 2.13).

Velazquez et al. (2000) reported test results of half-scale URM walls tested under out-of-plane cyclic loading. The test specimens had a width of 48-in. and a height of 56-in., with a slenderness ratio of 28. Two of the walls were strengthened on both faces with GFRP strips. By understanding that the balanced condition represents the failure of masonry and rupture of composite laminate at the same time, one wall had the reinforcement equivalent to the balanced ratio ($1.0\% \rho_b$). The other wall had three times the amount of reinforcement as compared as the first wall ($3.0\% \rho_b$). The specimen reinforced with $1.0\% \rho_b$ showed extensive delamination at failure. The first delaminated areas were observed on the central strip above the middle brick course. The specimen with $3.0\% \rho_b$ failed due to high in-plane shear stresses along the lower brick course. Substantial increases in strength and deformation capability were achieved. It was observed (see Figure 2.14) that the retrofitted walls resisted pressures up to 24 times the weight of the wall and deflected as much as 5% of the wall height. To avoid very stiff behavior and improve the hysteretic response, it was recommended to limit the reinforcement ratio to two times the balanced condition.

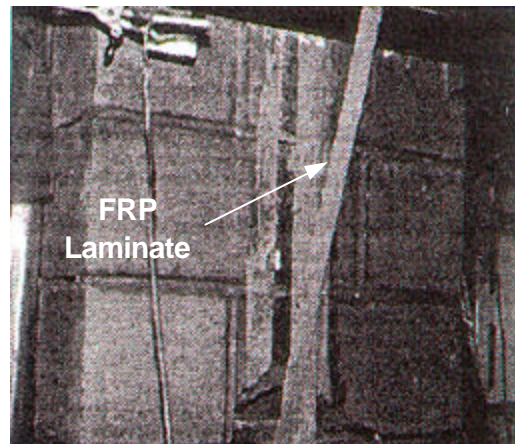


Figure 2.13. Debonding of FRP Laminate

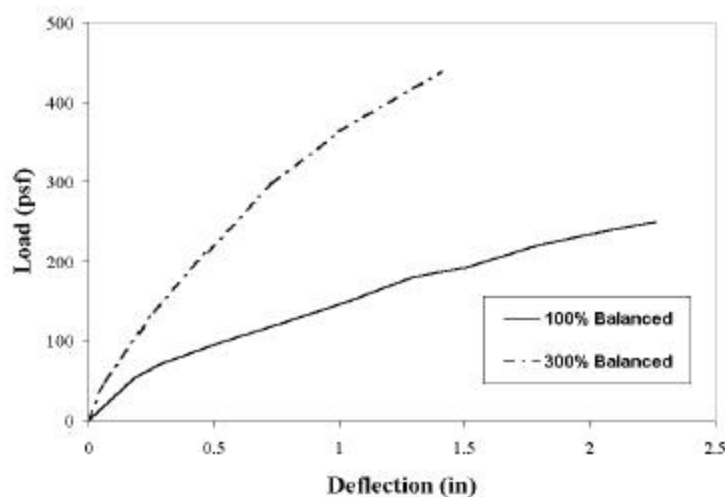


Figure 2.14. Test Results-Velazquez

2.2.2.2. Strengthening with FRP Rods. Hamid (1996) conducted an investigation aimed at strengthening of hollow concrete block walls using, similar to basement walls. As a vertical reinforcement # 4 FRP rods were used to strengthen a URM wall because of their corrosion resistance and ease of installation. The strengthening procedure consisted of: (1) cutting slots at the top course of the wall to place the reinforcing bars, (2) inserting the rods, (3) drilling holes of 2-in. diameter thorough the height of the cells to pump the grout; and (4) pumping grout starting from the lower holes; plug the holes after grouting to continue with the upper holes.

The 4 by 8.5-ft. walls were simply supported and tested under out-of-plane loading. In the strengthened wall, a 22-fold increase in flexural capacity compared to the unstrengthened wall was recorded. In addition, a large deformation capability beyond the first crack was observed, as seen in Figure 2.15. This is attributed to the presence of the reinforcing bars and the high tensile strength of the grout.

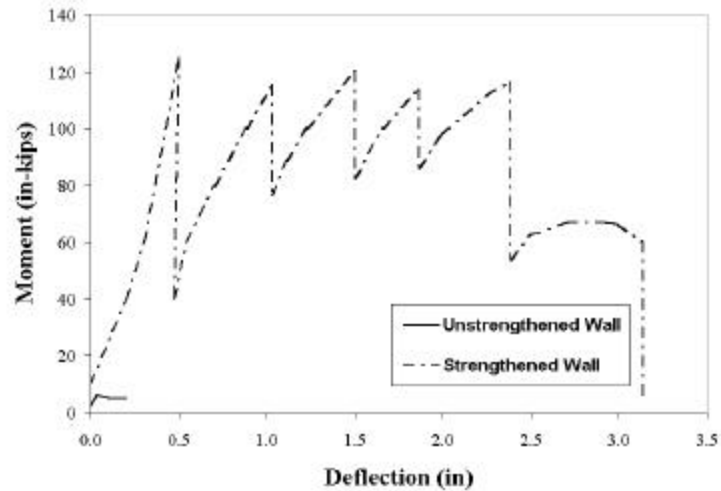


Figure 2.15. Test Results-Ahmid

Tinazzi et al. (2000) introduced the term “FRP Structural Repointing” and investigated the use of FRP rods to increase the shear capacity of masonry panels made of clay bricks. This technology consisted of placing # 2 GFRP rods in grooved horizontal joints. The rods were embedded in an epoxy-based paste. The nominal dimensions of the panels were 2 by 2 ft with a thickness of 3.5 inches. The failure of unreinforced panels consisted of the joint sliding along the compressed diagonal. In contrast, walls strengthened with FRP rods at each joint, showed increases in capacity of about 45% higher as compared to the unreinforced wall. The failure mode changed since joint sliding was prevented. The mechanism of failure indicated the sliding of the masonry-paste interface.

2.2.3. Final Remarks. The use of FRP composites for the retrofitting of masonry structures offers some advantages compared to the use of conventional retrofitting techniques. As an example, FRP composites do not add considerable mass to the structure. This extra weight could modify the dynamic response to seismic events, which may be observed when using masonry-RC composite walls or ferrocement overlays. From the architectural point of view, the use of conventional methods may violate the aesthetics of building facades and they may intrude on usable space adjacent

to the strengthened components. The aforementioned facts along with the outstanding properties of FRP materials make the use of FRP composites attractive for strengthening of masonry structures.

Studies on masonry walls strengthened with FRP composites have shown that increases in either out-of-plane or in plane capacities as well as ductility can be achieved. However, most of these studies have been carried out in laboratories, under ideal conditions such as considering free rotation of the supports. In this sense, some tests performed in this investigation offered an opportunity to observe the behavior of masonry walls under real boundary conditions, which are not commonly reproduced in the laboratory.

3. FRP COMPOSITE SYSTEMS

3.1. MECHANICAL PROPERTIES

FRP composites in the form of sheets and rods were used throughout this research to strengthen masonry walls. Three basic component materials are commonly used for the installation process of the FRP sheets; namely: primer, putty and impregnating resin or saturant. The combination of the latter and the fibers form the FRP laminate. The impregnating resin forms the matrix, which acts a binder for the reinforcing fibers. The matrix has two functions: to enable the load to be transferred among fibers and, to protect the fibers from environmental effects. The near-surface-mounted (NSM) rods system consists of two components: an epoxy-based paste, where the rods are embedded, and the rods themselves. The properties for primer, putty, saturant as well as epoxy-based paste are shown in Table 3.1.

Table 3.1. Resin Properties in Tension

Material	Tensile Strength (psi)	Tensile Elastic Modulus (ksi)	Tensile Strain (%)	Compressive Strength (psi)	Compressive Modulus (ksi)	Bond Strength (psi)
Primer	1800	105	3	3500	95	NA
Putty	1800	260	1.5	3500	155	NA
Saturant	7900	440	2.5	12500	380	NA
Paste	4000	NA	1	12500	450	> 2000

It is important to highlight that for the strengthening of masonry walls, the surface is commonly primed with the saturant used to bond and impregnate the fibers rather than the conventional primer used for concrete surfaces. This is due to the absorptive characteristics of masonry, which requires a high amount of primer. Three types of commercially available FRP sheets constituted of glass, aramid and carbon fibers, as well as glass FRP rods were used to strengthen the masonry walls. Their engineering properties according to the manufacturers are summarized in Table 3.2. Since FRP

sheets and #3 GFRP are broadly used, and their engineering properties have been well determined, no independent tests were conducted on them. Properties of the FRP sheets have been determined considering only the fibers, whereas, properties of the rods are based on the composite section (i.e. fiber and matrix). The #2 GFRP rods were subjected to tensile tests to determine their properties.

Table 3.2. Engineering Properties for FRP Sheets and GFRP Rods

Material	Tensile Strength (ksi)	Tensile Modulus (ksi)	Load per Sheet Width (lb/in)
GFRP – EG900	220	10,500	3050
AFRP – AK 40	290	17,000	3190
CFRP – CF 130	550	33,000	3580
#3 GFRP Rods	120	6,000	-----
#2 GFRP Rods	60	4,500	-----

3.2. INSTALLATION TECHNIQUES

The techniques used for the installation of FRP laminates and rods for field and laboratory experimentation are described. Field experimentation was conducted in the old City Hospital complex in St. Louis, Missouri, which was decommissioned and scheduled for demolition. Before the demolition takes place, one of the buildings, the Malcolm Bliss Hospital, was used as a research test bed (see Figure 3.1). The building of interest, a five-story reinforced concrete-frame addition built in 1964, had in its contour URM walls, which were strengthened with a variety of FRP composites. The walls had two wythes. Only the inner wythe, built with clay tiles, was strengthened.

For laboratory experimentation, the walls were strengthened with a technique denominated “FRP structural repointing”. This technique consists in placing RP rods in the mortar joints, which besides increasing the wall capacity, it preserves the masonry aesthetics.

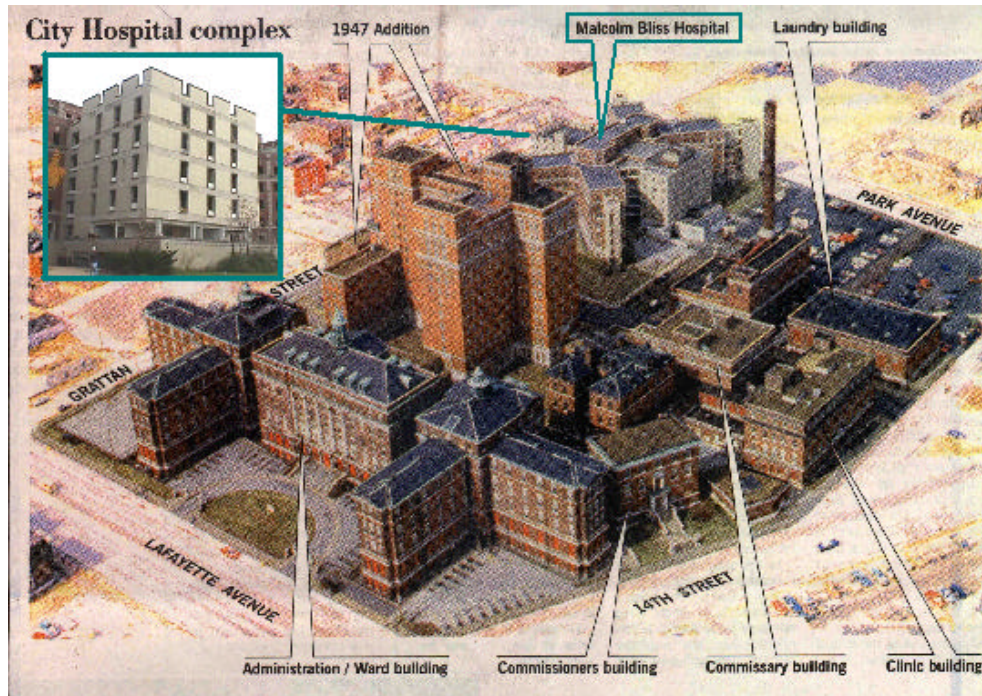
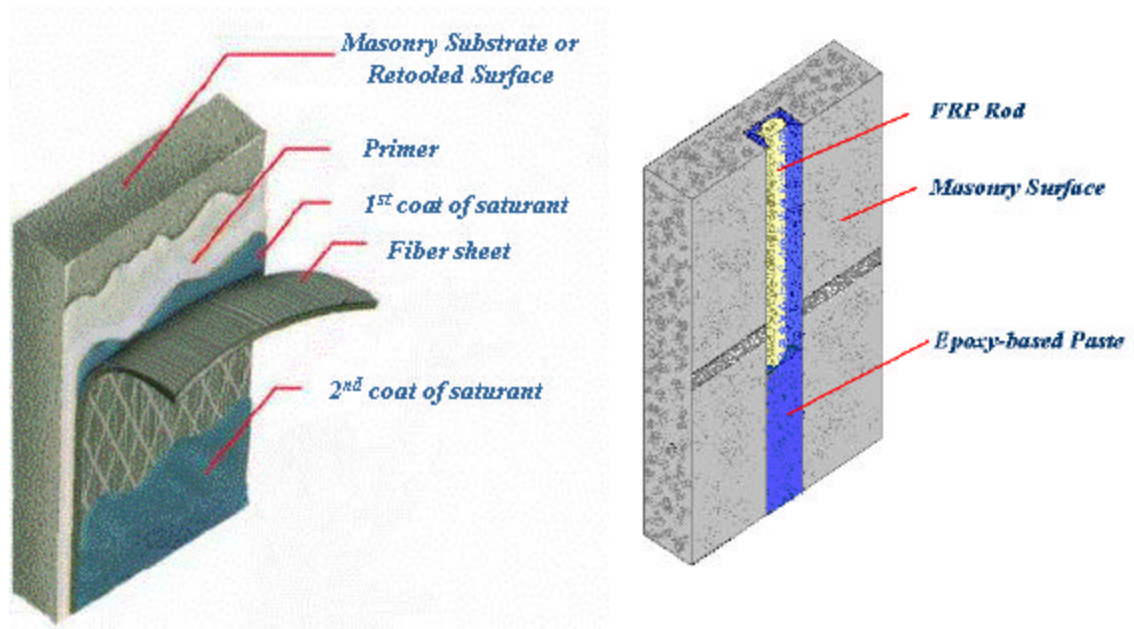


Figure 3.1. City Hospital Complex – St. Louis, Missouri

FRP laminates are formed by manual lay-up onto the surface of the member being strengthened. Prior to the fibers installation, the surface is prepared by sandblasting, application of primer, and puttying. Depending on the characteristics of the masonry surface, it may not need be sandblasted because the surface exhibits sufficient roughness. This is particularly evident in concrete units, which are extruded and thereby do not have laitance on their surface. The surface of the walls, particularly at the joints, is leveled with putty. After applying a first coat of saturant, the fibers are attached to the wall surface. The fibers are impregnated by a second coat of saturant, which after hardening enables the newly formed laminate to become integral part of the strengthened member (see Figure 3.2a).

Another available FRP technology consists of placing FRP rods into grooves made on the surface of the member being strengthened. The groove is filled with an epoxy-based paste, the rod is then placed into the groove and lightly pressed to force the paste to flow around the rod. Finally, the groove is filled with more paste and the surface is leveled (see Figure 3.2b).



(a) FRP Laminates

(b) NSM FRP Rods

Figure 3.2. FRP Systems

3.2.1. Laminate Manual Lay-up. The FRP sheets were attached to the wall surface by manual lay-up. For their installation a procedure recommended by the manufacturer was followed. Since the performance of the composite materials relies on bonding, surface preparation was to be performed before installing the sheets. Two installation methods were used depending on whether the FRP sheets were bonded to a plaster surface or directly to the masonry surface. In the first case, two procedures were investigated, herein referred to as Procedures A and B:

Procedure A: The paint and plaster of paris layers were removed using a grinder with a 4¹/₂ inch diamond blade. In terms of surface finishing this procedure gave good results, without excessive exposure of the aggregates present in the plaster (see Figure 3.3). A main disadvantage of this procedure was the preparation time, which for large scale projects may not be practical.

Procedure B: The surface was prepared by means of sandblasting, which was performed using an abrasive blast machine with a 300 lbs. sand capacity. This procedure was less labor intensive than the previous one; however, due to a lack of quality control the

aggregates were excessively exposed, requiring a larger amount of putty to level the surface (see Figure 3.3).

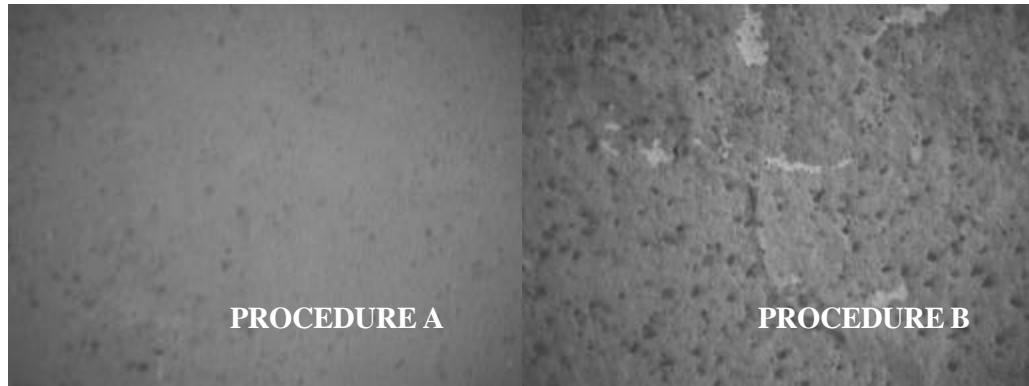


Figure 3.3. Aggregates Exposure

It may be concluded that each of these methods had pros and cons. The final adopted procedure was a combination of procedures A and B, which can be summarized as follows: sandblasting was employed to remove most of the plaster of paris layer; next the surface was finished with grinding (see Figure 3.4a).

Before the installation of the FRP sheets, the dust caused by the surface preparation was removed using air pressure to avoid potential bonding problems. The installation of the FRP sheets can be summarized as follows:

- Saturant was applied as a primer to fill cavities on the masonry wall surface. The constituent parts of the saturant were premixed independently using a 4-in. mixing jiffy paddle prior to being combined. The combined parts were mixed for three minutes using the proportions specified by the manufacturer, with a 2-in. mixing jiffy paddle.
- The primary purpose of using putty was to level the uneven surfaces present on the wall surface (see Figure 3.4b). After the putty set, the surface was smoothed to eliminate irregularities on the surface. This was carried out using a grinder.
- A layer of saturant was applied to the surface using a roller. Following this, the FRP sheets were adhered to the wall surface (see Figure 3.4c).

The FRP sheets were then cut to length. Once, the sheet was placed, it was pressed down using a “bubble roller” to eliminate entrapped air between the saturant and fibers. Finally, a second layer of saturant was applied as shown (see Figure 3.4d).



(a) Grinding of Wall Surface



(b) Putty Application



(c) Fibers Installation



(d) Saturant Impregnation

Figure 3.4. Installation of FRP Laminates

Before installing the FRP laminates on bare masonry walls the masonry surface was prepared. After sandblasting (see Figure 3.5a), the excess of mortar in the joints was eliminated using a grinder (see Figure 3.5b), and the uneven surface was leveled with putty material. After completing the surface preparation, the installation procedure of laminates is similar to that illustrated in Figure 3.4.



(a) Surface Sandblasting

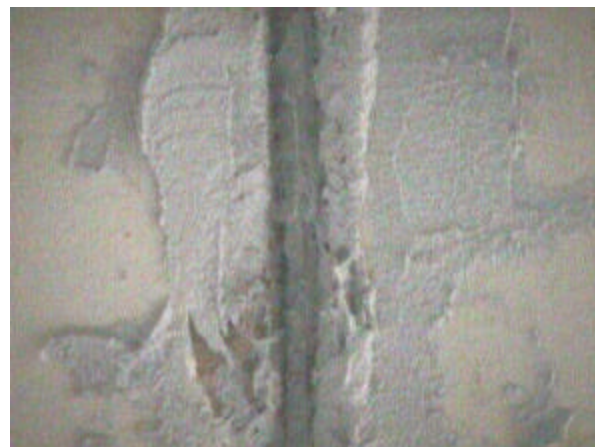
(b) Removal of Mortar Excess

Figure 3.5. Surface Preparation in Bare Walls

3.2.2. Near-Surface Mounted (NSM) Rods. The use of NSM rods is attractive since the removal of plaster is not required. For the walls where NSM rods were installed, the procedure can be summarized as follows: $\frac{3}{4}$ inch-wide lines were drawn on the wall at the desired location as traces for the specified width of the grooves. By using a grinder with a diamond blade, slots were then grooved (see Figure 3.6). The plaster and masonry material was then removed using chisel and hammer to complete the slots. The depth of the groove depended on the shell thickness of the clay tile.



(a) Grooving of Slots



(b) NSM Rod embedded in Paste

Figure 3.6. Installation of NSM Rods

An epoxy-based paste was used to provide bond between the masonry and the rods. First, using a mason trowel, a layer of paste was placed into the slots. Following this, a rod was nested in the slot (see Figure 3.11). The slot was then completely filled with the paste to encapsulate the FRP rod.

When the FRP rods are installed in either the horizontal or vertical (only for stack bond patterns) masonry joints, the aforementioned technique receives the name of FRP Structural Repointing. Repointing is a traditional retrofitting technique, commonly used in the masonry industry, which consists in replacing missing mortar in the joints. The term “structural” is added to describe a strengthening method aimed at restoring the integrity and/or upgrading the capacity of walls. This is achieved by placing into the joints deformed FRP rods, which are bonded to the masonry wall by the paste (see Figure 3.12).

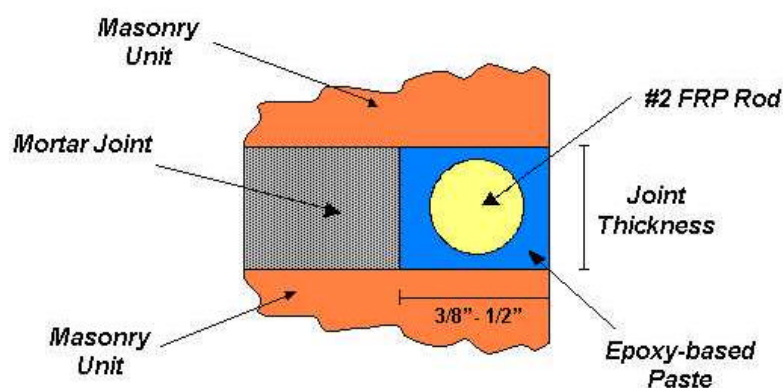


Figure 3.7. FRP Structural Repointing

Structural repointing offers advantages compared to the use of FRP laminates. The method itself is simpler since the surface preparation (sandblasting and puttying) is not required. In addition the aesthetic of masonry is preserved. The diameter size of the FRP rods is limited by the thickness of the mortar joint, which usually is $\frac{3}{8}$ inches. The FRP rods were placed into the joints by using a technique known as tuck pointing, which consists of: (1) cutting out part of the mortar using a grinder, the depth of the cut depends on the shell thickness of the masonry unit (see Figure 3.13), (2) masking of the masonry surface to avoid staining with the epoxy-based paste (see Figure 3.14), (3) filling the joints with an epoxy-based paste (see Figure 3.15), (4) embedding the rods in

the joint (see Figure 3.16), and (5) retooling. To ensure a proper bonding between the epoxy-based paste and masonry, it is recommended to remove the dust by means of an air blower once the grinding of the mortar joints has been completed.



(a) Grinding of Joints



(b) Masking of Masonry to avoid Staining



(c) Application of Epoxy-based Paste



(d) Installation of FRP Rods

Figure 3.8. Strengthening with FRP Structural Repointing

4. WALLS SUBJECTED TO IN-PLANE LOADING

Two experimental programs were conducted to study the in-plane behavior of masonry walls. The first program investigated the shear behavior of masonry panels strengthened with FRP composites, which were intended to represent infill walls. These walls were tested in the laboratory (In-Plane Laboratory), thereby they correspond to the Series IL. The second program dealt with the behavior of masonry walls under in-plane loads and without axial loads. These walls were part of a decommissioned building (In-Plane Field), and they belong to Series IF.

4.1. PROBLEM STATEMENT

Series IL had the objective to assess the behavior of URM panels similar to those found in infill walls. It is recognized that the behavior of these panels would be different in the presence of a surrounding structural frame. Masonry walls are commonly used as interior partitions or exterior walls bound by steel or concrete frames conforming the building envelope. For the latter case, depending on the design considerations, the infill walls may or not resist lateral and vertical loads. In order to simplify the design, the potential interaction between the infill walls and the structural frame has been ordinarily ignored. Ignoring the contribution of the masonry infill walls does not always represent a conservative design. The presence of infill walls can lead to stiffening their frames and thereby cause a redistribution of lateral loads in the building plan. The increase in stiffness of the frame can attract higher lateral loads than those expected according to the design. This may cause cracking of the wall and overstressing of the frame.

Previous investigations (Sabnis, 1976) have demonstrated that the composite action between the masonry infill and the surrounding frame is depending on the level of the in-plane load, bonding or anchorage at the interfaces, and geometry and stiffness of both the masonry infill and the structural frame. At a very low level of in-plane loading, a full composite action between the infill wall and the frame is observed. Once the load increases, the infill wall and the frame are no longer in contact, except in surrounding areas of the two corners where compression stresses are transmitted from the frame to the masonry which lead to the formation of a diagonal compression strut (see Figure 4.1).

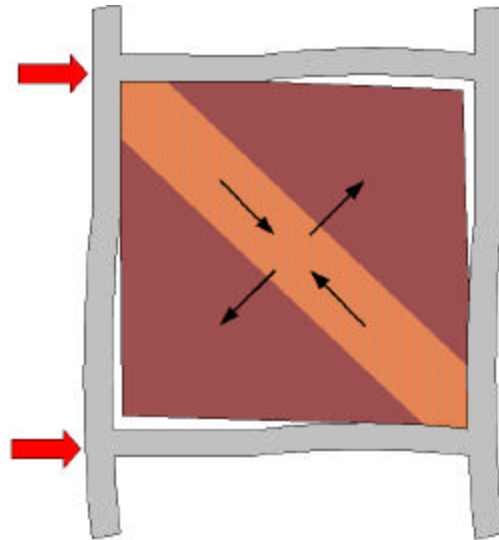


Figure 4.1. Diagonal Compression Strut

This resulting structural system is usually analyzed as a truss. The stiffness of the infill starts decreasing once cracking is developed. At a stage when higher in-plane loads are present, the contribution of the compressive strut begins to reduce as further cracking is developed. Also, the gap separating masonry from frame is increased, which eventually leads to shear failure (diagonal tension) of masonry as observed in Figure 4.2; and flexure (yielding) failure of the columns. Depending on the compressive strength of the masonry, the units in the corner areas may be crushed prior to developing diagonal cracking (see Figure 4.3).



Figure 4.2. Diagonal Tension Failure (Turkey, 1999)



Figure 4.3. Crushing of Infill Corners (Turkey, 1999)

Alternatively to the diagonal tension failure, a shear failure along a horizontal joint can be observed at a lower load level as compared to the load causing the latter mentioned failure. The resulting shear crack divides the infill in two parts, where the behavior is controlled by either the flexural or shear capacity of the columns. This failure mechanism is commonly known as Knee Brace or Joint-Slip (see Figure 4.4).

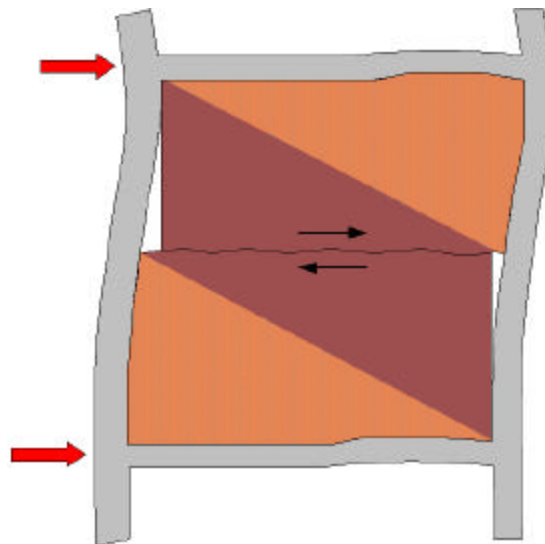


Figure 4.4. Joint-Slip Failure

Single-story buildings, such as schools and shopping centers, are very common in the United States. In these buildings, vertical and horizontal loads are resisted by shear walls. These unreinforced or lightly reinforced walls are prone to failing during an earthquake. Their capacity to withstand horizontal loads is limited by the strength of the masonry units and the mortar in the bed joints. At low axial loads, two modes of failure may be observed. One is sliding of the wall along the bed joints (see Figure 4.5a). The other is rocking on a horizontal crack at the wall bottom (see Figure 4.5b). The overall stability of the building is not compromised as long as the deformations are small. If the masonry wall bears high axial loads, the bed joint friction is increased and therefore sliding or rocking will not be observed. Instead, diagonal shear cracks will be developed. In this context, the specimens belonging to series IF offer the opportunity to perform fieldwork to evaluate the behavior of this kind of masonry walls.

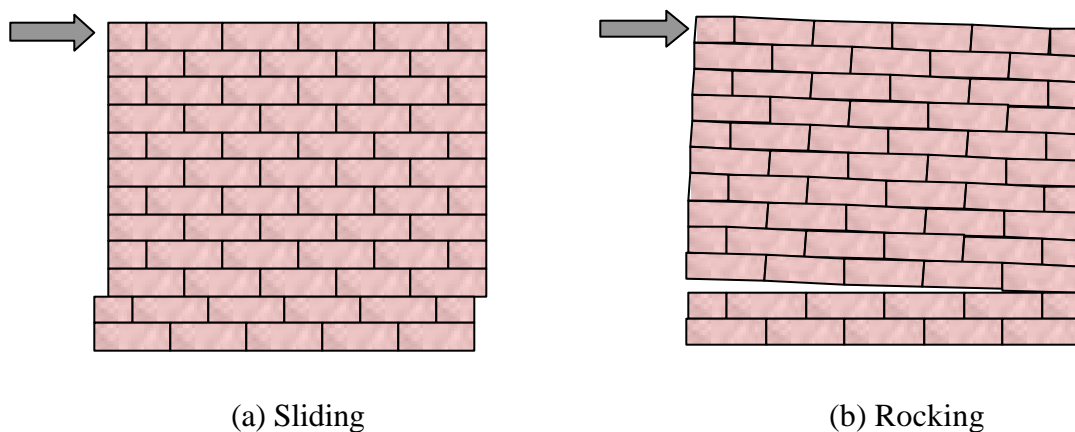


Figure 4.5. Potential Failures in Walls with No Axial Load

4.2. SERIES II

4.2.1. Test Specimens. A total of four masonry walls were manufactured for this experimental program, which were built with 6x8x16-in. concrete blocks in a stack bond pattern. The dimensions of the walls were 64 by 64-in. All the walls were built by a qualified mason to not introduce additional variables, such as handwork and different mortar workability that may arise from the construction of the specimens. The average compressive strength of the mortar was 1817 psi with a standard deviation of 15.3. These values were determined according to ASTM C109. The average compressive strength of masonry obtained from the testing of prisms was 2090 psi with a standard deviation of

19.7. The walls were strengthened with GFRP rods having a diameter of 0.25-in., a tensile strength of 60 ksi and modulus of elasticity of 5900 ksi. The GFRP rods were embedded into an epoxy-based paste. According to the manufacturer, the paste had the following mechanical properties: compressive strength of 12.5 ksi, tensile strength of 4 ksi, and modulus of elasticity of 450 ksi.

Two URM walls, Walls IL1-a and IL2-b were selected as control specimens for this test series. Wall IL2 was strengthened with GFRP rods at every horizontal joint (i.e. spacing equal to 8-in.). Wall IL3 was strengthened with GFRP rods in a grid pattern, which means that the rods were placed in every vertical and horizontal joint. Following the criterion provided by the Masonry Standards Joint Committee (MSJC, 1999) for cracking control, the vertical reinforcement was about one-third of the horizontal reinforcement. For Wall IL4 the amount of reinforcement was similar to that of Wall IL3 but the reinforcement was distributed in the two sides of the wall. The horizontal reinforcement was installed in the front side, whereas the vertical reinforcement was placed in the back side of the wall. Table 4.1 illustrates the matrix used for this experimental program. The strengthening schemes are presented in Appendix A.1.

Table 4.1. Test Matrix for Series IL

Specimen	Reinforcement	Front Side	Back Side
Wall IL1-a	None	None	None
Wall IL1-b	None	None	None
Wall IL2	#2 GFRP Rods	Every Horizontal Joint	None
Wall IL3	#2 GFRP Rods	Every Horizontal and Vertical Joint	None
Wall IL4	#2 GFRP Rods	Every Horizontal Joint	Every Vertical Joint

4.2.2. Test Setup. The specimens were tested in a closed loop fashion. Two 30-ton-capacity hydraulic jacks, activated by a manual pump, were used to generate the load along the diagonal of the wall being tested. When loading, the force was applied to the wall by steel shoes placed at the top corner, and transmitted to similar steel shoes at the

bottom corner through high strength steel rods. Figure 4.6 illustrates the test setup for Series IL.

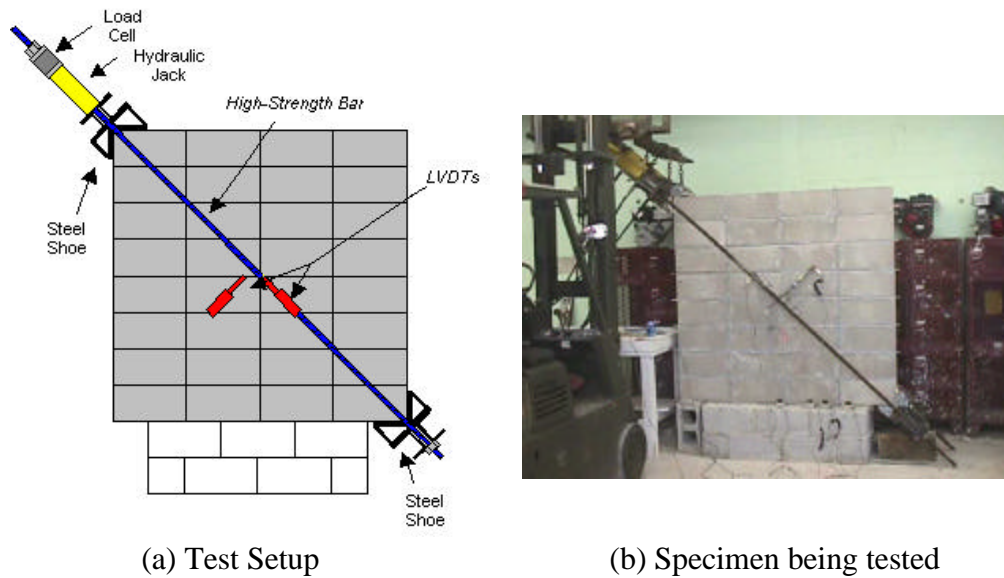


Figure 4.6. Test Setup for Series IL

The load was applied in cycles of loading and unloading, except in the control wall. An initial cycle for a low load was performed in every wall to verify that both the mechanical and electronic equipment were working properly. By applying the load by cycles, the stability of the system can be verified. The data acquired by the load cell and the Linear Variable Differential Transducers (LVDTs) were collected by a DAYTRONIC data acquisition system at a frequency of one point per second. A total of four LVDTs were used to collect displacements in the walls. A couple of LVDTs was placed on each side of the walls. One oriented along the line force and the other perpendicular to the line. The latter one was placed to register the crack opening.

4.2.3. Test Results. Figure 4.7 illustrates the envelopes of the load vs. crack opening curves recorded at the front and back sides for the five tested walls. The test results for each specimen are illustrated in Appendix A.2. It can be observed that at about 10 kips all the four test specimens experienced a reduction in their initial stiffness. Wall IL1-a maximum capacity was registered at about 27.6 kips; whereas Wall IL1-b exhibited a maximum capacity of 25.6 kips. As expected the capacity of these specimens

was sensitive to the weaker planes along the bed and head joints (see Figure 4.8a) with cracks developing only in these joints.

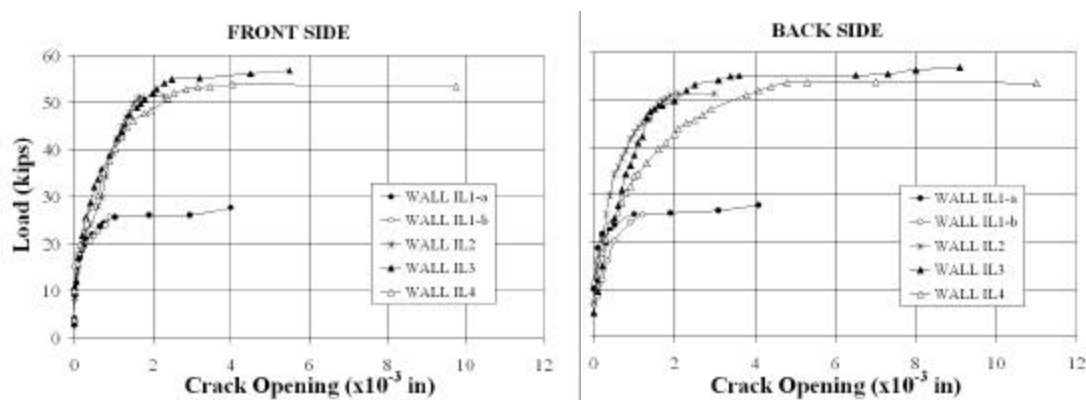


Figure 4.7. Envelopes of Load vs. Crack Opening

The maximum loads in Walls IL2, IL3 and IL4 were approximately the same, with an average load of 53 kips. In these strengthened walls, the presence of the reinforcement, forced the formation of diagonal cracks running through the masonry units (see Figures 4.8b, 4.8c and 4.8d). Thus, the tensile forces in the rods bridging the diagonal crack increased the shear capacity of the walls.

In the unstrengthened walls the failure was brittle, typical of a dominated shear failure. In this wall some material come loose after the ultimate load was reached which could potentially fail due to any out-of-plane loading. In a real building, this fact could cause injuries or loss of human life during a seismic event. On the other hand, at the final state, in all the strengthened walls no loose material was observed.

Wider cracks were mostly observed in the unstrengthened (back) side or where minimum amount of reinforcement was placed such as in Wall IL4. It should be noted that these cracks were not visible until the peak load was reached. In addition the strengthened walls tilted to the direction of the strengthened face, which was more evident in Wall IL3 (see Figure 4.9), which was strengthened with GFRP rods in the horizontal and vertical joints placed in one side of the wall. The cracking patterns are presented in Appendix A.3.



(a) Wall IL1-a



(b) Wall IL2



(c) Wall IL3



(d) Wall IL4

Figure 4.8. Specimens after Failure – Series IL



Figure 4.9. Strengthened Wall after Failure

4.2.4. Mechanism of Failure. In the strengthened walls, the failure was produced by the loss of bonding between the epoxy-based paste and the masonry units. Comparing the recorded crack widths in the front and back sides, the crack growth in the unstrengthened or less strengthened back side increased at a higher rate than the strengthened front side; as verified from Figure 4.7. The crack produced by debonding of the masonry units from the mortar in the back side, traveled through the wall thickness until debonding of the epoxy-based paste from the masonry units (see Figure 4.10). At this point the wall fails because the tensile stresses are not longer transferred to the rods.

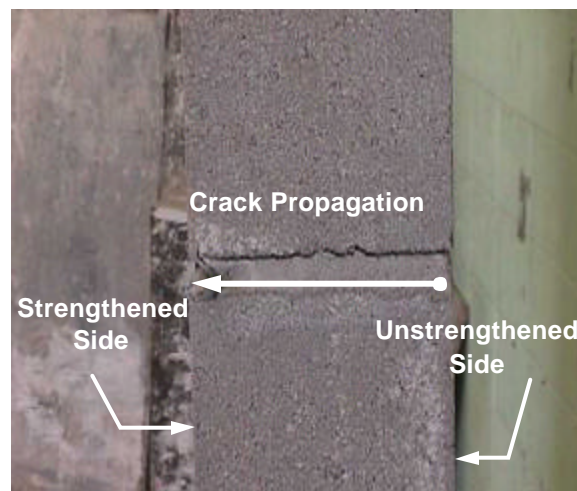


Figure 4.10. Mechanism of Failure – Series IL

4.2.5. Analytical Study. Diagonal tension tests do not completely reflect real loading conditions. The objective of these tests was to evaluate a new technology (FRP structural repointing) and to certain extent simulate the in-plane loads in an infill panel. It is recognized that the interaction of the masonry panel with a surrounding structural frame will modify the masonry panel behavior. To estimate the shear strength (R_n) of a URM wall strengthened with FRP structural repointing, the sum of the shear contributions of the masonry (R_m) and the FRP reinforcement (R_f) are considered:

$$R_n = R_m + R_f \quad (4.1)$$

R_f depends on the tensile stresses developed in the rods. Depending on the magnitude of the stresses two areas can be identified in a masonry panel: bond-controlled and rupture controlled regions (see Figure 4.11)

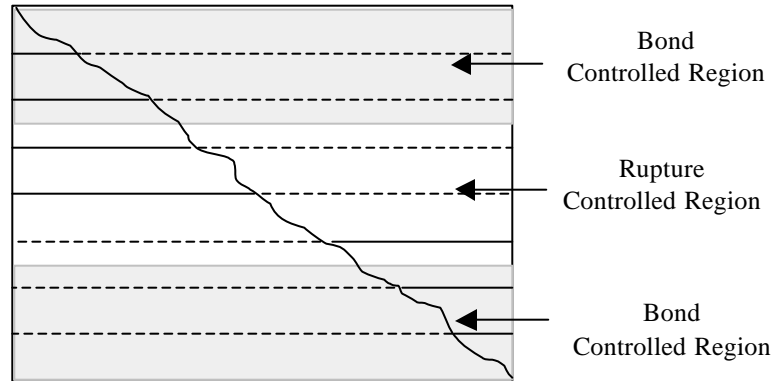


Figure 4.11. Controlling areas to estimate R_F

In contrast to grooving the surface of masonry units, grooving of the mortar joints is a simpler task. In addition, if grooving of the units is not carefully carried out, these may be locally fractured. That is the reason why the spacing of FRP rods is basically dictated by the size of the units. In the previous sections it was mentioned that the horizontal spacing between FRP rods was the height of the layer. In this research standard CMU were used, thus the horizontal spacing was equal to 8-in. When using vertical reinforcement, the rods were also placed in the joints since a stack bond pattern was used for the construction of the specimens. In this case the spacing was 16-in. For the analysis of the walls strengthened with FRP structural repointing, the following assumptions are considered:

- Inclination angle of the shear cracks constant and equal to 45° .
- Constant distribution of bond stresses along the FRP rods at failure of the panel.
- Although, it is recognized the potential existence of two controlling areas, all the rods to be intersected by the crack at failure are assumed to be subjected to the same tensile stresses.
- The observed mechanism of failure differs from that where debonding is observed along the three paste-masonry interfaces of the groove. Since neither debonding nor breaking of the GFRP rods were observed, it will be assumed for the estimation of the maximum shear capacity that the strength developed in the GFRP rods is half of the ultimate tensile strength.

Thus, the FRP shear contribution can be estimated as:

$$R_f = 0.5 \left(\frac{A_f}{s} \right) f_{fu}^* d_v \quad (4.2)$$

where:

A_f : cross-sectional area of FRP shear reinforcement

s : spacing of reinforcement

d_v : actual depth of masonry in direction of shear considered

f_{fu}^* : tensile strength of the rods reported by the manufacturer

This approach is similar to the proposed change to masonry standards by MSJC (MSJC, 2000) for the shear strength contribution of steel reinforcement in beams, piers, and columns. The factor of 0.5 for these elements was estimated empirically. Similarly, the factor of 0.5 in FRP structural repointing intends to account for the observed mechanism of failure by assuming an effective stress in the rods equal to half of the ultimate strength. However, it is recognized that this factor can change with future research.

For Wall IL2 strengthened with seven #2 GFRP rods, R_f is computed using equation 4.2 as:

$$R_f = 0.5 \left(\frac{(0.05 \text{in}^2)}{(8 \text{in.})} \right) (60 \text{ksi})(96 \text{in.}) = 18 \text{ksi}$$

The contribution of masonry is assumed to be the average of the shear strength of the two unstrengthened walls (Walls IL1-a and IL1-b); thus R_m is 26.6 kips. Finally, the shear strength is estimated as:

$$R_n = R_m + R_f = (26.6 \text{ kips}) + (18 \text{ kips}) = 44.6 \text{ kips} < 51.4 \text{ kips}$$

The difference can be attributed to additional compression resisted by the masonry diagonal strut.

Table 4.2 shows the experimental and analytical shear strengths. For Walls IL3 and IL4, the analytical shear strengths are considered to be the same as Wall IL2. The

contribution of the vertical FRP reinforcement may be fully realized in larger walls were more vertical reinforcing rods can bridge the diagonal cracks.

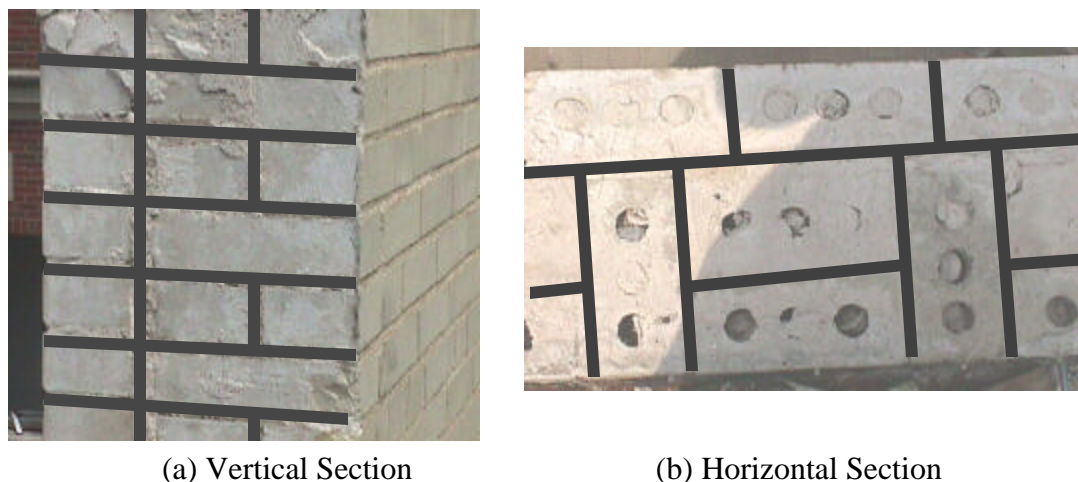
Table 4.2. Experimental and Analytical Values – Series IL

Specimen	Experimental			Analytical
	R _n (kips)	R _m (kips)	R _f (kips)	R _f (kips)
Wall IL1-a	27.6	27.6	---	---
Wall IL1-b	25.6	25.6	---	---
Wall IL2	51.4	26.6	24.8	18.0
Wall IL3	56.9	26.6	30.3	18.0
Wall IL4	53.5	26.6	26.9	18.0

Alternatively to the diagonal tension failure, a crack along a horizontal joint can be observed at a lower load level in infill masonry walls. The resulting horizontal crack divides the infill wall in two parts. This failure mechanism is commonly known as Knee Brace or Joint-Slip. Due to its premature characteristic and negative effects, this kind of failure should be avoided. A potential way to prevent it would be to place of vertical FRP reinforcement on the masonry infill, which would act as a dowel action.

4.3. SERIES IF

4.3.1. Test Specimens. Three multiwythe reinforced masonry walls built using clay units were tested as part of this experimental program. The testing dimensions were 5 x 5-ft. The overall thickness of the walls was 12.5-in. The multiwythe walls were built with cored bricks with the following physical dimensions, 3.75-in. wide, 2.25-in. high and 8-in. long, and three cores with a diameter of 1.5-in. Tests performed to the steel reinforcement showed that the yielding strength was 50 ksi. Details of the wall bond pattern are illustrated in Figure 4.12.



(a) Vertical Section

(b) Horizontal Section

Figure 4.12. Cross Section – Series IF

According to the building original drawings, the walls were reinforced with #3 steel bars, horizontally and vertically, which were placed in the joints between wythes (see Figure 4.13a). However, after being inspected, it was observed that many of the steel rebars were missing or irregularly placed as can be observed in Figure 4.13b. This fact made difficult to assess the actual capacity of the members.

Wall IF1 was selected as a control specimen. The remaining three specimens were strengthened with GFRP sheets and rods. Wall IF2 was strengthened with three GFRP strips with a width of 10-in. (vertically oriented), and six #3 GFRP rods spaced at 10 inches (horizontally oriented). The strengthening scheme for Wall IF3 was similar to that of Wall IF2 with regard to the FRP sheets. Conversely, ten #3 GFRP rods having a length of 36-in., two per slot, were placed in 18-in. at each wall toe. This additional reinforcement was placed with the purpose of increasing the flexural capacity of the wall and force a shear failure to occur. It would have been desirable to strengthen both sides of the walls, but since these walls were part of the parapets at the uppermost story only one side was easily accessible. Details of the strengthening schemes are presented in Appendix B.1.

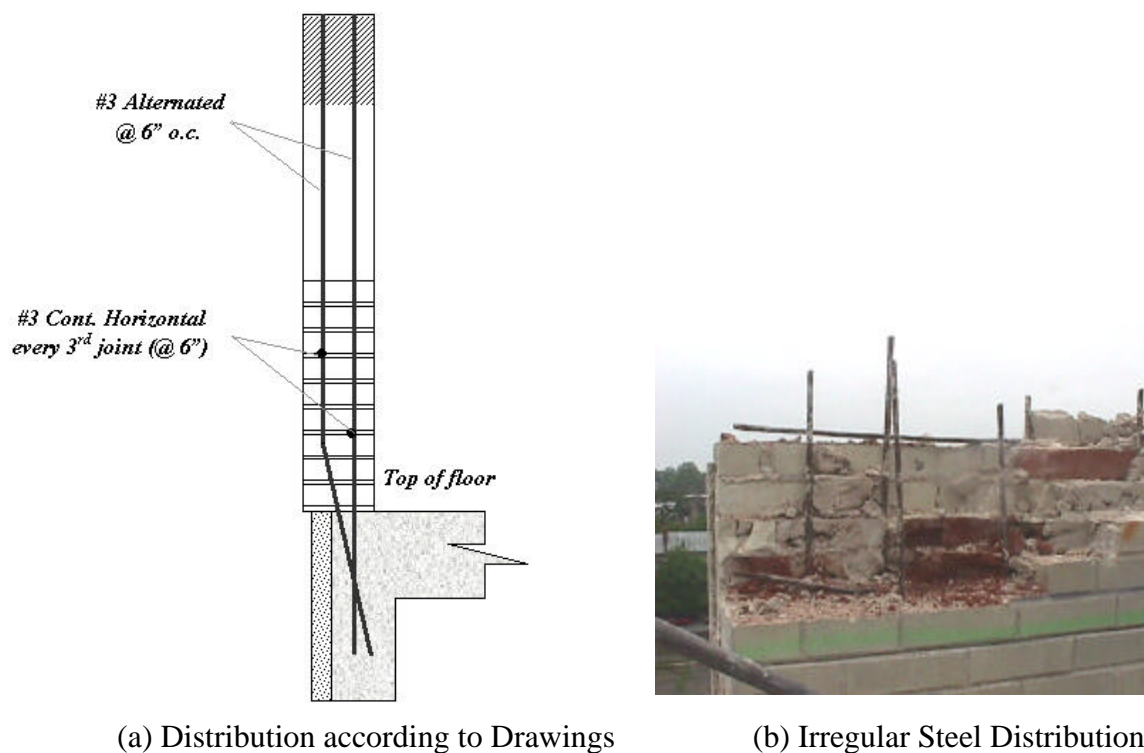


Figure 4.13. Steel Distribution – Series IF

4.3.2. Test Setup. The masonry walls were in-plane loaded as cantilever walls, with free rotation at the top and fixed rotation at the base. The loads were generated by the alternate use of two 200 kip hydraulic jacks, connected to a hydraulic pump. Thus, two walls could be tested in cycles at the same time. A positive cycle was defined when by using Jack 1 the wall had an inward displacement (see Figure 4.14a). The walls reacted against each other by means of two steel beams fabricated from C10x20 and two high strength rods. The in-plane forces were transmitted to the walls by 10x12-in. bearing plates, which had a steel rod to simulate a hinge connection. A negative cycle was defined when the load was applied by Jack 2, which generated an outward displacement as illustrated in Figure 4.14b. The loads were transmitted to the walls using similar plates. Once the weaker wall had failed, after two or three positive and negative cycles, the remaining wall was loaded to failure, using Jack 1, by reacting against a contiguous stiffer wall as illustrated in Figure 4.14c. The hydraulic jacks rested on a pile of concrete blocks and wood. Greased thin steel plates were placed underneath the jacks to reduce the frictional restraint and provide smooth action. A concentrated load was

applied to the top of the walls. The load was applied in cycles of loading and unloading. The walls were loaded in increments of 5 kips. The data was collected by a data acquisition system at a frequency of 1 Hz. Two LVDTs were used to monitor in-plane movement in each wall. The first one was placed at the top to record the top displacement. The second one was placed near to the floor to detect any sliding of the wall, if that was the case. An overall view of the in-plane test setup is shown in Figure 4.15.

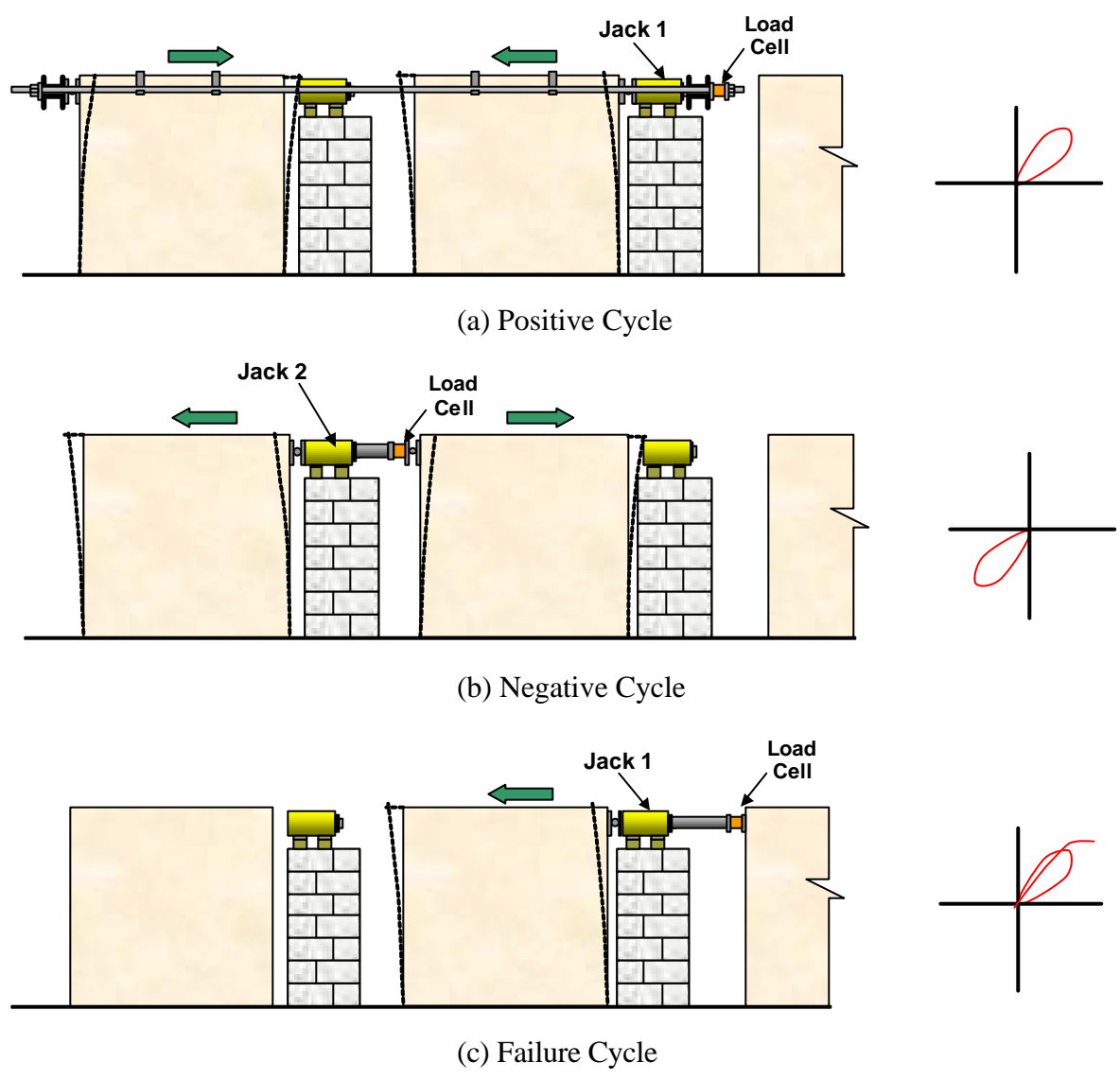


Figure 4.14. Test Setup -Series IF



Figure 4.15. In-Plane Test Setup

4.3.3. Test Results.

Wall IF1

This wall was used as control specimen to assess the flexural capacity from in-plane loading prior to being strengthened. A flexural crack was visible at the base of the wall for a load of 2 kips. A maximum force of 9.7 kips occurred for a displacement of about 0.03-in. The wall lost carrying capacity due to the crack growth caused by rocking. The crack length when the test was terminated covered approximately two-thirds of the base length (see Figure 4.16a). Base sliding was not observed at this final stage. The procedures followed to compute the expected flexural capacities are described later on this section. The capacity in Wall IF1 was significantly lower than expected. This fact can be attributed to a deficient anchorage of the existing vertical steel reinforcement, which was possibly pulled out from the wall. As it was mentioned, the steel reinforcement was placed in the space between the wythes, which was filled with the same mortar used to lay the masonry units.

Wall IF2

This wall was strengthened with GFRP sheets vertically oriented and GFRP rods horizontally oriented. Similarly to Wall IF1, a flexural crack was observed at the base of the wall for a load of 3.5 kips. Flexural failure was observed at about 12 kips for a displacement of 0.04-in. This slightly increment may be attributed to the bridging of

some secondary cracks near to the bottom by the FRP laminates. In the same way to Wall 1, the primary flexural crack causing the failure was observed at the bottom of the wall (see Figure 4.16b).

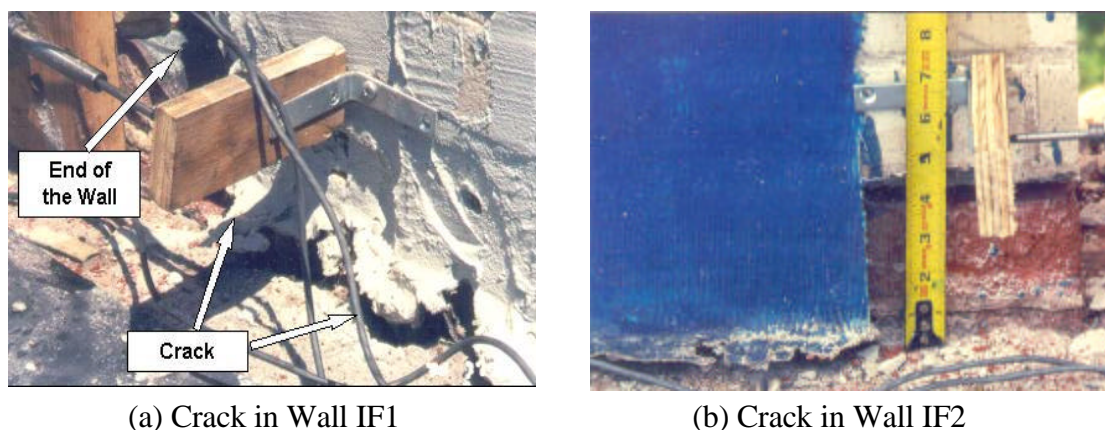


Figure 4.16. Flexural Cracks at the Bottom of Walls

Wall IF3

In order to increase the flexural capacity of the walls and induce a shear failure, anchor GFRP rods were installed in the toes of Wall IF3, as previously described. The strengthening scheme of Wall IF3 was similar to that of Wall IF2. A crack running along the base of the wall was visible at a load of 5 kips. A flexural failure was observed for a maximum load of 24 kips with a corresponding displacement of about 0.18-in. After reaching a displacement of about 0.3-in., significant load degradation was observed. The opening of the horizontal crack in the strengthened side was controlled by means of the GFRP rods. However, the eccentric tensile forces in the GFRP rods caused by the anchoring of only one face of the wall, made the wall tilt, which forced to stop the test. An envelope of the load vs. top displacement curves is illustrated in Figure 4.17. This envelope includes the cycle where the failure occurred, either positive or negative cycle. The curves showing the positive and negative cycles, as defined in the previous subsection, are shown in Appendix B.2. In Figure 4.17, by comparing Wall IF3 to the previous wall, without near-surface-mounted rods in the toes regions, the increment in capacity was over 100%. Since the steel reinforcement was pulled out, the concept of ductility defined as the ratio between the deflection at the ultimate state of failure and the

deflection at the yielding of steel can not be applied. However, in Wall IF3, due to the contribution of the GFRP rods in the toes, a notable increase in pseudo-ductility was attained.

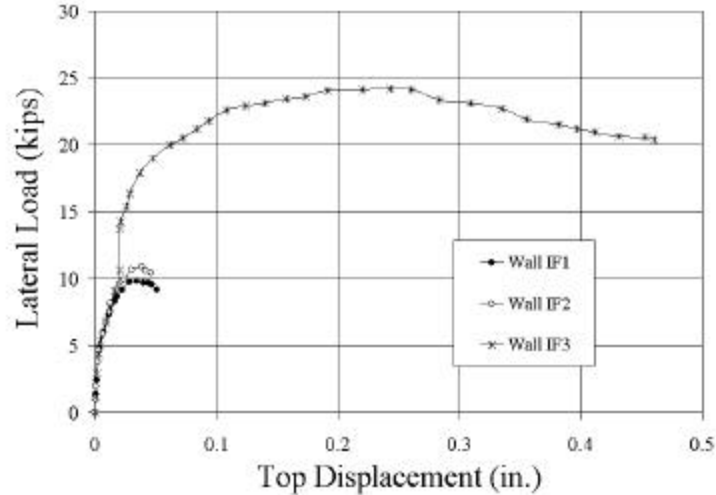


Figure 4.17. Lateral Load vs. Top Displacement – Series IF

4.3.4. Analytical Study. The nominal flexural capacity of the masonry walls was computed by adding the FRP contribution to the relationship proposed by Shing et al. (1990) for reinforced masonry walls:

$$M_n = 0.72f'_m c b \left(\frac{L}{2} - \frac{0.85c}{2} \right) - \sum_{i=1}^n A_{s_i} f_{s_i} \left(d_{s_i} - \frac{L}{2} \right) - \sum_{i=1}^n A_{f_i} f_{f_i} \left(d_{f_i} - \frac{L}{2} \right) \quad (4.3)$$

where considering a maximum strain of 0.0035 for clay masonry the following expressions can be derived.:

$$f_{s_i} = 0.0035 E_s \frac{d_{s_i} - c}{c} \leq f_{s_y} \quad (4.4a)$$

$$f_{f_i} = 0.0035 E_f \frac{d_{f_i} - c}{c} \leq f_{f_u} \quad (4.4b)$$

The computation of the moment capacity for walls with and without NSM rods in the toe regions is shown in Appendix B.3. The analytical shear forces for Wall IF1, IF2, and IF3 are illustrated in Table 4.3. The shear force V_1 was estimated considering the walls as cantilevers with a height of 5-ft., whereas, the shear force V_2 was computed according to the MSJC provisions.

Table 4.3. Experimental and Analytical Values – Series IF

Specimen	Analytical			Experimental
	M (ft-kips)	V ₁ (kips)	V ₂ (kips)	V (kips)
Wall IF1	134.2	26.8	70.0	9.7
Wall IF2	134.2	26.8	70.0	12.0
Wall IF3	479.1	95.8	70.0	24.0

In Wall IF3 the objective was to achieve a shear failure to observe the contribution of the FRP reinforcement. The MSJC provisions specify an allowable stress in-plane shear stress, f_{vall} equal to $1.5\sqrt{f'_m}$. The masonry compressive strength was estimated as 1400 psi; therefore the allowable stress is:

$$f_{vall} = 1.5\sqrt{1400 \text{ psi}} = 56 \text{ psi}$$

The MSJC provisions take the nominal strength of masonry, f_{vn} , as $2^{1/2}$ times the allowable stress value. Thus:

$$f_{vn} = 2.5(56 \text{ psi}) = 140 \text{ psi}$$

The acting shear stress can be estimated from equation 4.5:

$$f_v = \frac{VQ}{It} = \frac{1.5V}{A} \quad (4.5)$$

where V is the acting shear force, Q is the first moment of area, I is the moment of inertia and t is the wall thickness.

Thus, solving equation 4.5 for V: $(140 \text{ psi}) = \frac{1.5V}{(12.5 \text{ in.})(60 \text{ in.})} \therefore V = 70 \text{ kips}$

From these results, shear cracks would be expected to form; however due to tilting of the wall caused by eccentricities of the FRP reinforcement in the toe regions this was not observed.

5. WALLS SUBJECTED TO OUT-OF-PLANE LOADING

The masonry walls tested at the Malcolm Bliss Hospital correspond to Series OF. These field tests allowed observing the out-of-plane behavior of URM walls under real boundary conditions. Using the results of previous laboratory investigations a provisional design approach was developed. The influence of the boundary conditions are introduced in this approach.

5.1. PROBLEM STATEMENT

URM walls depend on the tensile strength of masonry to resist out-of-plane loads caused by high wind pressures or earthquakes. URM walls can collapse due to this limitation. In addition, relatively stiff frames may restrain the movement of the wall when subjected to out-of-plane loading. As a consequence, in-plane compressive forces are built, which produce a load resisting mechanism referred as to arching action that improve the initial flexural behavior of the wall. At the ultimate state, due to the compressive stresses generated by this mechanism at the upper and lower zones of the wall, the masonry units along the edges are fractured. Thereby, the influence of arching mechanisms in the behavior of retrofitted walls needs to be taken into account to fully realize the effectiveness of strengthening strategies.

5.2. SERIES OF

5.2.1. Test Specimens. Ten full-scale URM walls, constructed of clay units, were tested. The nominal dimensions of these walls were 8 by 8-ft.; their overall thickness, including the two wythes and plaster was 13-in. The upper and lower boundaries for these walls were RC beams which were cast integrally with the floor system. The studied walls, classified as infill, belong to a masonry typology commonly used during a time frame from late 1940's through the early 1960's. A section view of a typical wall is shown in Figure 5.1. The walls under investigation consisted of two wythes of masonry units spaced at 0.75-in., joined only by header units placed at each fourth course, and at each fourth unit within that course. The outer wythe, corresponding

to the veneer wall, was built using cored units with width of 4-in., height of 2.25-in., and length of 8-in., the units had three cores of 1.5 in diameter. The inner wythe or backup wall was constructed using two kinds of clay units. Tiles and bricks were laid in alternated courses (see Figure 5.1). The actual dimensions of the tile units were 7.5-in. wide by 7.5-in. high by 12-in. long. The brick units were solid, their dimensions were 4.25-in. wide, 2.25-in. high and 8.5-in. long. The walls were finished with one-inch thick cementitious plaster, reinforced with a two-directional welded steel mesh at mid-depth.

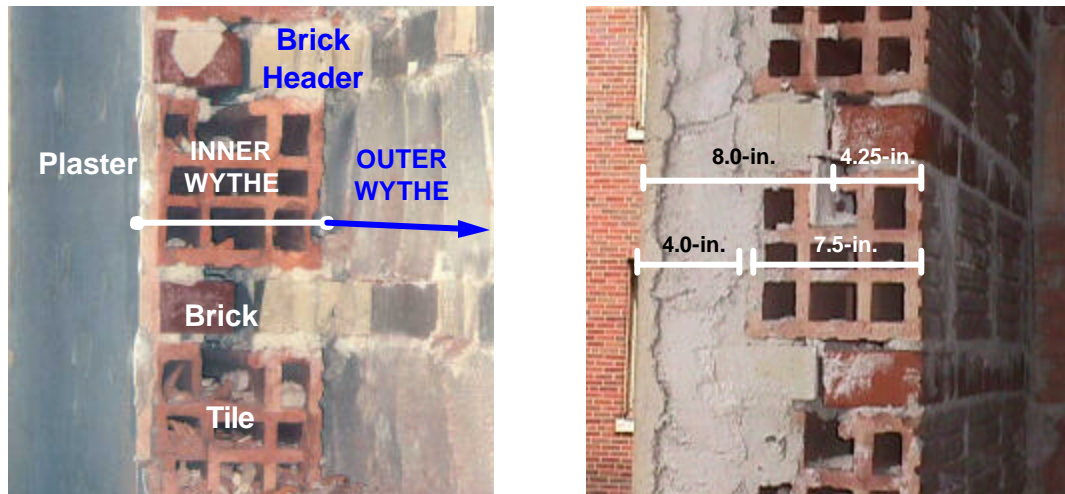


Figure 5.1. Vertical Cross Section of Typical Wall

One inherent difficulty when conducting a testing program in-situ is to characterize the materials. In order to attain this task, samples obtained from similar walls in the building were collected. These samples included bricks, tiles, and mortar. Due to their brittle characteristic, it was not possible to recover masonry assemblage from the interior wall. However, in the case of the veneer wall some assemblages consisting of two courses of bricks were attained for laboratory analysis. The compressive strength of these assemblages was 1403 psi with a standard deviation of 15.2. The compressive strength of the mortar was 814 psi with a standard deviation of 7.6. It is important to mention that the latter value was not obtained from standard tests, but from cylinder shaped mortar entrapped in the cores of the brick veneer. Using the average compressive strength, the mortar can be classified as Type N according to the ASTM C270.

A summary of the experimental program is shown in Table 5.2; the typical strengthening schemes are shown in Appendix C.1. Two URM walls, Wall OF1 and Wall OF2, were selected as control specimens. In Wall OF1 the plaster remained on its surface; whereas, in Wall OF2 the plaster was removed. The remaining specimens were strengthened with different composite materials, namely GFRP, AFRP, CFRP and deformed GFRP rods. Thus, Wall OF3 was strengthened with three 20-in. wide GFRP strips attached to the plaster surface. The strengthening scheme for Wall OF4 was similar to that of Wall OF3, except that the GFRP strips were applied directly to the masonry, meaning without the presence of plaster. The purpose of testing this group of walls was to observe the difference in behavior, if any, in walls strengthened with FRP attached to plaster and to masonry under out-of-plane loading. One of the advantages of using composite materials is that little disruption is caused during its installation. That was the purpose of studying the behavior of walls strengthened without the removal of plaster. Thus, in the remaining walls the strengthening was carried out with the presence of plaster.

Wall OF5 was strengthened with three 10-in. wide GFRP strips, with the purpose of comparing it to Wall OF3, which had twice the amount of reinforcement. In Wall OF6 and Wall OF7 the strengthening geometry was similar to Wall OF3. In the first case the URM wall was strengthened with AFRP; whereas, in the latter case CFRP was used as strengthening material. Wall OF8 was strengthened using two different composite systems: GFRP laminates and near-surface-mounted GFRP rods. Four #3 pieces with a length of 26-in., two in each end, were placed under each strip of GFRP. With the purpose of providing continuity to the GFRP laminates, the rods were anchored to the RC beams, with a development length of 8-in.

The fact that the anchorage of near-surface-mounted rods into adjacent RC members (i.e. slabs, columns and beams) is a relatively simple, it makes their use attractive for increasing the flexural strength of masonry walls. Thereby, Wall OF9 and Wall OF10 were strengthened with eight #3 GFRP rods spaced at 12-in. In the first case the rods were not anchored to the adjacent beams; whereas, in the latter case the rods were anchored 6-in. into the upper and lower beams.

Table 5.1. Test Matrix for Series OF

Specimen	Strengthening System	Reinforcing Scheme	Plaster
Wall OF1	Control	None	Yes
Wall OF2	Control	None	No
Wall OF3	GFRP Laminates	Three strips (width=20 in)	Yes
Wall OF4	GFRP Laminates	Three strips (width=20 in)	No
Wall OF5	GFRP Laminates	Three strips (width=10 in)	Yes
Wall OF6	CFRP Laminates	Three strips (width=20 in)	Yes
Wall OF7	AFRP Laminates	Three strips (width=20 in)	Yes
Wall OF8	GFRP Rods and GFRP Laminates	Three strips (width=20 in), anchored with rods	Yes
Wall OF9	GFRP Rods	Eight #3 near-surface mounted rods	Yes
Wall OF10	GFRP Rods	Eight #3 anchored near-surface mounted rods	Yes

5.2.2. Test Setup. The masonry walls were tested under two out-of-plane loads, which were distributed by 12 x 12 x ½-in. steel plates to the external face of the wall (see Figure 5.2). The loads were generated by means of a 200 kip hydraulic jack activated by a manual pump. The force created by this jack reacted against a five foot steel girder made of two C10x20, hereafter called Beam A, and an 11 foot steel girder made of two C15x40, hereafter referred as Beam B. When loading, two reacting forces were created on Beam A. These forces were transmitted to the masonry wall using two high strength

rods, which through of steel plates pulled the wall from its exterior face. On the reaction side, the force generated by the hydraulic jack reacted against Beam B, which transmitted the load to the upper and lower RC beams, and floor system. A scheme of the test setup is shown in Figure 5.3.



Figure 5.2. Plates on the external face of the wall

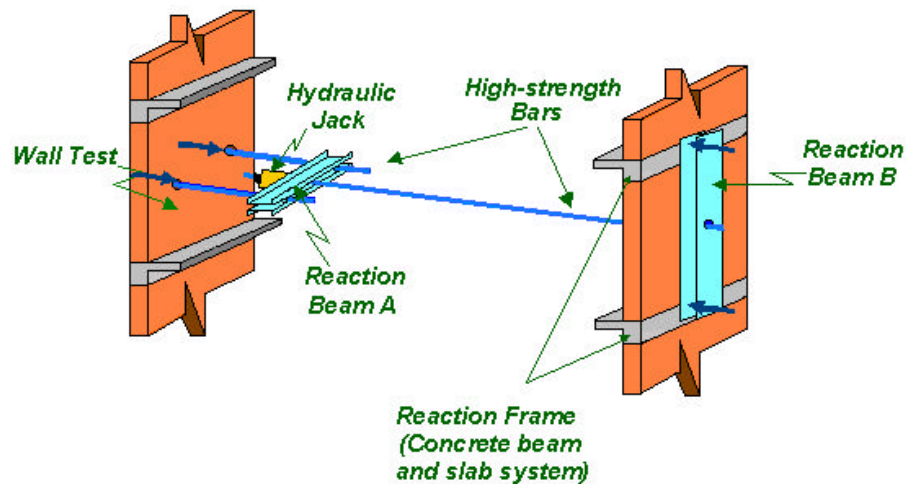


Figure 5.3. Test Setup-Series OF

Beam A was supported by a wooden panel resting on concrete blocks. Thin plates, which were greased, were placed between Beam A and the panel to reduce the friction restraint and provide smooth action (see Figure 5.4a). Beam B was erected into place using an electric hoist located at the roof level (see Figure 5.4b). The hoist was

restrained by a steel frame located on the roof of the building (see Figure 5.5). In this manner Beam B could be raised or lowered, depending on what wall was being tested.

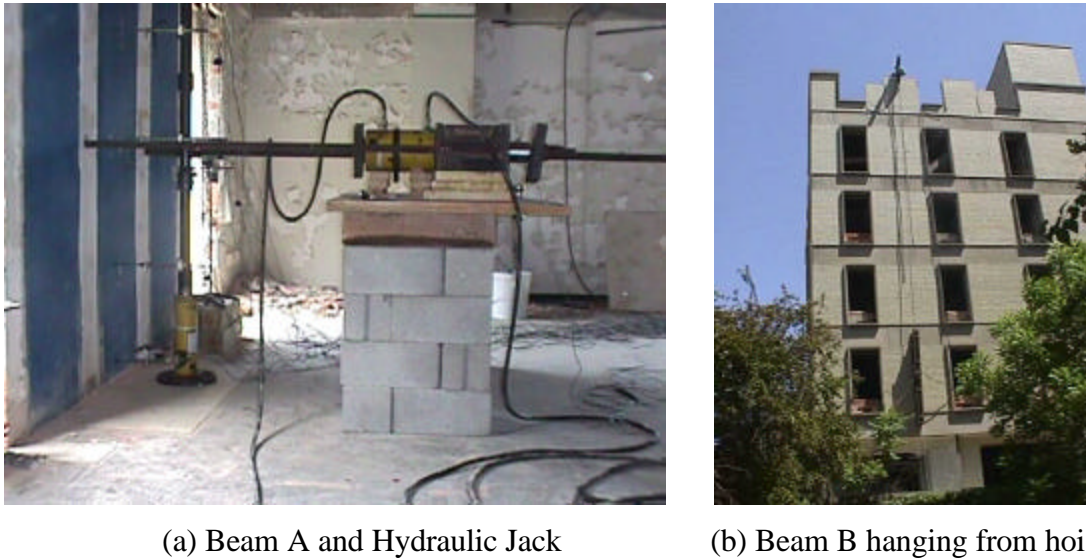


Figure 5.4. View of Test Setup for Series OF



Figure 5.5. Hoist and Metallic Frame

The test setup was designed to load the URM walls with two concentrated loads, and measure deflections, strains and rotations due to these loads. The top and bottom beams provided some fixity to the walls. The test conditions were those of walls away from corners, since both vertical edges were free. The load was applied in cycles of

loading and unloading. Each URM wall was loaded to 10 kips and then unloaded prior to continuing with the test. This procedure allowed checking the instrumentation and reacting systems. The walls were loaded in increments of 10 kips, and unloaded to a low threshold of 5 kips. The data obtained from a 200 kip load cell, Linear Variable Transducer (LVDTs), strain gages, and inclinometers were collected by a data acquisition system at a frequency of 1 Hz (see Figure 5.6). For the tests carried out in this experimental program eight LVDTs were used. LVDTs 1 to 5 intended to record out-of-plane deflections along the wall height. LVDTs 1 and 5 measured the wall movement at the boundaries. LVDT 3 recorded midheight deflection, LVDT 6 monitored any movement in the upper RC beam, and LVDTs 7 and 8 intended to register the deflections along the wall length with the purpose of observing two-way action. Five channels to record strains were employed, the strain gages were placed on the FRP laminates or rods. Three inclinometers were used to record rotations in the upper and lower borders, as well as in one of the free edges.

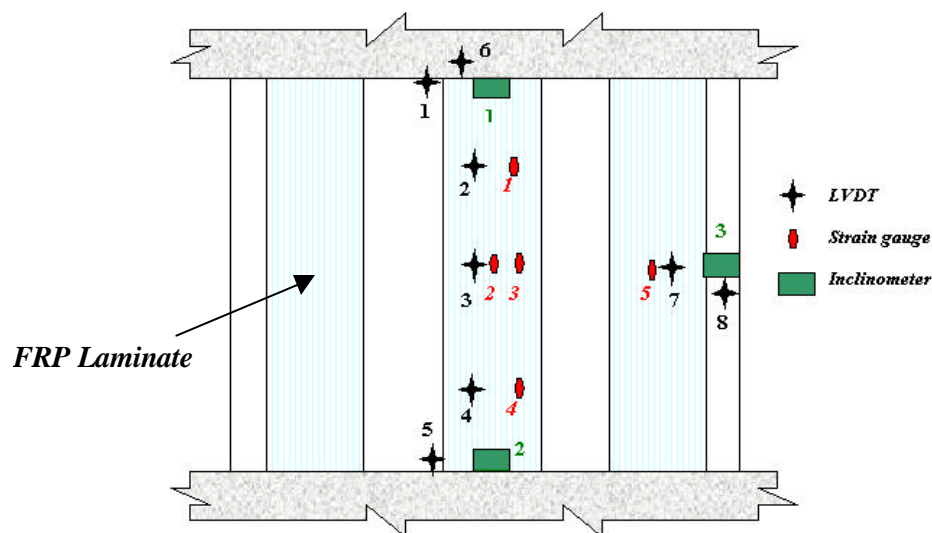


Figure 5.6. Test Instrumentation –Series OF

5.2.3. Test Results.

Wall OF1

This wall was tested as a control specimen to determine the load-carrying capacity with the inclusion of the cementitious plaster. At 12 kips a first major horizontal crack was visible at mid-height, along the full bed joint (see Figure 5.7). At an applied load of

26 kips a second horizontal crack is formed, measured at a quarter height from the top of the wall. The peak load was reached at 30 kips for a mid-height deflection of 0.16 in as can be observed in Figure 5.8. The final failure is produced by a shear-compression combination effect, which ended with the fracture of the tiles placed at the bottom region of the wall. At the final stage part of the plaster, located at the bottom region of the wall is delaminated. In this specimen as well as in the remaining ones, no damage was observed on the exterior face of the veneer wall. From the recorded displacements in this and the remaining walls an insignificant two-way action was observed (see Appendix C.2). The cracking patterns did not show evidence of important two-way action. Since the two vertical edges were free, this action can be attributed to the test setup (i.e. two concentrated loads).



Figure 5.7. Horizontal crack in Wall OF1

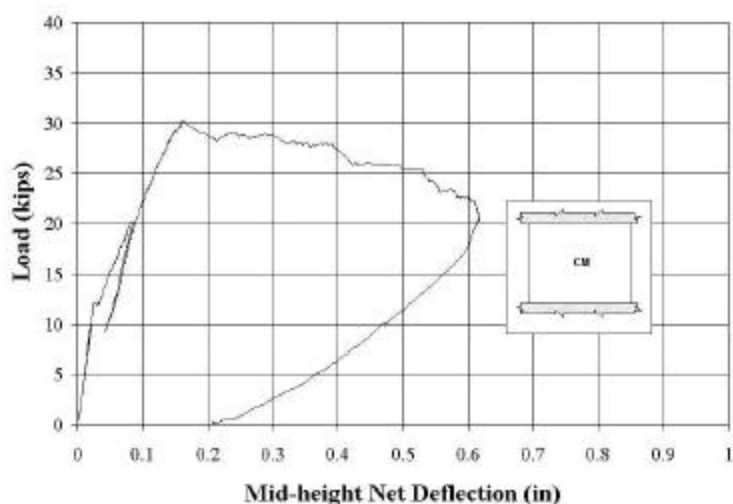


Figure 5.8. Load vs. Mid-height Net Deflection Curve – Wall OF1

Wall OF2

This wall was also tested as control specimen; however, in this case the cementitious plaster was removed from its surface. The first visible crack was observed at a load of 10 kips, running above the central brick course, along the bed joint. The peak load was reached at 24 kips for a mid-height deflection of 0.16-in., the failure, similar to that observed in Wall OF1, was caused by a shear-compression combination effect at the upper region of the wall. Once its peak was reached the load decreased to 20 kips and only the deflection increased. In comparison to Wall OF1, this wall was less stiff, and it had pseudo elasto-plastic behavior up to failure (see Figure 5.9).

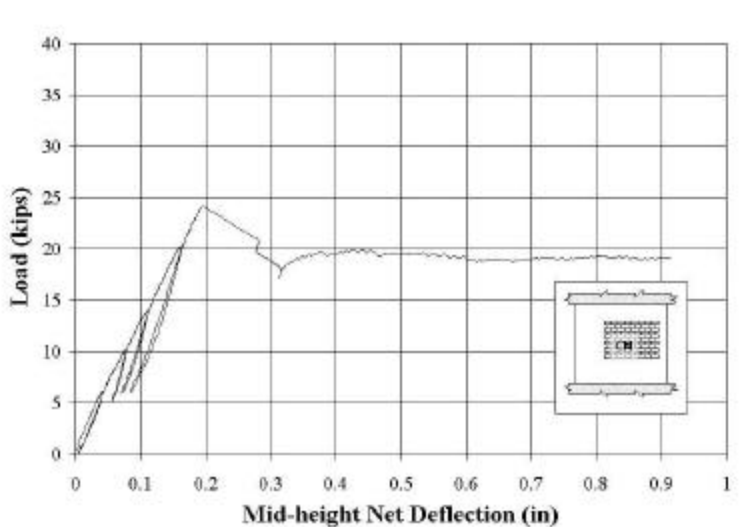


Figure 5.9. Load vs. Mid-height Net Deflection Curve – Wall OF2

Wall OF3

This wall was strengthened with three strips 20-in. wide of GFRP laminates. The first visible crack was observed at a load of 20 kips; at this stage the stiffness is slightly reduced. Two horizontal cracks are observed above the mid-height course. As shown in Figure 5.10, the wall failed at a load of 29 kips with a mid-height deflection of 0.1-in. at that stage. Delamination of the plaster at the lower area of the wall could be observed due to the loss of bonding between the plaster and the adjacent bricks and tiles, which were fractured by a shear-compression combination effect. In comparison with Wall OF1, the presence of glass fibers delayed the first cracking, reduced the crack width but did not increase the ultimate capacity.

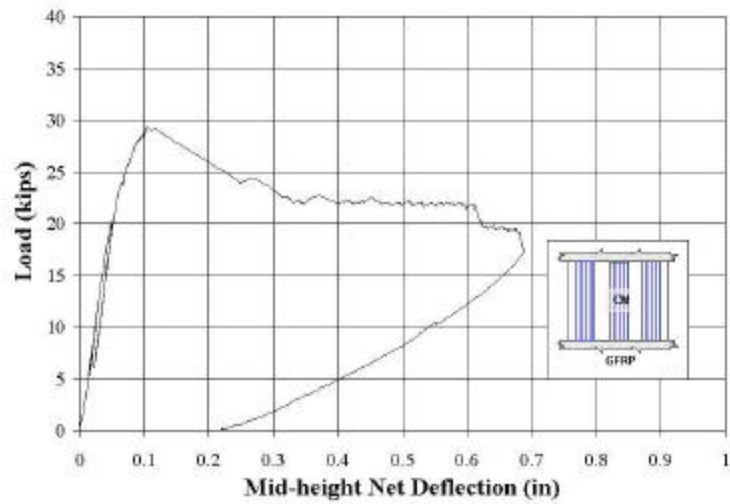


Figure 5.10. Load vs. Mid-height Net Deflection Curve – Wall OF3

Wall OF4

This wall had a similar strengthening scheme to Wall OF3. The significant difference was that the GFRP laminates were applied directly on the masonry. It was observed that the FRP reinforcement performed in a better fashion than in the previous wall. The failure was caused by fracture of the masonry units located at the top of the wall (see Figure 5.11). For this case, the load drop was less pronounced and more gradual after reaching the peak. The maximum load recorded was 34 kips with a corresponding mid-height deflection of 0.2 in (see Figure 5.12)



Figure 5.11. Fracture of Tile Unit

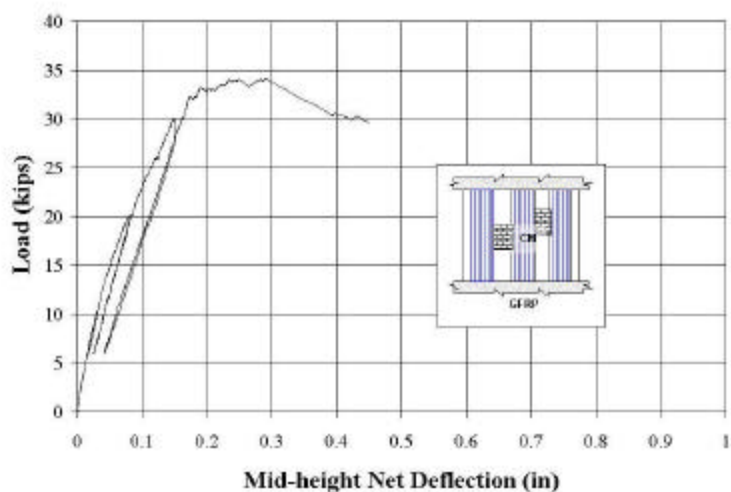


Figure 5.12. Load vs. Mid-height Net Deflection Curve – Wall OF4

Wall OF5

This wall was strengthened with half of the reinforcement used in Walls OF3 and OF4, meaning three strips 10-in. wide of GFRP fibers were attached to the wall surface. A horizontal crack above the mid-height course was observed at a load of 13 kips. Similarly to the previous walls, the failure was caused by a shear-compression combination effect at the lower region of the wall. The failure occurred at a load of 33 kips for a corresponding mid-height deflection of 0.12 in (see Figure 5.13). By comparing this wall to Wall OF3, a larger presence of cracks spread for almost 50% of the area was observed (see Figure 5.14).

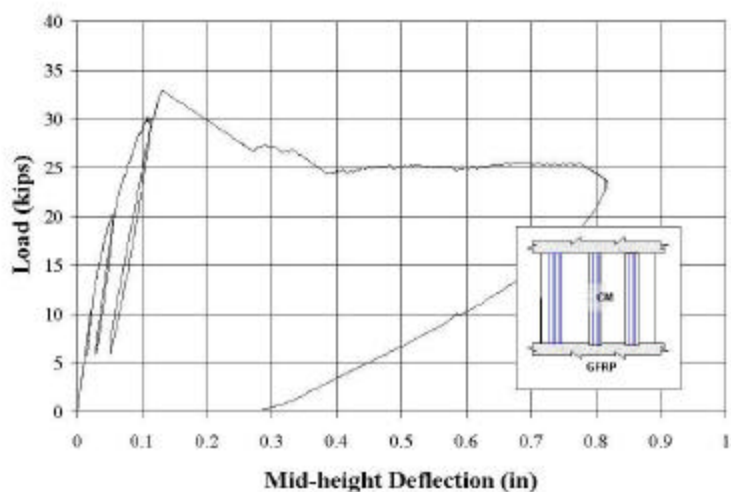


Figure 5.13. Load vs. Mid-height Net Deflection Curve – Wall OF5

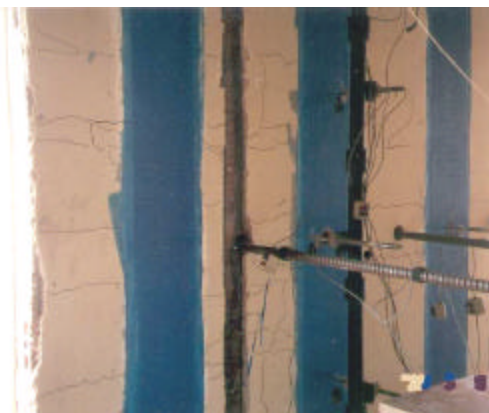


Figure 5.14. Cracking in Wall OF5

Wall OF6

This wall was strengthened with three strips 20-in. wide of CFRP laminates. A major horizontal crack was observed at a load of 24 kips, running along the bed joint located above the mid-height course. The maximum registered load was 30 kips, for 0.06 in mid-height deflection, as observed in Figure 5.15. The failure was caused by a shear-compression combination effect, which fractured some tile units located at the bottom of the wall. As a consequence, with the deflection increasing the plaster layer delaminated from the adjacent tiles as can be observed in Figure 5.16. This wall showed an atypical behavior compared to the other walls. As can be observed in the corresponding Height vs. Displacement curve in Appendix C.2-21, the upper region of the wall displaced in opposite direction to the applied load.

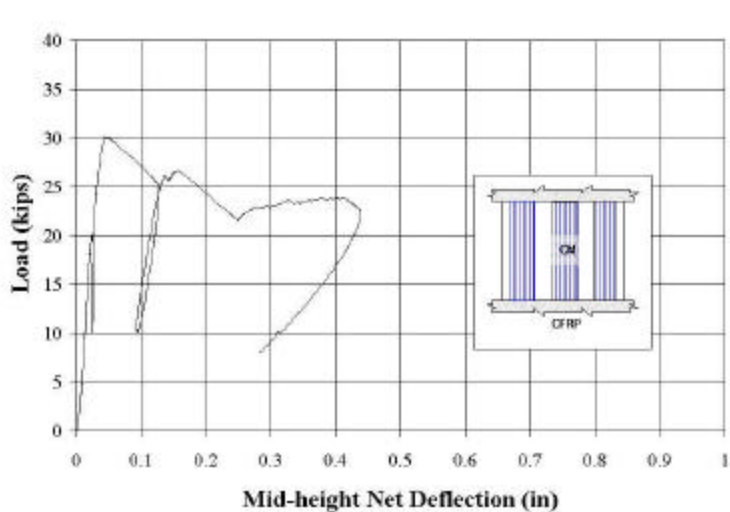


Figure 5.15. Load vs. Mid-height Net Deflection Curve – Wall OF6



Figure 5.16. Fracture of units at the bottom of Wall OF6

Wall OF7

The strengthening geometry of this wall was similar to the previous wall, only that in this case AFRP laminates were used. This wall did not show large areas of cracking, only a major horizontal crack running along the mid-height was detected at a load of 24 kips. The peak load was 36 kips with a corresponding mid-height deflection of 0.12-in. (see Figure 5.17). Delamination of the plaster on the top region of the wall was observed as a consequence of the fracture of the tiles, as shown in Figure 5.18.

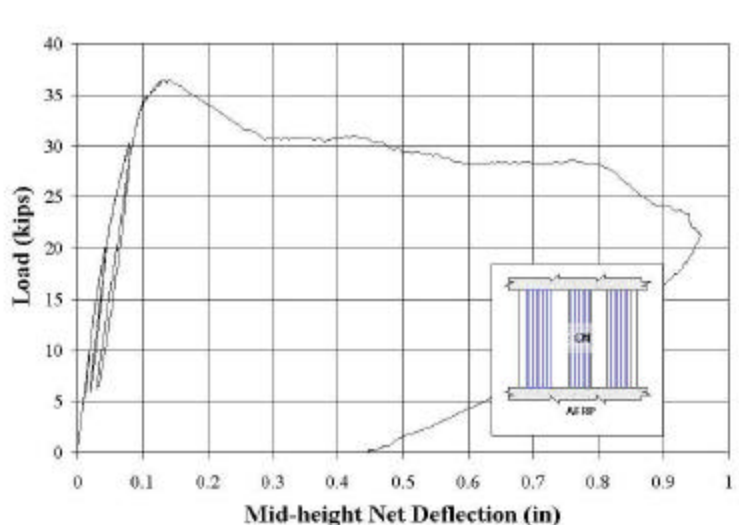


Figure 5.17. Load vs. Mid-height Net Deflection Curve – Wall OF7



Figure 5.18. Plaster Delamination

Wall OF8

The strengthening geometry of Walls OF3 and OF8 were similar. The only difference was the employment of GFRP rods in Wall OF8 in order to give continuity to the GFRP laminates into the RC beams. Since the controlling factor was the fracture of the tiles located at the bottom region of the wall, the results were identical to those found in Wall OF3. The peak load was 29 kips with 0.1 in mid-height deflection, as observed in Figure 5.19.

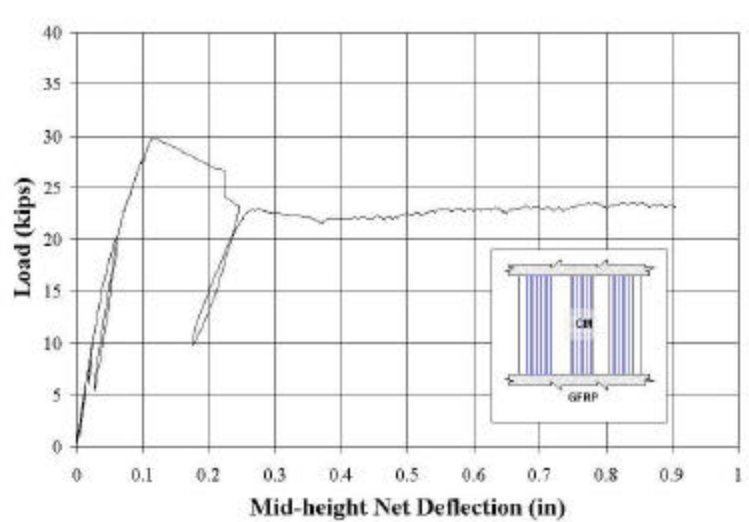


Figure 5.19. Load vs. Mid-height Net Deflection Curve – Wall OF8

Wall OF9

This wall was strengthened with eight #3 GFRP rods. The first visible crack was observed at 22 kips running along the upper joint of the mid-height course (see Figure 5.20). The wall failed at 24 kips for a mid-height displacement of 0.06 in (see Figure 5.21). The lower capacity may be attributed to factors such as pre-existing cracking formed during the installation of the rods or poor workmanship during the construction of the walls. The failure was caused by fracture of tiles at the lower part of the wall.



Figure 5.20. Horizontal crack in Wall OF9

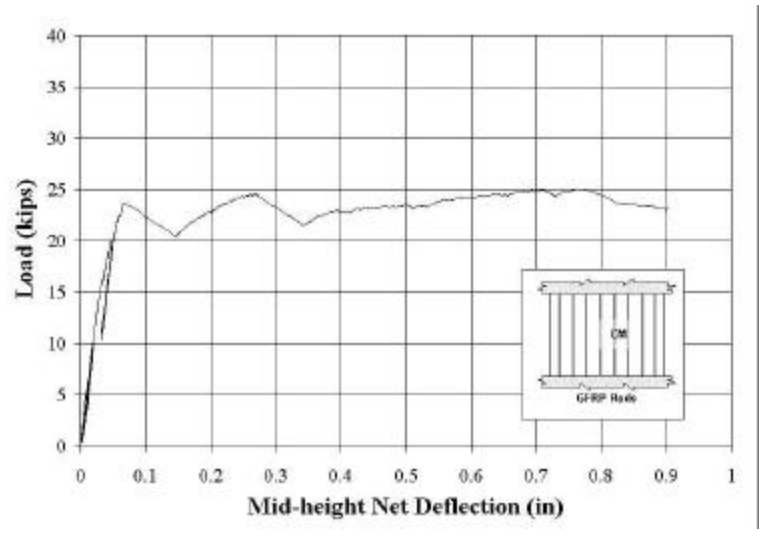


Figure 5.21. Load vs. Mid-height Net Deflection Curve – Wall OF9

Wall OF10

This specimen was also strengthened with eight #3 GFRP rods. As previously mentioned, the NSM rods were anchored to the upper and lower beams. The first visible crack, at mid-height course, was observed at 20 kips for a corresponding displacement of 0.09-in. As observed in Figure 5.22, the wall failed at 26 kips, in similar way to the previous one.

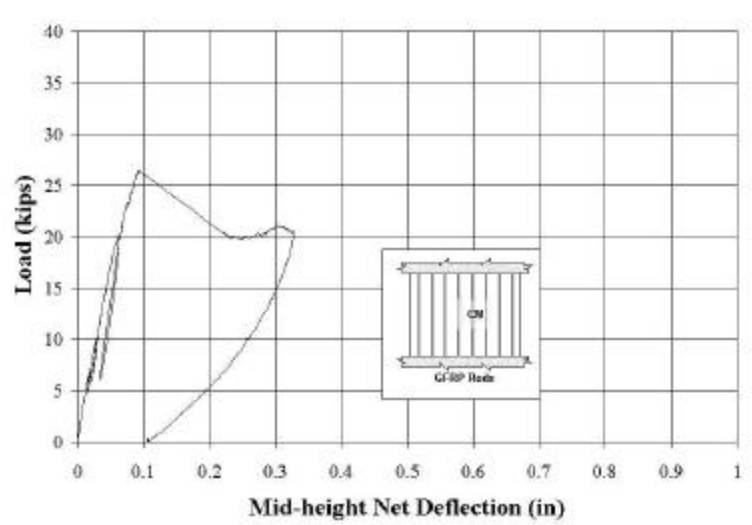


Figure 5.22. Load vs. Mid-height Net Deflection Curve – Wall OF10

By observing Figure 5.23, control Wall OF1, with plaster, showed a capacity 25% larger than that found in control Wall OF2, without plaster. After reaching 12 kips, point where the first horizontal cracks occurred in Wall OF1, a substantial difference in the stiffness K ($K \propto EI$) is observed. This difference is attributed to an increment in the overall moment of inertia of the wall due to the extra inch of the plaster thickness, and due to the different modulus of elasticity in the masonry and cementitious plaster. From the same figure it is observed that FRP laminates do not perform adequately when they are attached to the plaster surface, as can be concluded from the corresponding tests performed on Wall OF1 and Wall OF3, where no increment in capacity was registered. In contrast, when the FRP was attached directly on the masonry by removing the plaster, an increment of 40% in capacity was observed by comparing Wall OF4 to the Control Wall OF2.

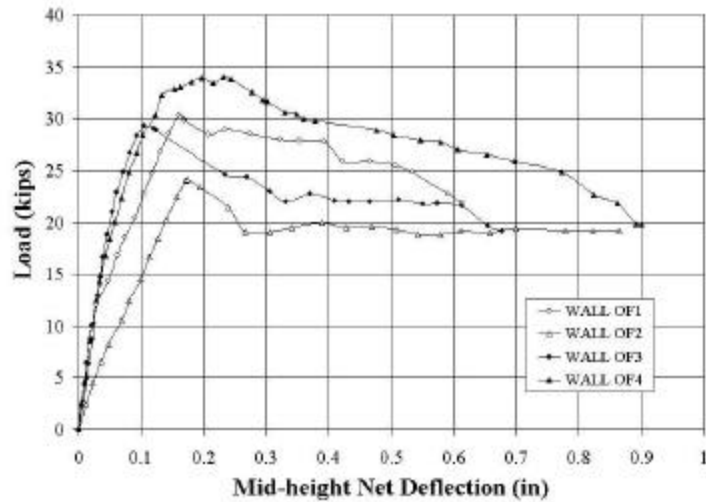


Figure 5.23. Behavior Comparison of Walls OF1, OF2, OF3 and OF4

The aforementioned increment in capacity is attributed to a better engagement of the FRP laminates to the surface when the out-of-plane bending increases. This can be corroborated from Figure 5.24, where up to a load of 20 kips the strains developed in the FRP laminates attached to Wall OF4 doubled those of Wall OF3. In the walls strengthened with the presence of plaster, the recorded strains were in the range of 0.4% to 0.6% for laminates, and in the range of 0.3% to 0.5% for the rods. The strains were not associated to increases in carrying capacity; only increases in the stiffness of the walls were observed.

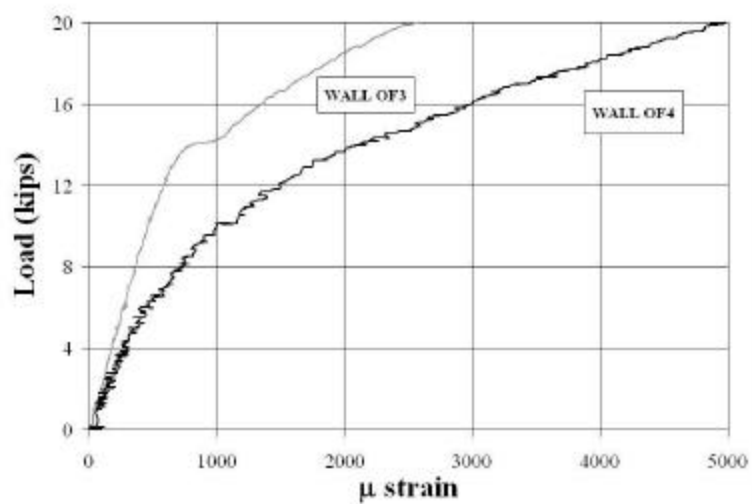


Figure 5.24. Strain Comparison for Walls OF3 and OF4

Figure 5.25 compares the behavior of walls strengthened with GFRP laminates without the removal of plaster. It is observed that Wall OF3 and Wall OF8 had the same behavior. The rods placed in Wall OF8 did not have influence since the failure was controlled by a shear-compression effect, which fractured the tiles in the boundary regions of the wall. Also, it can be observed that Wall OF5, with half amount of reinforcement respect to the other walls, showed a slightly higher capacity.

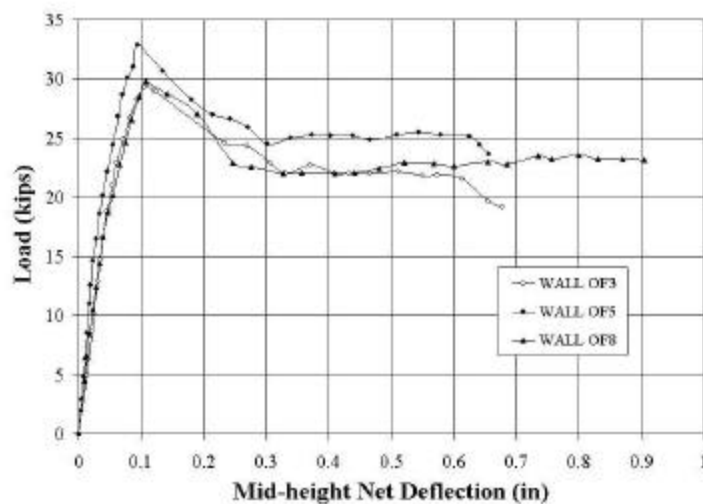


Figure 5.25. Behavior Comparison of Walls OF3, OF5 and OF8

In Figure 5.26 the behavior of walls strengthened with FRP rods are compared, Wall OF9 and Wall OF10 showed lower capacities than the Control Wall OF1, which may be attributed to a weakening of the masonry units during the installation of the rods. FRP rods were mounted into slots grooved on the masonry surface using a grinder and chisel. This procedure may have pre-cracked the wall. The use of near-surface-mounted rods is attractive since the removal of plaster is not required; however, their installation should be limited to strengthening of walls built of solid brick units or grouted concrete walls.

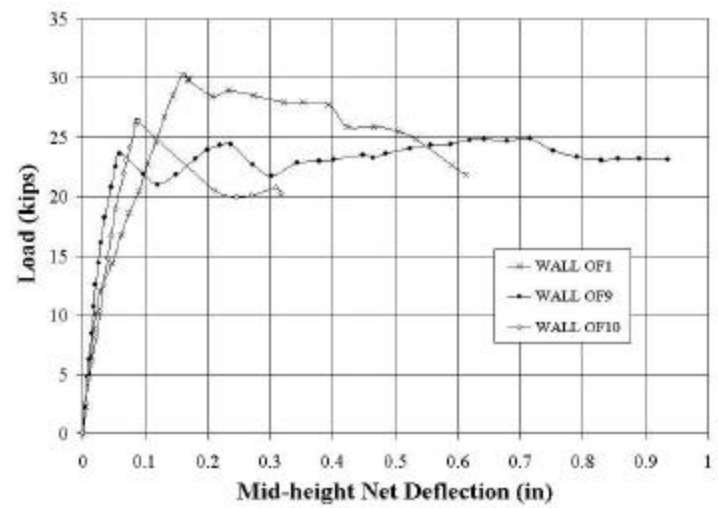


Figure 5.26. Behavior Comparison of Walls OF9 and OF10

Figure 5.27 illustrates the load vs. deflection curves of walls strengthened with different types of fiber. It is observed the increment of stiffness, from smaller to larger, when GFRP, AFRP and CFRP laminates were used. The higher capacity of Wall OF7 compared to the other walls is not statistically significant since its value is within the variability of the capacity values and because the fracture of tiles is controlling its behavior. During the tests, it was observed that the employment of FRP laminates delayed the presence of the first visible cracks, and also, that the crack widths were reduced.

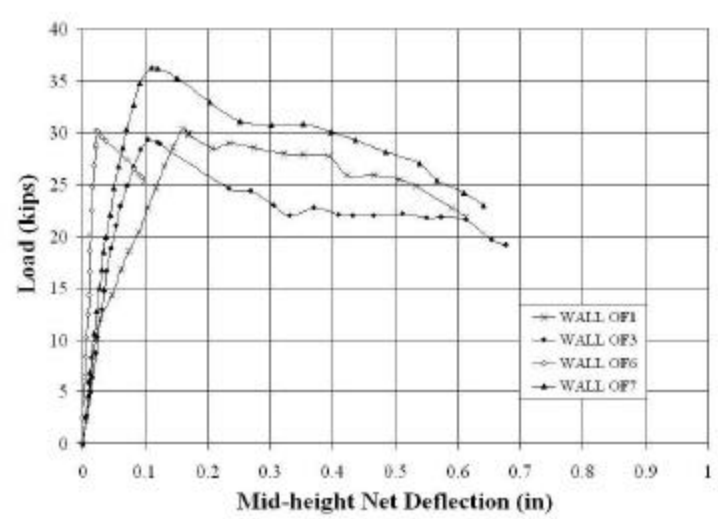


Figure 5.27. Behavior Comparison of Walls OF1, OF3, OF6 and OF7

The walls suffered more rotations in the zone where the main fracture occurred. The values recorded by the inclinometers were small, averaging 0.25° , they produced angular distortion, which is critical in a masonry unit composed of thin walls such as the case of the clay tiles. These values showed good correlation with the slope values of the walls at the supports, which averaged 0.16° , and were obtained from the Height vs. Deflection curves shown in Appendix C.2. The angular distortion along with a shear-compression combination effect caused the fracture of the units located either at the top or bottom of the wall. Larger rotations were accompanied, most of the times, by larger displacements at that zone due to either starting of plaster delamination or spalling of the tile shell, which were caused by the fracture of the tiles (see Height vs. Deflection and Out-of-Plane Load vs. Rotation curves in Appendix C.2). As example the Load vs. Rotation curve corresponding to Wall OF7 is presented in Figure 5.28, in this case fracture of tiles was observed at the top of the wall.

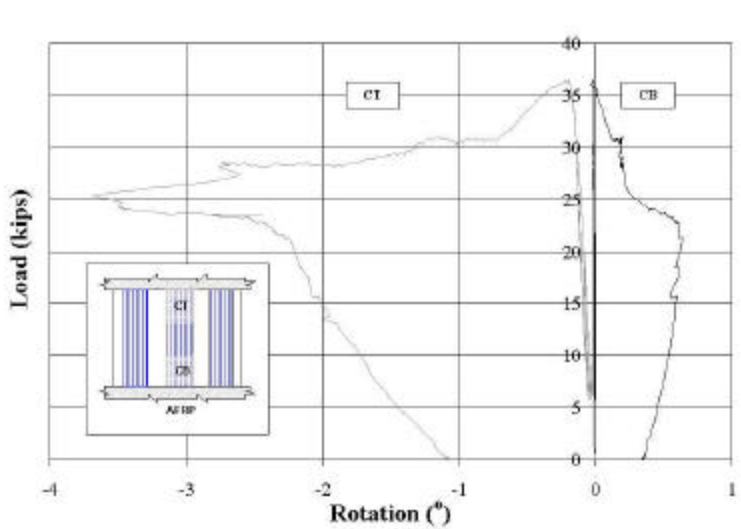


Figure 5.28. Rotations in Wall OF7

5.2.4. Mechanism of Failure. The failure of the URM walls was caused by the fracture of the tile units placed on the uppermost or bottommost courses due to arching action. The fracture of these tiles is caused by angular distortion due to out-of-plane rotation, and mainly by a force generated by a shear-compression combination effect. Flexural cracking occurs at the supports due to negative moments followed by cracking at

mid-height due to positive moments, as a result a three-hinged arch is formed. When the deflection increases due to out-of-plane bending the wall is restrained against the supports, in this case the upper and lower beams. This action induces an in-plane compressive force (F_V in Figure 5.29), which accompanied by the shear force (F_H in Figure 5.29) in the support create a resultant force that causes the fracture of the tile (F_R in Figure 5.29). It is important to mention that normally the crushing is associated to the mortar joint; however, due to the brittle characteristics of the tile, the failure here was associated with the tiles. Once the fracture of the tiles was initiated, the adjacent plaster layer began to delaminate from the masonry surface. At this stage, since the FRP adhered to the plaster surface was not able of engaging the flexural cracks, the wall capacity degraded. In contrast where the externally bonded FRP strips were attached directly to the masonry, the failure was delayed because the FRP were able to engage the flexural cracks running through the bed joints. Consequently, the wall capacity was improved but the mechanism of failure did not change. It has been reported that for slenderness ratios (h/t) larger than 30, the effect of arching action is small (Angel et al., 1994).

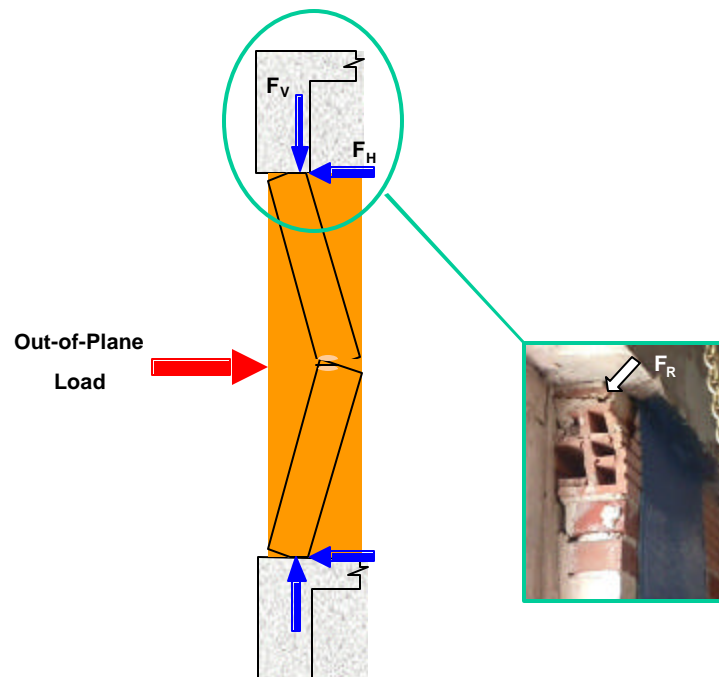


Figure 5.29. Out-of-Plane Mechanism of Failure

5.2.5. Analytical Study. A model is presented for determining the transverse load that both unreinforced and externally strengthened infill walls can resist. The infill wall is idealized as a strip of variable width, which is subjected to a concentrated load applied normal to the plane of the wall. This model can be used for distributed loads, after modifying the load distribution shown in the initial equilibrium.

As described in the previous section, the failure of the URM walls was caused by the fracture of the tile units placed on the uppermost or bottommost courses. Clamping forces in the supports, originated by arching action, led to increasing the out-of-plane resistance of URM walls. Previous researchers (Fricke, 1992, Angel 1994) have found this resistance to be many times greater than the predicted by conventional theories that do not consider post-cracking mechanisms. Also, it was described that when externally bonded FRP laminates were attached to the masonry surface, the out-of-plane capacity of the wall was improved because the FRP was able to engage the flexural cracks running through the bed joints. However, the controlling mechanism of failure was the same as the URM wall.

5.2.5.1. Analytical Derivations for URM Wall. Once the wall has been cracked at mid-height, it can be assumed that the two resulting segments can rotate as rigid bodies about the supports as illustrated in Figure 5.30.

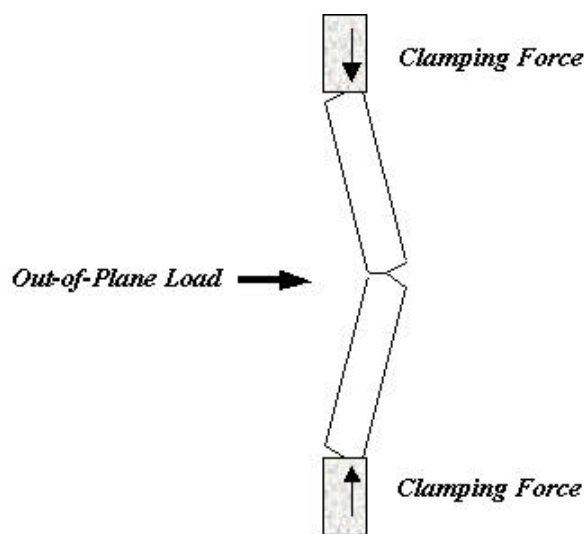


Figure 5.30. Behavior of Infill URM Wall

Analyzing the top segment of the URM wall shown in Figure 5.30, the following free-body diagram can be derived:

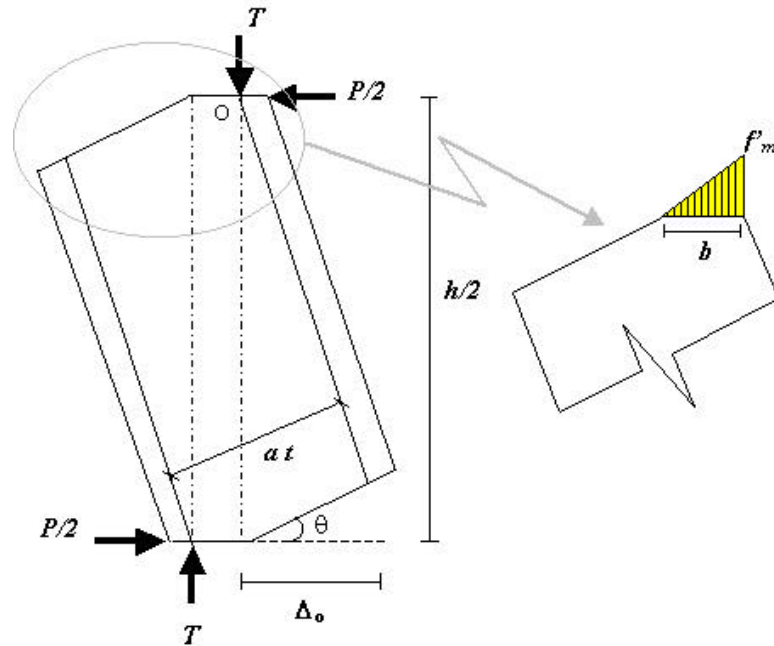


Figure 5.31. Free-body Diagram of Upper Part of URM Wall

The variables in Figure 5.31 are defined as follows:

P = out-of-plane load

T = clamping force

h = height of the wall

t = thickness of the wall

a = arm distance between clamping forces

b = bearing width

Δ_o = wall deflection (rigid-body assumption)

f'_m = compressive strength of masonry

Taking moments about “o” and assuming that the angle θ is very small:

$$\left(\frac{P}{2}\right)\left(\frac{h}{2}\right) = T(a - \Delta_o) \quad (5.1a)$$

$$P = \frac{4T}{h}(a - \Delta_o) \quad (5.1b)$$

The clamping force by unit width acting on the restrained end of the wall can be calculated as:

$$T = \frac{1}{2}(f'_m)(b) \quad (5.2)$$

The wall deflection can be estimated by similar triangles from Figure 5.32 as:

$$\frac{\Delta_o}{h/2 - \Delta_1} = \frac{\Delta_1}{b} \quad (5.3a)$$

$$\Delta_o = \frac{h \Delta_1 - 2 \Delta_1^2}{2b} \quad (5.3b)$$

Where Δ_1 is the axial shortening at the restrained end. The value for Δ_1^2 can be neglected, so that the following relationship is obtained:

$$\Delta_o = \frac{h \Delta_1}{2b} \quad (5.3c)$$

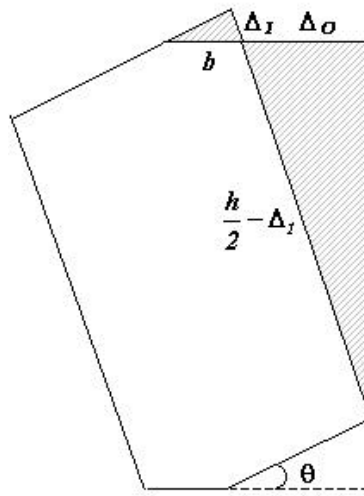


Figure 5.32. Computation of Δ_o

It is assumed that the compressive strains at the tensile fiber of the wall segment vary linearly along the half of the wall. Thereby, the strain at the restrained region is

maximum, whereas, at the midspan they are relieved due to the crack opening (Angel, 1994). In this way Δ_1 can be estimated by integrating the following expression:

$$\Delta_1 = \int_0^{h/2} \epsilon(x) dx = \int_0^{h/2} \left(\frac{\epsilon_{\max}}{h/2} \right) x dx = \frac{1}{4} \epsilon_{\max} h \quad (5.4a)$$

Angel also introduced the dimensionless parameter c :

$$c = \frac{\Delta_1}{h} = \frac{1}{4} \epsilon_{\max} \quad (5.4b)$$

Also, the bearing width can be computed from the equation shown below (Angel, 1994):

$$b = 0.25 t \left[1 + \sqrt{1 - 2c \left(\frac{h}{t} \right)^2} \right] \quad (5.5)$$

In addition, from Figure 5.32 the rotation θ of the wall segment can be determined by:

$$\theta = \arcsin \left(\frac{\Delta_1}{b} \right) = \arcsin \left(\frac{\Delta_o}{h/2 - \Delta_1} \right) \quad (5.6)$$

5.2.5.2. Analytical Derivations for Strengthened Wall. For an URM wall externally strengthened the following free-body diagram for the top part can be derived:

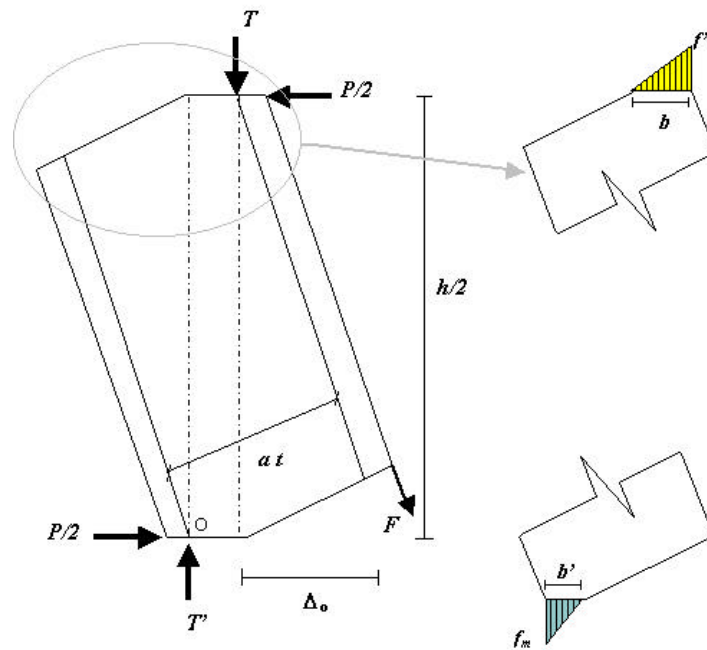


Figure 5.33. Free-body Diagram of Upper Part for Strengthened Wall

Most of the variables have been previously defined for the case of URM walls; additional variables are:

F = Force due to the external reinforcement

T' = clamping force at mid-height

b' = bearing width for T'

f_m = compressive stress of masonry

In similar way to the URM wall, taking moments about “o”:

$$\left(\frac{P}{2}\right)\left(\frac{h}{2}\right) = T(a - \Delta_o) + F\left(t - \frac{b'}{3}\right) \quad (5.7a)$$

$$P = \frac{4T}{h}(a - \Delta_o) + \frac{4F}{h}\left(t - \frac{b'}{3}\right) \quad (5.7b)$$

Since the rotation in the wall is very small, the force in the external strengthening can be approximated as:

$$F = T' - T \quad (5.8)$$

The clamping force by unit width acting on the restrained end at mid-height is calculated as:

$$T' = \frac{1}{2}(f_m)(b') \quad (5.9)$$

The deformations in the restrained ends at the support and wall mid-height can be related to each other from Figure 5.34.

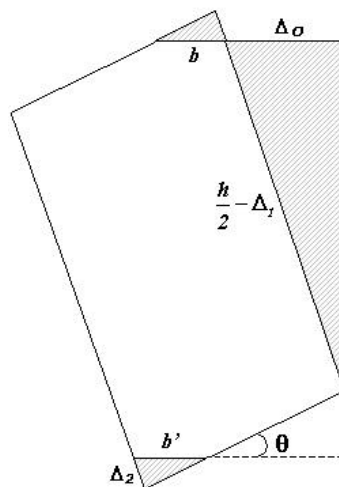


Figure 5.34. Relation between Δ_1 and Δ_2

Thus:

$$\frac{\Delta_1}{b} = \frac{\Delta_2}{b'} \quad (5.10)$$

Similarly to equation, Δ_2 can be related to the strain ϵ_m in the restrained end at mid-height by:

$$\frac{\Delta_2}{h} = \frac{1}{4} \epsilon_m \quad (5.11)$$

ϵ_m is the strain developed in the compressive fiber of the wall segment when the maximum strain ϵ_{max} is reached in the restrained end at the support.

5.2.5.3. Validation of the Analytical Model.

URM Wall

Estimate the out-of-plane load P causing the failure of the two-wythe URM wall (Wall OF2 in Table 5.1), described in the previous sub-sections. This wall had the following properties:

Geometric Properties:

Height = 8 ft = 96-in.

Length = 8 ft = 96-in.

Thickness = 12-in.

Engineering Properties:

Inner Wythe: $f'_m = 300$ psi

$\epsilon_{max} = 0.0015$

Outer Wythe: $f'_m = 1400$ psi

$\epsilon_{max} = 0.0035$

For the inner wythe, the value for f'_m was estimated as an average of compressive strengths of some prisms built with clay tiles studied in research investigations conducted prior to 1964, date of the construction of the Malcolm Bliss Hospital, as can be observed in Table 5.2. The value for ϵ_{max} was obtained from a previous investigation (Bennett, 1997) on compressive properties of structural clay tile prisms. For the outer wythe, f'_m equal to 1400 psi was determined from reclaimed masonry assemblages. A value of

0.0035 for the maximum strain of clay masonry was considered based on the MSJC provisions (1999).

Table 5.2. Compressive Strengths of Clay Tile Prisms

Whittemore and Hathcock (1923)	$f'_m = 392$ psi
Stang (1926)	$f'_m = 363$ psi
Stang (1926)	$f'_m = 232$ psi
Whittemore (1938)	$f'_m = 276$ psi

- Estimate bearing width 'b'

Using equations 5.4b and 5.5:

$$c = \frac{1}{4}(0.0015) = 3.75 \times 10^{-4}$$

$$b = 0.25(12 \text{ in}) \left[1 + \sqrt{1 - 2(3.75 \times 10^{-4}) \left(\frac{96 \text{ in}}{12 \text{ in}} \right)^2} \right] = 5.93 \text{ in.}$$

- Estimate the wall deflection ' Δ_o '

From equation 5.4a the deformation at the support is:

$$\Delta_1 = (3.75 \times 10^{-4})(96 \text{ in}) = 0.036 \text{ in.}$$

Thus, using equation 5.3c the wall deflection is:

$$\Delta_o = \frac{(96 \text{ in})(0.036 \text{ in})}{2(5.93 \text{ in})} = 0.29 \text{ in.}$$

- Estimate the clamping force 'T'

From equation 5.2, and considering a one foot wide strip:

$$T = \frac{1}{2}(300 \text{ psi})(5.93 \text{ in}) \left(\frac{12 \text{ in}}{1 \text{ strip}} \right) \left(\frac{1 \text{ kip}}{1000 \text{ lbs}} \right) = 10.68 \text{ kips / strip}$$

- Estimate the out-of-plane load 'P'

Using equation 5.1b:

$$a = (12 \text{ in}) - 2 \left(\frac{5.93 \text{ in}}{3} \right) = 8.05 \text{ in.}$$

$$P = \frac{4(10.68 \text{ kips / strip})}{(96 \text{ in})} ((8.05 \text{ in}) - (0.29 \text{ in})) = 3.45 \text{ kips / strip}$$

For the total length of the wall:

$$\therefore P = (8 \text{ strips}) (3.45 \text{ kips / strip}) = 27.6 \text{ kips}$$

The out-of-plane load vs. mid-height deflection curve for Wall OF2 tested to failure is shown in Figure 5.35. It is observed that the experimental and predicted values for predicting the out-of-plane load are close. Based on the free-body assumption, the predicted deflection, Δ_0 , should underestimate the real deflection. Δ_0 depends primarily on the maximum compressive strain the tiles, ϵ_{\max} , which was assumed to be 0.0015 (Bennett et al., 1997). If ϵ_{\max} is considered to have a less value than the initially assumed, Δ_0 will decrease. Due to the loading characteristic, which caused local failure at the corner of the walls, ϵ_{\max} should depend more on the brittle characteristics of the clay tile itself (i.e. ϵ_{\max} is less than the assumed).

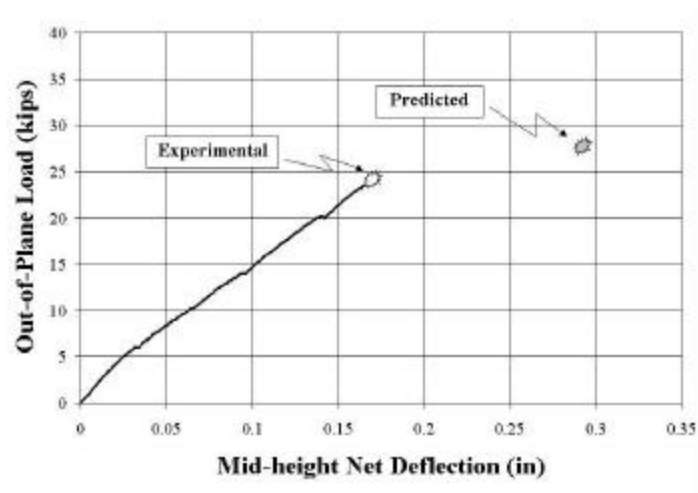


Figure 5.35. Experimental and Predicted Values –URM Wall

Strengthened Wall

Estimate the out-of-plane load P causing the failure of the URM wall, after being strengthened with GFRP laminates (Wall OF4 in Table 5.1).

- Estimate the strain ' ϵ_m ' at mid-height

Assume the only the veneer is carrying out the compressive forces at the final stage, so that:

$$b' = 2.75 \text{ in (width of brick veneer)}$$

Combining equations 5.10 and 5.11:

$$\epsilon_m = \frac{4 (0.036 \text{ in}) \left(\frac{2.75 \text{ in}}{5.93 \text{ in}} \right)}{(96 \text{ in})} = 0.0007$$

- Estimate the clamping force 'T'

According to specifications provided by MSJC (1999), the modulus of elasticity for clay masonry can be estimated as: $E_m = 700f'_m$

In this way the modulus of elasticity for the outer wall is taken as:

$$E_m = 700(1400) = 9.8 \times 10^5 \text{ psi}$$

Thus, the stress in the outer wall at mid-height is:

$$f_m = \epsilon_m E_m = (0.0007)(9.8 \times 10^5 \text{ psi}) = 686 \text{ psi} = 0.69 \text{ ksi}$$

Finally the clamping force T' for a 32 inch-wide strip (see Figure 5.36) can be estimated using equation 5.9:

$$T' = \frac{1}{2}(0.69 \text{ ksi})(2.75 \text{ in})(32 \text{ in}) = 30.4 \text{ kips}$$

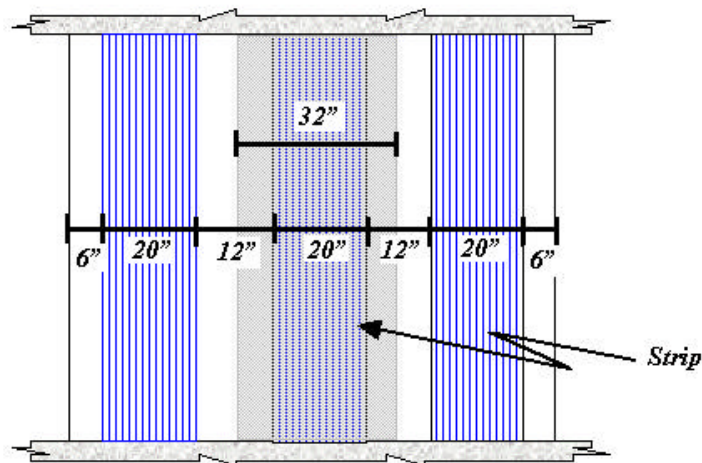


Figure 5.36. Wall Strip for Analysis

- Estimate the out-of-plane load 'P'

For a wall strip of 32 inches, the clamping force T can be recalculated using equation 5.2 as:

$$T = \frac{1}{2}(300\text{psi})(5.93\text{in}) \left(\frac{32\text{ in}}{1\text{strip}} \right) \left(\frac{1\text{ kip}}{1000\text{lbs}} \right) = 28.5\text{ kips / strip}$$

In equation 5.8, the force in the external strengthening is:

$$F = (30.4\text{kips / strip}) - (28.5\text{kips / strip}) = 1.9\text{kips / strip}$$

The arm 'a' is determined as follows:

$$a = t - \frac{1}{3}(b + b') = 12 - \frac{1}{3}((5.93\text{in}) + (2\text{in})) = 9.36\text{in}$$

The out-of-plane load for the wall strip being considered is calculated using equation 5.7b:

$$P = \frac{4(28.5\text{kips / strip})}{(96\text{in})}(9.36\text{ in}) + \frac{4(1.9\text{kips / strip})}{(96\text{in})} \left((12\text{in}) - \frac{(2.75\text{ in})}{3} \right)$$

$$P = 11.35\text{kips / strip}$$

For the total length of the wall:

$$\therefore P = (3\text{ strips})(11.35\text{ kips / strip}) = 34.1\text{ kips}$$

As evidence of the validity of this process, the out-of-plane load vs. mid-height deflection curve for the strengthened wall is plotted in Figure 5.37. The results show that the experimental and predicted values for the out-of-plane load are very close.

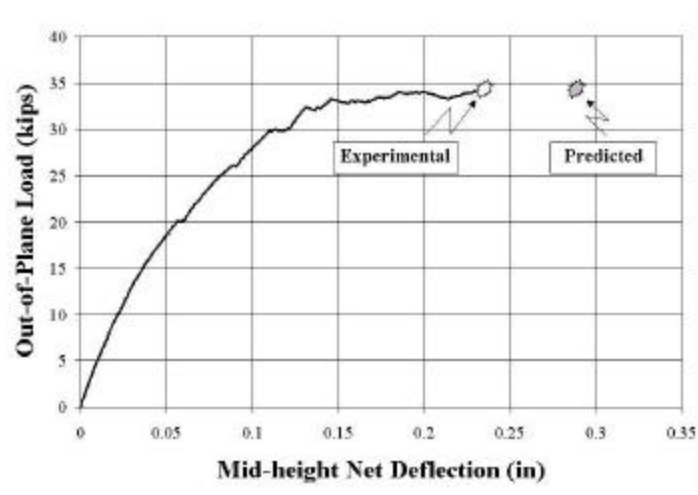


Figure 5.37. Experimental and Predicted Values –Strengthened Wall

6. PROVISIONAL DESIGN APPROACHES

6.1. SHEAR STRENGTHENING WITH FRP RODS

Load reversal causes cracking and reduction in compression-shear transfer, aggregate interaction, and dowel action (Priestley, 1986). Therefore, for design purposes it may not be too conservative to carry all the shear demand by the FRP reinforcement (i.e. $R_n = R_f$). The ultimate strength design requires that the design shear capacity must exceed the shear demand:

$$R_u \leq \phi R_n \quad (6.1)$$

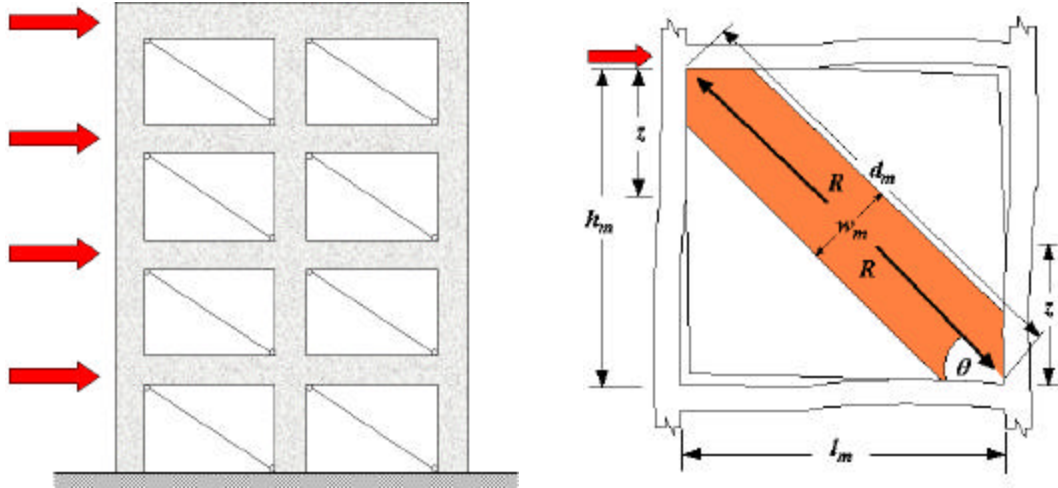
The following assumptions are considered:

- Inclination angle of the shear cracks is constant and equal to 45°.
- The effective strength is reached in all the rods intersected by the diagonal crack.
- The effective strength is one half of that reported by the manufacturer.

6.1.1. Protocol.

1. Determine the critical diagonal compression force in a masonry infill.

A building with infill walls laterally loaded can be idealized as a diagonally braced frame, where the diagonal compression struts have an area bounded by the effective width w_m and the wall thickness. The diagonal strut is idealized as a truss element, which is connected by pins to the frame corners (see Figure 6.1a). There are different approaches to estimate w_m ; for example the New Zealand Code (1990) suggests taking w_m as one-fourth of the length of the infill diagonal, d_n . The expressions showed herein intend to determine the forces in the infill wall for three failure conditions. These failure conditions are diagonal tension, sliding shear, and compression failure of diagonal strut. The lowest value initiates the failure of the infill panel. Figure 6.1b illustrates the geometry of the infill panel.



(a) Equivalent braced frame

(b) Geometry of Infill Panel

Figure 6.1. Equivalent Bracing Action of Infill Panel

Diagonal Tension Failure

The diagonal force to initiate diagonal cracking (R_d) can be estimated by equating the shear stress caused by R_d and the allowable in-plane shear stresses provided by MSJC. Defining the horizontal net area as A_n , The acting stresses are computed based on the diagonal net area, which is expressed as A_n divided by the cosine of the angle θ . Assuming that $1.5\sqrt{f'_m}$ controls, the following derivations can be made:

$$\frac{R_d}{A_n / \cos \theta} = 1.5\sqrt{f'_m} \quad (6.2a)$$

$$R_d = 1.5\sqrt{f'_m} A_n \left(\frac{d_m}{l_m} \right) \quad (6.2b)$$

Sliding Shear Failure

It is assumed that the masonry panel does not carry vertical loads due to gravity effects. The assumption is based on the absence of a tight connection with the surrounding frame, and the separation of the frame and infill panel when the members are laterally loaded.

The maximum shear force resisted by the infill, V_p , can be expressed as:

$$V_p = \tau_o A_n + \mu N \quad (6.3a)$$

where τ_o is a shear bond, μ is a coefficient of friction, and, N is a normal (clamping) force to the shear plane. The vertical component of the diagonal force to initiate sliding shear (R_s) is the only normal force across the sliding plane. V_p is the horizontal component of R_s . Thus:

$$R_s \cos \theta = \tau_o A_n + \mu R_s \sin \theta \quad (6.3b)$$

$$R_s = \frac{\tau_o A_n d_m}{1_m - \mu h_m} \quad (6.3c)$$

Consider $\tau_o = 0.03f'_m$ and $\mu = 0.3$ (Paulay et al., 1992) or use the values provided by MSJC.

Compression Failure of Diagonal Strut

The following expression to determine the force causing compression failure of the diagonal strut has given a conservative agreement with test results (Paulay et al., 1992)

$$R_c = \frac{2}{3} z t f'_m \sec \theta \quad (6.4a)$$

where z is the vertical contact length between infill and column, and it can be estimated as:

$$z = \frac{\pi}{2} \left(\frac{4E_c I_g h_m}{E_m t \sin 2\theta} \right)^{1/4} \quad (6.4b)$$

where E_c and I_g are the modulus of elasticity and moment of inertia of the concrete columns, and E_m is the modulus of elasticity of the infill.

2. The shear force carried by the FRP reinforcement is computed from equation 4.2. Changes to the masonry standards proposed by MSJC (2001) suggest a reduction factor ϕ equal to 0.8 when considering shear with or without axial load. Since long-term exposure to various types of environments may reduce the tensile properties of the FRP reinforcement, the material properties used in design equations should be reduced based on the environmental exposure condition by an appropriate environmental reduction factor C_E (ACI-440, 2000). Thus:

$$f_{ft} = C_E f_{ft}^* \quad (6.5)$$

The environmental reduction factors given in Table 6.1 are conservative estimates based on the relative durability of each fiber type.

Table 6.1. C_E Factor for Various Fibers and Exposure Conditions

Exposure Condition	Fiber Type	C_E
Enclosed Conditioned Space	Carbon	1.00
	Glass	0.80
	Aramid	0.90
Unenclosed or Unconditioned Space	Carbon	0.90
	Glass	0.70
	Aramid	0.80

6.1.2. Design Example. A RC frame is infilled with a 6-in. hollow concrete block masonry wall with dimensions of 8-ft. long by 8-ft. high. The surrounding RC columns are 6-in. wide and 12-in. deep. Due to increased load demand, the load to be resisted by the infill wall has been computed as 20 kips. Assume the wall has the masonry units face shell mortar bedded. Determine if the infill wall can resist the required load. If the demand is exceeded, use FRP structural repointing to upgrade the shear capacity.

Masonry Properties: $f'_m = 1500$ psi

$$E_m = 900 f'_m = 1,350,000 \text{ psi (MSJC, 1999)}$$

Concrete Properties: $f'_c = 4000$ psi

$$E_m = 57,000 \sqrt{f'_c} = 3,605,000 \text{ psi (ACI-318, 1999)}$$

FRP Properties: $f_{fu}^* = 120$ ksi

$$A_{rod} = 0.05 \text{ in}^2$$

- Estimate the critical diagonal force in the masonry infill

Diagonal Tension Failure:

Length and height of infill panel are $l_m = 8$ -ft. and $h_m = 8$ -ft., respectively. Thus, the diagonal can be computed as: $d_m = 11.31$ -ft.

The shell mortar bedded thickness of 1.0-in. for 6-in. block results in the effective area:

$$A_n = 2 (1.0\text{-in.})(8 \text{ ft})(12 \text{ in}) = 192 \text{ in}^2$$

Then, the diagonal force initiating cracking can be estimated from equation 6.2b as:

$$R_d = 1.5\sqrt{1500 \text{ psi}}(192 \text{ in}^2) \left(\frac{11.31 \text{ ft.}}{8 \text{ ft.}} \right) = 15770 \text{ lbs} = 15.77 \text{ kips}$$

The load demand of 20 kips exceeds R_d , therefore the infill panel needs to be strengthened.

Sliding Shear Failure:

The MSJC provisions suggest the use of τ_o equal to 37 psi, and μ equal to 0.45. Thus the diagonal force initiating shear sliding is estimated from equation 6.3c as:

$$R_s = \frac{(37 \text{ psi})(192 \text{ in}^2)(11.31 \text{ ft.})}{(8 \text{ ft.}) - (0.45)(8 \text{ ft.})} = 18270 \text{ lbs} = 18.27 \text{ kips}$$

Compression Failure of Diagonal Strut:

The cross section of the RC columns is specified as 6-in. wide and 12-in. deep. Thus, the moment of inertia is estimated as: $I_g = 864 \text{ in}^4$. The vertical contact length, z , between infill and column is estimated from equation 6.4b as:

$$z = \frac{\pi}{2} \left(\frac{4(3605 \text{ ksi})(864 \text{ in}^4)(8 \text{ ft.})(12 \text{ in.})}{(1350 \text{ ksi})(5.625 \text{ in.})(\sin 2(45^\circ))} \right) = 31.29 \text{ in.}$$

The force to cause compression failure of the diagonal strut is computed by equation 6.4a:

$$R_c = \frac{2}{3}(31.29 \text{ in.})(5.625 \text{ in.})(1500 \text{ psi})(\sec 45^\circ) = 248930 \text{ lbs} = 548.93 \text{ kips}$$

- Determine the amount of FRP reinforcement

The shear demand was specified to be 20 kips; therefore considering a ϕ factor equal to 0.8, the nominal shear force R_f to be entirely carried by the FRP reinforcement is:

$$R_f = \frac{20 \text{ kips}}{0.8} = 25 \text{ kips}$$

The ultimate strength is calculated as: $f_{fu} = C_E f_{fu}^* = 0.8(120 \text{ ksi}) = 96 \text{ ksi}$

The environmental factor C_E equal to 0.8 is determined from Table 6.1 for enclosed conditioned space and for glass fibers.

The spacing of reinforcement is estimated from equation 4.2 as:

$$s = 0.5 \left(\frac{A_f}{R_f} \right) f_k d_v = 0.5 \left(\frac{(0.05 \text{ in}^2)}{(25 \text{ kips})} \right) (96 \text{ ksi})(96 \text{ in.}) = 9.2 \text{ in.}$$

∴ Use 11 # 2 GFRP rods, place them at every joint (spacing = 8.0-in.)

6.2. FLEXURAL STRENGTHENING WITH FRP LAMINATES

Three ultimate states can be considered in a masonry wall strengthened with FRP laminates:

State 1: Debonding of the FRP laminate from the masonry substrate

State 2: Rupture of the FRP laminate

State 3: Crushing of masonry in compression

The flexural capacity of a FRP strengthened masonry wall can be determined based on strain compatibility, internal force equilibrium, and the controlling mode of failure. Previous investigations (Velazquez, 1998, Hamilton et al., 1999, and Roko et al. 1999) suggest that most of the times, the controlling state is the debonding of the FRP laminate (State 1). If a large amount of FRP is provided, shear failure may be observed.

Debonding may have a direct relationship with the porosity of the masonry unit, which is characterized by initial rate of absorption tests. Roko et al. (1999) observed that the absorption of the epoxy is limited in the extruded brick units as compared to the absorption in molded bricks. This is attributed to the glazed nature of their surface, which leads to a reduction of the bond strength between the FRP laminate and the masonry surface.

Figure 6.2 illustrates the relationship between the experimental-theoretical flexural capacity ratio, and the reinforcement ratio ω_f , expressed as $\frac{\rho_f E_f}{f'_m (h/t)}$. The introduction of the slenderness ratio h/t is justified since this parameter is identified as one of the most important in the out-of-plane behavior of masonry walls. The slenderness ratios and the out-of-plane capacity are inversely proportional. As the slenderness ratios decrease, the out-of-plane strength becomes very large (Angel et al., 1994). Since the strength is directly proportional to the compressive strength, then the slenderness ratio and the compressive strength are inversely proportional. Therefore, it is reasonable to express the relation between the compressive strength and the slenderness

factor as a product. The experimental data used for plotting Figure 6.2 was obtained from previous investigations (Velazquez, 1998, and Hamilton et al., 1999) and from two specimens tested during the present investigation. The test specimens were built with clay and concrete masonry units. AFRP and GFRP laminates were used as strengthening material. Mostly, the tests showed that the strengthened specimens failed due to debonding of the laminate. In the case of the two specimens tested in this investigation, shear failure was observed. These masonry assemblages were built with standard concrete blocks, and had nominal dimensions of 24-in. by 48-in. The reinforcement consisted of GFRP and AFRP laminates with reinforcement ratios of 0.06% and 0.04%, respectively. The characteristics of the specimens being considered as well as the calculations conducted to developing Figure 6.2 are presented in Appendix C.3.

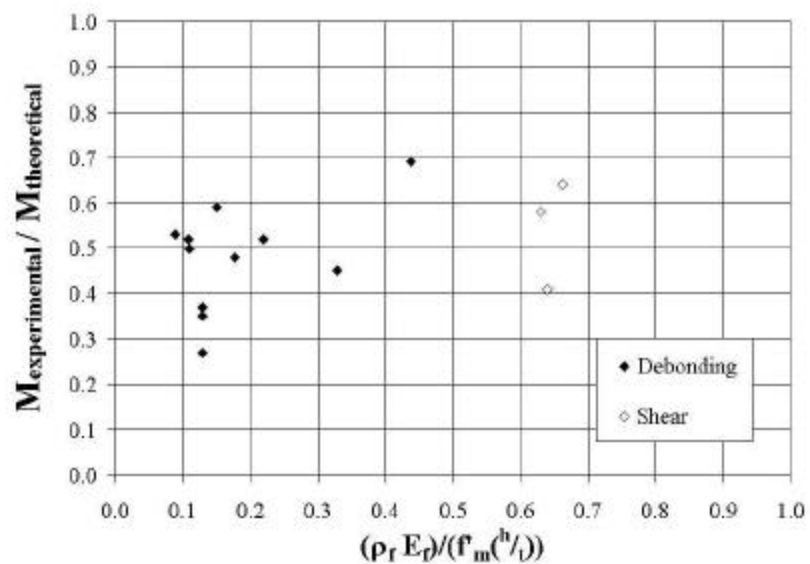


Figure 6.2. Influence of Amount of FRP Reinforcement

Theoretical flexural capacities of the strengthened walls were estimated based on the assumption that no premature failure was to be observed. This means that either rupture of the laminate or crushing of masonry would control the wall behavior. For simplicity and similarly to the flexural analysis of RC members, a parabolic distribution is used in the computation of the flexural capacity of the strengthened masonry. Thus:

$$f_m = f'_m \left[2 \left(\frac{\epsilon_m}{\epsilon'_m} \right) - \left(\frac{\epsilon_m}{\epsilon'_m} \right)^2 \right] \quad (6.6a)$$

From the parabolic distribution, the coefficient α and β_1 that bound the equivalent compressive block can be determined from the following relationships:

$$\alpha\beta_1 = \left(\frac{\epsilon_m}{\epsilon'_m} \right) - \frac{1}{3} \left(\frac{\epsilon_m}{\epsilon'_m} \right)^2 \quad (6.6ba)$$

$$\alpha\beta_1 \left(1 - \frac{1}{2} \beta_1 \right) = \frac{2}{3} \left(\frac{\epsilon_m}{\epsilon'_m} \right) - \frac{1}{4} \left(\frac{\epsilon_m}{\epsilon'_m} \right)^2 \quad (6.6cb)$$

The strain and stress distributions in a masonry cross-section strengthened with FRP laminates are illustrated in Figure 6.3.

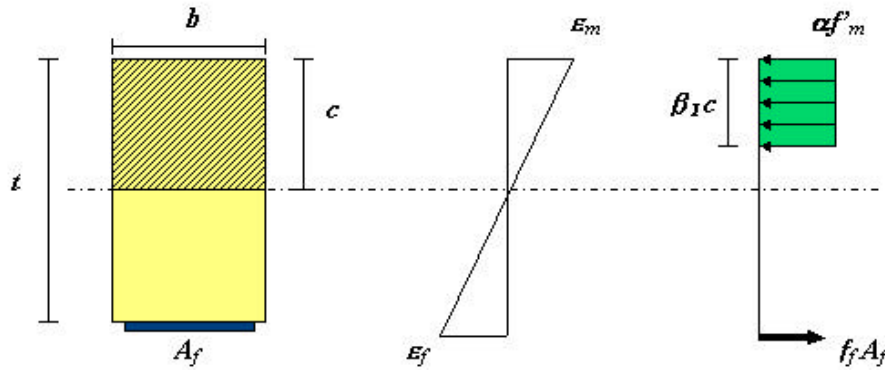


Figure 6.3. Strain and Stress Distribution

In order to satisfy the internal force equilibrium:

$$(\gamma f_m)(\beta_1 c)(b) = A_f f_f \quad (6.7a)$$

$$f_f = E_f \epsilon_f \quad (6.7b)$$

The effective strain in the reinforcement ϵ_{fe} and the strain in the masonry are related by:

$$\frac{\epsilon_m}{c} = \frac{\epsilon_f}{t - c} \quad (6.7c)$$

The following assumptions provided by MSJC (1999) are considered:

- The maximum usable strain ϵ_{mu} is assumed to be 0.0035 in./in. for clay masonry, and 0.0025 in./in. for concrete masonry.
- The tensile strength of masonry is neglected.

Using the previous relationships, the depth of the neutral axis 'c', the theoretical flexural capacity can be estimated by:

$$M_{\text{theoretical}} = A_f f_f \left(t - \frac{\beta_1 c}{2} \right) \quad (6.8)$$

Since the ratio $M_{\text{experimental}} - M_{\text{theoretical}}$ shown in Figure 6.2 averages about 0.5, for design considerations the effective strain e_{fe} in the FRP laminate can be limited as about half of the strain at ultimate in the laminate e_{fu} . It is suggested to use a value equal to 0.008 for e_{fe} as a limit strain. The index ω may be limited to 0.5 to prevent the occurrence of shear failure. These assumptions are taken with the premise that further research needs to be conducted to fully validate the veracity of the assumed limits. Based on the strain levels achieved by the FRP reinforcement at ultimate, it can be considered that the actual ultimate capacity of the strengthened wall can be calculated from a cracked section under elastic stresses, where the two materials behave elastically, or very nearly so in the case of masonry (see Figure 6.4).

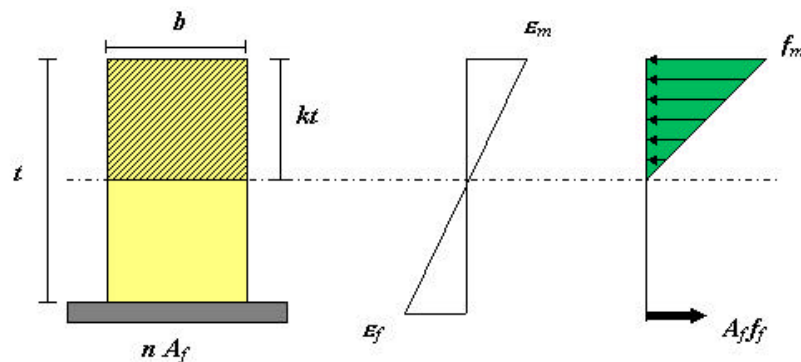


Figure 6.4. Strain and Stress Distribution in Cracked Transformed Section

Thus, the depth of the neutral axis and the flexural capacity can be estimated from the equilibrium of forces:

$$\frac{1}{2}(f_m kt) b = f_f A_f \quad (6.9a)$$

and the following relationships:

$$f_m = \varepsilon_m E_m \quad (6.9b)$$

$$f_{\text{fe}} = \varepsilon_f E_{\text{fe}} \quad (6.9c)$$

$$n = \frac{E_{\text{fe}}}{E_m} \quad (6.9d)$$

Thus, the coefficient 'k' is obtained from the "well-known" relationship:

$$k = \sqrt{(n\rho_f)^2 + 2(n\rho_f)} - n\rho_f \quad (6.10)$$

Finally the flexural capacity is estimated as:

$$M_n = A_f f_{\text{fe}} \left(t - \frac{kt}{3} \right) \quad (6.11)$$

If the modulus of elasticity of masonry, E_m , is unknown, it can be estimated as $E_m=700f'_m$ for clay masonry and $E_m=900f'_m$ for concrete masonry (MSJC, 1999). Figure shows the relationship between the experimental and analytical flexural capacity, estimated following the proposed approach. The results show an acceptable correlation between the experimental and analytical values as observed in Figure 6.5. The corresponding calculations were conducted for an effective strain equal to 0.008 in the laminates, and are presented in Appendix C.3.

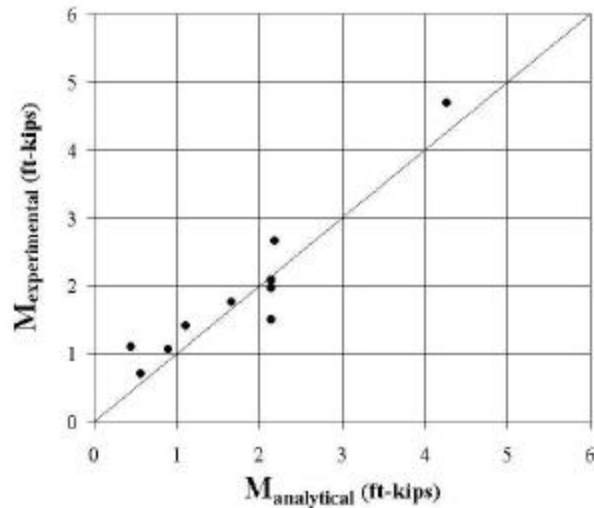
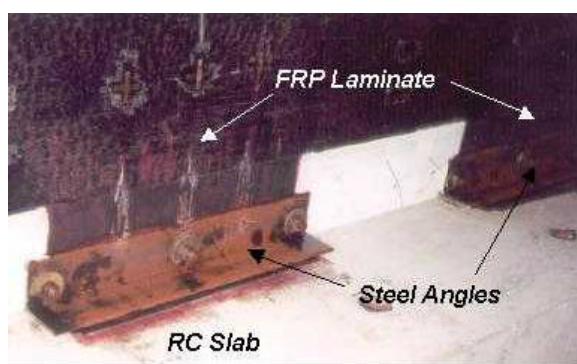
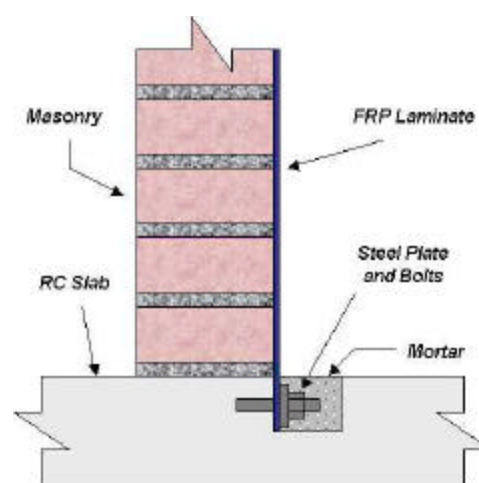


Figure 6.5. Correlation between Experimental and Analytical Values

During strong seismic events the strengthened walls can displace as a whole or partially collapse under out-of-plane loads. To avoid this, anchorage systems can be installed. Some anchorage systems include the use of steel angles (see Figure 6.6a), steel bolts (see Figure 6.6b), and NSM rods. The use of steel angles can locally fracture the wall in the anchorage regions due to the restraint caused when the wall starts deflecting. Thereby, it is advisable that the anchorage system is not in contact with the masonry surface. Schwegler et al.(1996) investigated the use of bolts, which even though showed effectiveness, represent a demanding installation effort.



(a) Steel Angles



(b) Steel Bolts

Figure 6.6. Anchorage Systems

The nature of the NSM installation technique and the shortened installation time make their use suitable to be used as part of the strengthening strategy of masonry walls. NSM rods have been successfully used for anchoring FRP laminates in RC joists strengthened in shear (Anaiah et al., 2000). The installation technique consists of grooving a slot in the upper and lower boundary members. The fibers are then placed in the slot, rounding a FRP rod which will act as anchorage after being bounded by a suitable epoxy-based paste (see Figure 6.7).

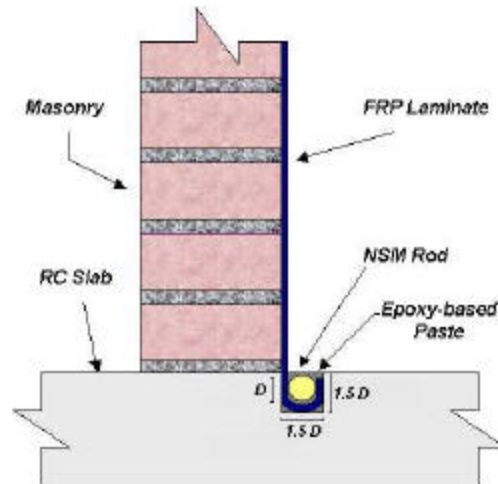


Figure 6.7. Anchorage with NSM rods

6.2.1. Protocol. The ultimate strength design criteria states that the design flexural capacity of a member must exceed the flexural demand.

$$M_u \leq \phi M_n \quad (6.12)$$

The following assumptions are taken:

- The strains in the reinforcement and masonry are directly proportional to the distance from the neutral axis.
- The maximum usable strain, ϵ_{mu} , at the extreme compressive fiber is assumed to be 0.0035 in./in. for clay masonry and 0.0025 in./in for concrete masonry.
- The maximum usable strain in the FRP reinforcement is assumed to be 0.0008 in./in.
- The tensile strength of masonry is neglected.
- The FRP reinforcement has a linear elastic stress-strain relationship up to failure.

The design protocol can be outlined as follows:

1. Compare the allowable tensile stresses provided by MSJC with the acting stresses to determine the need for strengthening.
2. Verify that local crushing will not occur in the boundary regions.

In the previous subsections a method to predict the out-of-plane load causing local crushing in the masonry wall was presented. This behavior is critical in walls constituted of brittle units with a very low compressive strength.

3. The nominal flexural capacity is computed by considering a reduction factor ϕ equal to 0.70.

The approach for the reduction factor is similar to that of the ACI-318, where a section with low ductility must be compensated with a higher reserve of strength. The higher reserve of strength is attained by applying a strength reduction factor of 0.70 to sections prone to have brittle or premature failures such as debonding of the laminate.

4. The amount of FRP reinforcement is estimated by modifying equation 6.11 as follows:

$$M_n = \rho_f f_k b t_m^2 \left(1 - \frac{k}{3}\right) \quad (6.13)$$

where ρ_f is the FRP reinforcement ratio, b is the width of the section being analyzed, and t_m is the overall wall thickness.

A maximum usable strain FRP strain is used based on experimental observations. Thus, the effective usable stress can be computed as:

$$f_k^* = 0.008 E_f \quad (6.14)$$

Similarly, to the shear design protocol, an environmental reduction factor C_E (ACI-440, 2000) is also considered. The C_E factors are estimated from Table 6.1.

$$f_k = C_E f_k^* \quad (6.15)$$

5. The maximum clear spacing between FRP strips can be defined as follows:

$$s_f = \min \{2t_m, L\} \quad (6.16)$$

For block units: $L = l_b$

For brick units: $L = 2l_b$

Where t_m is the thickness of the wall being reinforced without including the wall veneer, and l_b is the length of the masonry unit.

There is no scientific evidence for the recommendations on maximum clear spacing. s_f equal to two times the wall thickness is based on stress distribution criteria along the thickness. For s_f equal to the length of the masonry unit, the rationale is to engage most of the masonry units and avoid loosening of units, which could cause the partial collapse of the wall. Low amount of reinforcement as determined from item 4 can lead to large clear spacing between strips. For that case the criterion of minimum spacing described in this item should prevail; even though, additional reinforcement, no needed to satisfy load demands, would have to be placed.

6.2.2. Design Example. The flexural capacity of a non-bearing URM concrete block wall needs to be verified due to increased wind load demands. The nominal dimension of the concrete units is 8x8x16-in. The wall has only two boundary elements (i.e. lower and upper beams), and it can be assumed to have only one-way bending behavior. The dimensions of the wall are 12-ft. by 12-ft. The moment demand has been estimated as 1.15 ft-kips/ft. If strengthening is needed, a glass/epoxy system will be used to upgrade the shear capacity.

Masonry Properties: $f'_m = 2000$ psi

$\epsilon_{mu} = 0.0035$ in./in.

$t_m = 8$ -in.

FRP Properties: $f_{ti}^* = 120$ ksi

$E_f = 10500$ ksi

GFRP Sheet thickness, $t_t = 0.0139$ -in.

- Check the flexural tension stress:
Assuming face shell mortar bedding, the moment of inertia of the section is estimated by the ASTM C90 to be equal to 309 in⁴ per foot of wall.
According to the MSJC provisions the allowable flexural tension is 25 psi.
Considering the $1/3$ increase for wind loading, the allowable stress is 33.3 psi.
The acting tensile stress is:

$$f_t = \frac{M(t_m/2)}{I} = \frac{(1.15 \text{ ft} - \text{kips} / \text{ft})(12)(7.625 \text{ in} / 2)}{309 \text{ in}^4} = 170 \text{ psi}, \text{ which greatly exceeds}$$

the allowable tensile stress. Therefore, the URM wall needs upgrading.

- Check the occurrence of local crushing

Recognizing that the loads generated by wind pressures are distributed, using the procedure presented for URM walls, an out-of-plane force causing local crushing equal to 4.5 kips/ft can be calculated. This force is associated to a moment:

$$M_c = \frac{(4.5 \text{ kips} / \text{ft})(12 \text{ ft})}{4} = 13.5 \text{ ft} - \text{kips} \gg 1.15 \text{ ft-kips}$$

Therefore, local crushing in the boundary regions will not be observed.

- Compute the nominal flexural capacity

The ultimate moment due to wind loads can be estimated as:

$$M_u = 1.3(1.15 \text{ ft} - \text{kips} / \text{ft}) = 1.5 \text{ ft} - \text{kips} / \text{ft}$$

The nominal flexural capacity is calculated as:

$$M_n = \frac{M_u}{\phi} = \frac{(1.5 \text{ ft} - \text{kips} / \text{ft})}{0.7} = 2.1 \text{ ft} - \text{kips} / \text{ft}$$

The effective usable stress is estimated from equation 6.15 as:

$$f_{fe}^* = 0.008E_f = 0.008(10500 \text{ ksi}) = 84 \text{ ksi}$$

Considering an environmental factor C_E equal to 0.8, the effective stress is:

$$f_{fe} = C_E f_{fe}^* = 0.8(84 \text{ ksi}) = 67.2 \text{ ksi}$$

To determine the ratio n between the modulus of elasticity of FRP reinforcement and masonry, the latter can be estimated as $E_m = 900f_m^*$ (MSJC, 2000). Thus:

$$E_m = 900(2000 \text{ psi}) = 1800 \text{ ksi}, \text{ and } n = \frac{E_f}{E_m} = \frac{(10500 \text{ ksi})}{(1800 \text{ ksi})} = 5.83$$

The coefficient k is computed by equation 6.10 as:

$$k = \sqrt{(5.83\rho_f)^2 + 2(5.83\rho_f)} - 5.83\rho_f$$

The amount of required reinforcement is computed by solving equation 6.13:

$$(2.1 \text{ ft} - \text{kips} / \text{ft}) = \rho_f (67.2 \text{ ksi})(12 \text{ in})(7.625 \text{ in})^2 \left(1 - \frac{\sqrt{(5.83\rho_f)^2 + 2(5.83\rho_f)} - 5.83\rho_f}{3} \right)$$

Solving for trial and error or another numerical method: $\rho_f = 0.00056$

The amount of strengthening is estimated as: $A_f = (0.00056)(8 \text{ in})(12 \text{ in}) = 0.054 \text{ in}^2/\text{ft}$

The width of GFRP is: $w_f = \frac{A_f}{t_f} = \frac{(0.054 \text{ in}^2)}{(0.0139 \text{ in})} = 3.8 \text{ in} / \text{ft} \therefore \text{Use } 4.0 \text{ in} / \text{ft}$

The total length of required reinforcement is: $(12 \text{ ft})(4.0 \text{ in}/\text{ft}) = 48\text{-in.}$ The strengthening layout is illustrated in Figure 6.8.

- Determine the clear spacing s_f

t_m and l_b are equal to 8-in. and 16-in., respectively.

Thus, in the relationship 6.16 the clear spacing can be calculated as:

$$s_f = \min \{2(8 \text{ in.}), 16 \text{ in.}\} = 16 \text{ in.}$$

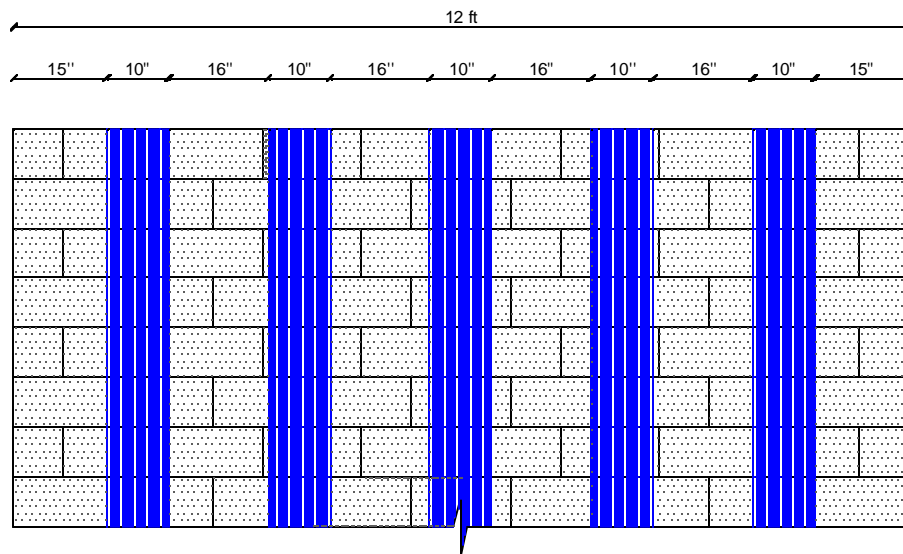


Figure 6.8. Strengthening Layout

7. FINANCIAL JUSTIFICATION

7.1. BACKGROUND

Currently in the United States, large investments are being directed to retrofitting projects. It is estimated that the national average spending on reconstruction is about 25% of new construction investment (U.S. Census Bureau 1998). Under the URM Building Law of California, passed in 1986, approximately 25,500 URM buildings were inventoried throughout the state. Even though this number is a relatively small percentage of the total building inventory in California, it includes many cultural icons and historical resources. The building evaluation showed that 96 % of the URM buildings in California needed to be retrofitted, which would result in approximately \$4 billion in retrofit expenditures (California Seismic Commission, 2000). To date, it has been estimated that only half of the owners have taken remedial actions, which may be attributed to high retrofitting cost. Therefore there is an urgent need to develop effective and affordable retrofitting techniques for masonry elements. In that context, FRP composites provide solutions for the strengthening of URM walls subjected to high in-plane and out-of-plane stresses caused by wind or earthquake loads.

7.2. RETROFITTING ALTERNATIVES

Retrofitting techniques can be classified according to the problem to be addressed: damage repair or structural upgrading (strengthening). FRP materials can be primarily used in cases where structural upgrading of masonry elements is required; therefore, the present discussion will be limited to situations in which strengthening of the structural elements is necessary. Structural retrofitting or strengthening can be performed using either conventional materials, such as steel and grout, or FRP composite materials.

7.2.1. Conventional Strengthening Methods. For strengthening or upgrading of structures some of the available conventional methods are:

- Grout injection of hollow masonry units with non-shrink portland cement grout or epoxy grout to strengthen or stiffen the wall. This method often requires disruptive

activities such as drilling of holes and utilization of relatively heavy equipment, which could increase the cost.

- Construction of an additional masonry wythe to increase the axial and flexural strength. This method will cause the loss of valuable space. In addition, the normal operations of the building area being strengthened are affected during construction, which could require the relocation of building inhabitants. These factors could increase the cost of the project.
- Post-tensioning of an existing construction. This method is particularly effective to increase the flexural capacity of masonry elements. In addition, post-tensioning does not affect the masonry aesthetics. However, it demands high-skilled labor, which increases the cost.
- External reinforcement with steel plates and angles. This is a relatively simple method to implement; however, one of the main disadvantages is that it can affect the aesthetics of the building. This fact can increase the intangible costs. In addition, additional costs can be incurred due to maintenance.
- Surface coating with reinforced cement, such as a welded mesh. This method causes disruption to normal operations of the building as well as it requires relatively heavy equipment.

7.2.2. Strengthening with FRP Composite Materials. FRP materials in the form of laminates and rods are available for the strengthening of masonry elements. The use of laminates involves the application of fiber sheets by manual lay-up to the surface of the member being strengthened. The fibers are impregnated by an epoxy resin, which after hardening enables the newly formed laminate to become integral part of the strengthened member. Another available FRP technology is the use of rods, which consists of placing FRP rods into grooves made on the surface of the member being strengthened. The groove is filled with an epoxy-based paste, the rod is then placed into the groove and lightly pressed to force the paste to flow around the rod. The groove is then filled with more paste and the surface is leveled.

The cost of material and construction of these two alternatives are compared in section 7.4.

7.3. FINANCIAL ANALYSIS

When initially considering an URM building structure for potential structural retrofit, the stakeholders (i.e. owners, contractors, and consultants) need to consider leaving the structure as is without improvements (“no action” alternative), demolishing the deficient URM walls and erecting new walls, or performing structural retrofitting.

7.3.1. The “no action” Alternative. This is the option to not take any remedial action. In the long term the costs associated to this option can be very high if there is a significant probability of damage due to earthquakes or high winds. URM buildings may be used as office space, apartment complexes, warehousing, etc. Failure of those structures with human occupancy can result in drastic damages and in loss of human lives, which would generate extremely large preventable costs. On the other hand, if only material goods were stored in the building, damages caused to equipment, inventory, etc, the cost of the “no action” alternative may be less. The probability and severity of an earthquake or high-wind pressures occurrence determines the need to retrofit an URM building. For example, in the Western United States the probability of a severe earthquake are higher than in the Eastern region. An expected cost of the “no action” alternative can be estimated based on the cost of failure and the probabilities of its occurrence. This cost of “no action” can then be used to determine the financial justification of the retrofit costs. If the cost of “no action” is greater than the cost of retrofit, the retrofit activity is financially justified.

The costs of reconstruction or retrofit also include the cost of failure and probability of occurrence. If the retrofit reduces the risk to a minimal level it can be ignored. However, if it only makes a small improvement in the survivability of the structure then the value gained by the activity is significantly smaller. Therefore, when determining the value of the reconstruction or retrofit activity the impact to the probability of failure should be considered.

An important point to consider is that some of the URM buildings in existence have become part of the cultural and historical heritage of the towns where they are located, and as such have become irreplaceable. No level of structural damage to these structures can be tolerated and structural improvements must be undertaken in order to save the structure’s integrity. In this case the cost of “no action” is extremely high.

In addition, due to changes in building codes, old URM structures do not comply with the minimum structural requirements and retrofit becomes necessary. As a consequence some states like California have passed regulations to promote the retrofit of deficient URM buildings. In these cases, the “no action” option is not a legal alternative.

7.3.2. Demolition and Reconstruction. This option requires the substitution of a deficient wall by a new one complying with new specifications. This option can generate large expenditures associated to disruption of activities, removal of debris and transportation of new material within the site. In the case of a historical building, this is not a viable option since it would alter its historical value.

If the “demolition and reconstruction” alternative is a possibility, then it should be compared against the “no action” alternative and the retrofitting option, be it with conventional or FRP materials.

7.3.3. Structural Retrofitting. This alternative involves determining whether to use conventional or FRP materials to retrofit the structure. As mentioned previously, URM buildings located in regions subject to potential earthquake or high wind pressures may need to be retrofitted. In those areas, the expected cost of not retrofitting an URM building could be extensive, providing a clear financial justification for the retrofit.

7.3.4. Comparison of Alternatives. In this section a method to analyze the alternatives dealing with the reconstruction and retrofitting of masonry members is presented. It is based on comparisons that include both direct and indirect costs. These comparisons also include up-front costs as well as follow-on costs and are consistent with a life-cycle cost (LCC) approach. LCC is particularly useful in making effective decision in projects where the decision has major implications in the maintenance costs and expected life of the structure. The procedure of the life-cycle cost method for building economics is described in ASTM E917.

The reality of retrofitting operations is that the costs and benefits of any of these alternatives vary widely. Consequently, it is not possible to determine exact costs for any of the activities being considered. Appropriate estimates must take into account the specific conditions for each case. However, based on common sense, widely accepted practices and observations in this area, general guidelines can be provided that compares

these costs in typical and normal cases. This is the objective of the cost analysis that follows.

Cost analysis is an effective way to support logical decision-making and select the most viable economic option. Table 7.1 presents comparative costs of alternatives when considering reconstructing URM walls, and use of conventional and FRP materials. For each activity the normal costs are compared for each of the three major alternatives. The level of costs is represented by a level 1, 2 or 3. Level 1 represents the most economical option and 3 the most expensive option. For each of the major alternatives, the levels of cost have been taken as an average of the appropriate methods.

Table 7.1. Comparative Costs of Alternatives

Items	Reconstruction	Conventional Strengthening	FRP Strengthening
DIRECT COSTS			
Initial Costs			
• Design	1	2	2
• Material	1	2	3
• Construction			
Equipment	2	3	1
Labor	3	2	1
Inspection	1	2	2
Partial or Total			
Demolition	3	1	1
Maintenance Costs			
• Maintenance	1	2	1
• Repair	2	1	1
Sub-Total	2	3	1
INDIRECT COSTS			
• Aesthetics	2	3	1
• Occupants Relocation	3	2	1
• Lost Business	3	2	1
Sub-Total	3	2	1
Total	2	2	1

7.3.4.1. Direct Costs. The direct costs include the initial costs related to the design process, material used and, construction activities. The direct costs also include maintenance costs.

Design: A thorough assessment of a masonry wall and adjacent regions before retrofitting is extremely important before deciding an appropriate method. The reconstruction alternative will represent the most economic alternative since new and different design ideas are not considered. Design is the engineering process conducted to determine the strengthening strategy. Since the use of a particular material will not be always suitable for every project (i.e. FRP will not be the best alternative every time), it is considered that design with conventional and FRP materials will have approximately the same cost. The variables considered in the assessment include the following:

- *Masonry typology:* Construction practices vary from region to region. Furthermore, masonry typologies vary by years. For instance, masonry construction practices are different in the Western and the Eastern regions of the United States. Similarly current practices are different than they were 30 years ago. This is due to loading requirements (wind and earthquake), construction practices, and material availability. As a consequence different kind of masonry typologies can be observed. These differences include masonry units (e.g. bricks or blocks, clay or concrete), type of mortar, and wall arrangement (number of wythes). The masonry typology sometimes determines the most suitable strengthening strategy for that particular kind of masonry. For instance, it has observed that due to their installation nature, the use of rods in masonry walls made of brittle masonry units (tiles and hollow units) are not recommended. For those cases the use of FRP laminates would be more appropriate.
- *Connections:* During an earthquake or high wind pressures URM walls can tear off and collapse; therefore, it is important to determine if the masonry walls are properly connected to adjacent members such as beams, slabs or other walls. If the walls are not adequately connected, the use of steel rods or angles should be considered to anchor the wall. Due to the characteristics of the acting stresses in the masonry wall boundary region and some mechanical properties of the FRP

rods, their use may not be suitable to solve this problem. In this case conventional materials will offer a more viable alternative.

- *Seismic requirements:* In the Western region, especially in California, seismic criteria prevail when developing a strengthening strategy. The use of conventional materials to retrofit an URM walls in a building can increase the mass. As a consequence larger seismic forces will be attracted which can have effects on the overall structural systems (i.e. beams, slabs, columns, and foundation). Due to their reduced thickness and light weight, the use of FRP laminates and rods has the advantage of not increasing significantly the building mass as other strengthening methods. The cost of using conventional materials or FRP composites will depend on the characteristics of the project and seismic requirements.
- *Environment:* Since masonry walls are subject to water infiltration from rain, conventional reinforcing materials such as steel can be corroded. In contrast, FRP composites are non-corrosive and can be used in harsh environments. Also, some building components contain hazardous materials such as asbestos and lead. Their presence imposes limitations on activities that produce odor, smoke, or noise. Therefore, the use of strengthening methods with minimum surface preparation such as “FRP structural repointing” might be required.

Material: FRP materials are generally more expensive than traditional materials used for retrofitting. Materials used for wall reconstruction include masonry units (bricks or blocks), mortar and steel rebars. Therefore, reconstruction generally offers the lowest cost of all the alternatives.

Construction: Cost estimates and schedules of potential strengthening strategies should be analyzed. In this area design/build projects are common in which the retrofitting strategy is designed and executed by the same company. This management approach has proven to be efficient in terms of cost, and time is improved since there is a single-point of responsibility. However, since not many construction companies are specialized in the installation of FRP composites, it can also have negative effects because there is a limited cost competition.

The characteristics of the equipment to be used during the retrofitting activities have influence on the selection of the retrofit method. The installation of FRP generally requires the use of less equipment than those used by conventional methods, which helps make this alternative more economical.

In general, labor is the most important direct cost factor; therefore, alternatives that require considerable use of labor have a cost disadvantage. Since the use of FRP composites can reduce the project's duration, and simplify the work required it can provide an advantage in this area.

Because masonry walls are many times connected to other adjacent walls, these walls may need to be partially or totally demolished to perform the strengthening activities. Demolition generates similar costs for strengthening with conventional or FRP materials. The reconstruction alternative implies a high amount of demolition because new masonry walls will be erected which generates additional costs.

Many times due to the uniqueness of many retrofitting projects, more inspection is required by the owner, which would increase the project cost. In this case the reconstruction alternative will represent a minimal cost. The costs for the strengthening options would be similar to each other but higher than reconstruction.

Maintenance and Repair: The maintenance of a new wall and a wall retrofitted with FRP materials exhibit the lowest costs. Traditional strengthening methods may need larger maintenance efforts, which can slightly lead to increasing future costs. Some of these methods involve the use of steel plates, which can be subject to corrosion.

Repair can be required sometimes when using FRP systems; basically due to mistakes during the installation process. Depending on the masonry exposure, future repairs of a reconstructed wall may represent higher costs due to environmental effects.

7.3.3.2. Indirect Costs. The indirect costs are those that are harder to identify and quantify. They are related to aesthetics, occupants' relocation and loss of business.

Aesthetics: In some cases, it is important that the retrofit work should be carried out with the least possible irrevocable alteration to the building's appearance. Many URM buildings are part of the cultural heritage of the city or country. Therefore, to preserve their aesthetic and architecture is critical. Since the use of external reinforcing overlays of steel or FRP can alter the aesthetics of masonry. "FRP structural repointing"

is a valuable alternative to strengthen masonry walls in these cases. Since the reinforcing rods are placed in the mortar joints, this method has the advantage of maintaining the original appearance of the masonry surface.

Occupants Relocation: Any retrofit project involves some disruption activities to the building occupants. Conventional strengthening may require the use of relatively heavy equipment such as welding machines, saws, etc, which can produce dust and noise that can disrupt the normal activities of the building users. The use of FRP laminates can lessen these effects to some extent. However, it is recognized that surface preparation requirements prior to the FRP installation can also be disruptive. Since the surface preparation for “FRP structural repointing” is much less (only grooving of the joints is required), this method is ideal when it is important to minimize the impact to the normal operations of the building. The time length of relocation and the need to utilize other spaces will have an impact to additional cash outlays and loss in productivity. Conventional strengthening may require the building occupants to temporarily move, which would add significant costs and additional inconvenience. The movement of personnel or assets will undoubtedly increase the cost of the retrofitting project due to rental costs, inadequate resources and lost of productivity. Since FRP strengthening is usually performed faster than conventional methods, it provides a significant advantage in this area.

Lost Business: During the retrofit work, shutdown of the building operations should be considered. However, it will cause temporary loss of business for the owners. The possibility of work during off-hours (night and weekends) should be evaluated to see if it is cost-effective as compared to the shutdown of the building operations. However, this alternative will probably increase the labor cost and slowdown the process. “FRP structural repointing” has the characteristic of causing less disruption and it can be cost-effective when the shutdown alternative is too expensive. Therefore, strengthening with FRP materials can minimize these lost business costs.

7.4. MATERIAL AND CONSTRUCTION COST OF FRP RETROFITTING

Two alternatives using FRP systems to strengthen a concrete masonry wall are evaluated on direct material and construction costs. The wall dimensions are 28 ft by 15 ft. Strengthening Scheme A (see Figure 7.1) consists of GFRP laminates placed on 40 inches on center; whereas, Strengthening Scheme B (see Figure 7.2) consists of #3 GFRP rods placed at every 10 inches. To be considered structurally equivalents, the amount of reinforcement in both schemes is similar.

7.4.1. Strengthening Scheme A. To complete this alternative, the following activities are normally required:

- Removal of paint from the wall surface by using an abrasive blasting machine.
- Surface preparation of masonry substrate, which includes leveling of uneven surfaces such as mortar joints with a suitable epoxy-based paste. The equipment includes an air compressor, abrasive blasting machine, and grinder.
- Removal of dust from masonry surface using air pressure
- Strengthening of wall with GFRP system by manual lay-up. The materials include GFRP sheets, epoxy saturant, and primer.

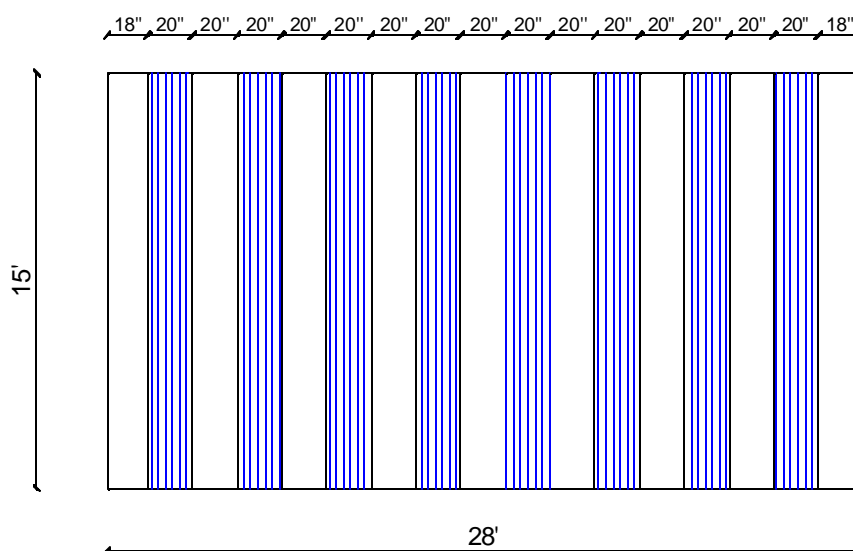


Figure 7.1. Strengthening Scheme A

7.4.2. Strengthening Scheme B. The following activities are normally required to complete this alternative:

- Grooving of vertical slots on the masonry surface using a grinder.
- Removal of dust from slots using air pressure generated by an air compressor.
- Installation of #3 GFRP rods, which are embedded in an epoxy-based paste.

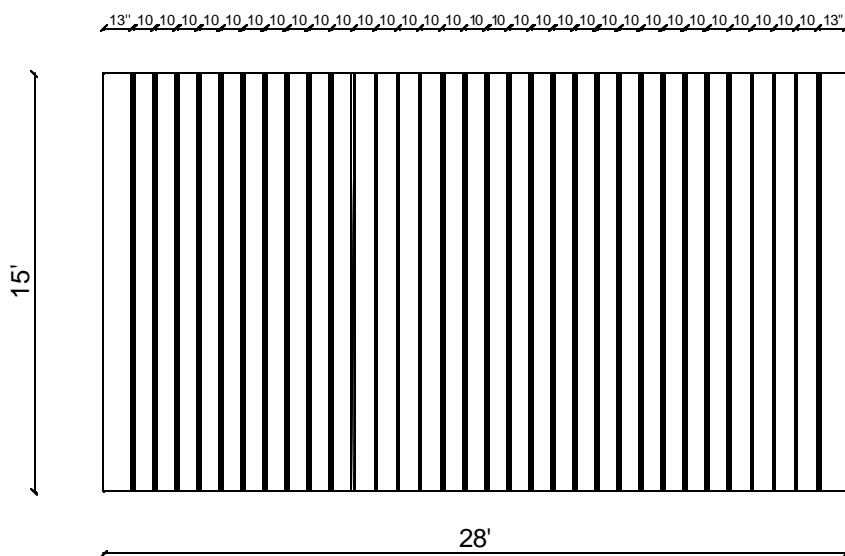


Figure 7.2. Strengthening Scheme B

Based on the described activities, the costs for the execution of schemes A and B were estimated with the assistance of a contractor company with significant experience in the use of FRP composites for infrastructure rehabilitation (see Table 7.2). As a result, it is observed that both alternatives have similar actual costs. In addition, these costs are mostly (70%) labor costs. The cost of labor includes surface preparation and installation. These costs are estimated based on a four-man crew. The cost of material includes the tools needed for the installation of the FRP systems (i.e. rollers, trowels, etc) For the specific case of FRP structural repointing most of the material cost share is attributed to the epoxy-based paste to embed the rods. This cost can diminish if alternative embedding materials having lower costs can be developed.

Table 7.2. Cost Comparison

Item	Strengthening Scheme A	Strengthening Scheme B
Labor	\$6,250.00	\$6,250.00
Equipment	\$1,525.00	\$1,300.00
Material	\$1,200.00	\$ 1,500.00
TOTAL	\$8,975.00	\$9,050.00

7.5. SUMMARY

A method to analyze reconstruction and retrofitting alternatives was presented. It is based on comparison of direct and indirect costs that include up-front and follow-on costs.

The most important characteristic of the cost of typical strengthening work is the predominance of labor and shutdown costs as opposed to material costs, time and site constraints and long-term durability. Advantages of FRP composites versus conventional materials for strengthening of structural and non-structural elements include lower installation costs, improved aesthetics preservation, improved corrosion resistance, on-site flexibility of use, and minimum changes in the member size after repair. In addition, disturbance to the occupants of the facility being retrofitted is minimized. It should be recognized that each retrofitting project is unique, and depending on the project's characteristics, the use of FRP materials can offer a significant total cost reduction.

8. CONCLUSIONS AND FUTURE WORK

The present investigation has demonstrated that FRP composites offer great benefits for the strengthening of masonry elements. FRP systems have been proven to increase remarkably flexure and shear capacities of URM elements. Provisional design protocols and recommendations for proper engineering and installation procedures, which are key to success, are presented.

8.1. MASONRY WALLS UNDER IN-PLANE LOADING

The following conclusions can be drawn from the walls strengthened by FRP structural repointing (Series IL):

- Remarkable improvements of about 100% in shear wall capacity were registered. However it is recognized that this increase can be less when the wall panel interacts with a surrounding structural frame.
- Walls strengthened with same amount of reinforcement, distributed over one or two faces, exhibited similar behavior. However, the contribution of the vertical reinforcement may be fully realized in larger walls where more vertical rods may bridge the diagonal crack.
- In contrast with URM walls, strengthened walls were stable after failure. In a real building, this fact can avoid injuries or loss of human life due to collapse.
- By assuming that the effective stress developed in the FRP rods is equal to a half of the ultimate stress, a provisional design protocol was presented. This assumption needs to be verified studying different strengthening schemes and masonry typology.

For the field evaluation conducted on the walls belonging to Series IF, the following remarks can be made:

- To be effective, FRP shear strengthening depends on the development of the wall flexural capacity, which in turns relies on the anchorage of the existing steel reinforcement. For series IF, construction details such as spacing between steel bars and anchorage of the reinforcement were assumed based on original construction documents, which did not show agreement with the actual detailing after inspecting the test specimens.

- Due to pullout of the vertical reinforcement and the absence of some of the horizontal and vertical steel reinforcing bars, the full benefits of the FRP strengthening were not realized. It is important to note that good performance of the strengthening strategy rests with the building plans, which are assumed to have been materialized following adequate construction standards.
- In spite of the difficulties found during the execution of this experimental program, the test results demonstrated that, under in-plane loading, the use of FRP rods confined to the toe region of the walls were able to increase the flexural capacity and provide a ductile behavior for masonry walls.

8.2. MASONRY WALLS UNDER OUT-OF-PLANE LOADING

The singular opportunity of testing URM Walls at the Malcolm Bliss Hospital (series OF), allowed to conclude the following:

- A mechanism of failure that is not commonly observed in tests performed in a laboratory environment was identified, where simply supported boundary conditions are considered. This mechanism of failure is not usually considered in the quantification of upgraded wall capacities, which can dangerously lead to overestimate the wall response during a seismic event.
- In addition, it was observed that the wall where the FRP laminates were applied directly to the masonry surface, after the removal of plaster, exhibited a better performance than its counterpart, strengthened without the removal of plaster. The increase in capacity was about 17 % compared to the wall strengthened with the presence of plaster, and 45 % compared to the control wall without plaster. Therefore, it is recommended to remove any plaster or paint layer before the strengthening of masonry walls.
- The use of NSM rods is attractive since the removal of plaster is not required. To avoid the creation of local damage in masonry walls, special care needs to be taken during their installation.
- In order to fully realize the benefits of the use of FRP composites, the strengthening techniques should address the boundary components. For the test walls investigated

herein, one strengthening alternative could be to grout the tiles to force the failure to occur into the FRP rather than in the boundary regions.

- An analytical model is presented for determining the transverse load that both unreinforced and externally strengthened infill walls can resist. The model shows adequate correlation with experimental results.

Finally, a provisional design protocol, which is based on experimental results reported by previous investigations, is presented. From this protocol the following can be concluded:

- The design protocol provides a good correlation between experimental and expected flexural capacities.
- From previous investigations, debonding of the FRP laminate from the masonry surface is considered to be the governing mode of failure.
- The effective strain in the laminates is assumed to be 0.008 in./in. The assumptions taken for the masonry material are based on the MSJC provisions.

8.3. FUTURE WORK

The following recommendations for future work are formulated:

- For masonry walls strengthened with FRP laminates, research results have shown that debonding of the FRP laminate from the masonry substrate is the controlling mechanism of failure (Schwegler et al., 1995; Hamilton et al., 1999; Velazquez et al., 2000). This has been evident from test results conducted on masonry walls strengthened to resist either in-plane or out-of-plane loads. Therefore, there is a need to determine the effective strain of the laminate as a function of the amount of strengthening. Since debonding may have a direct relationship with the porosity of the masonry unit, the determination of the effective laminate strain, walls built with different and representative types of masonry units should be investigated.
- For the developing of design protocols for the flexural strengthening of URM walls under out-of-plane loads, different amounts of FRP reinforcement can be studied to observe its incidence in different modes of failure such as rupture or laminate, debonding and shear. Other variables to be studied should include different types of FRP materials, masonry surfaces, and wall slenderness ratios.

- Based on the premise of debonding as a controlling mode of failure, anchorage systems to avoid collapse of the wall need be developed. The use of NSM rods is an alternative to be investigated.
- For masonry walls strengthened by FRP structural repointing, the effective strain developed in the rods needs to be estimated for different strengthening schemes (i.e. spacing of rods) and masonry typologies.
- For FRP structural repointing, more economical embedding materials to encapsulate the FRP rods in the mortar joints need to be explored. These materials might be mortars with improved bond properties, which can transfer tensile stresses to the reinforcement.
- It is important to investigate the interaction of strengthened walls with the surrounding structural elements (i.e. beams and columns) since the effectiveness of the strengthening may be dangerously overestimated due to premature failures in the masonry or structural elements.
- Investigation on surface preparation methods and amount of impregnating resins is also needed. To date, there is a tendency to use types and quantities of resin similar to those used for the strengthening of RC elements. For instance, there is a predisposition in the construction industry to use the impregnating resins, used for bonding the fibers, to prime the masonry surface. This is attributed to economical reasons because the amount of required primer increases due to the high initial rate of absorption of masonry.

APPENDIX A

SERIES IL

Appendix A.1: Strengthening Schemes

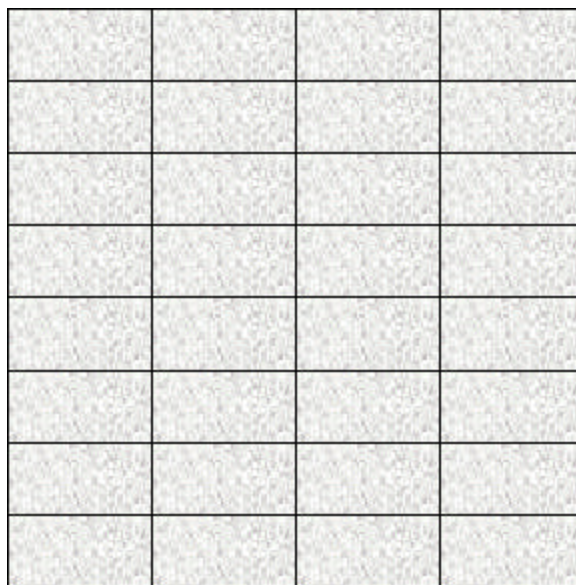


Figure A.1 - 1. Control Specimens – Walls IL1-a and IL1-b

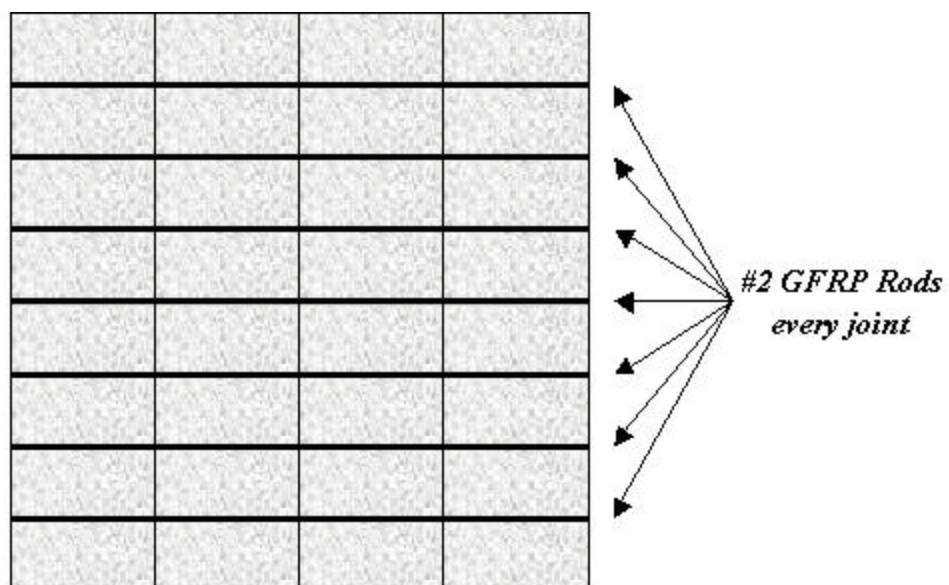


Figure A.1 - 2. Strengthening Scheme for Wall IL2

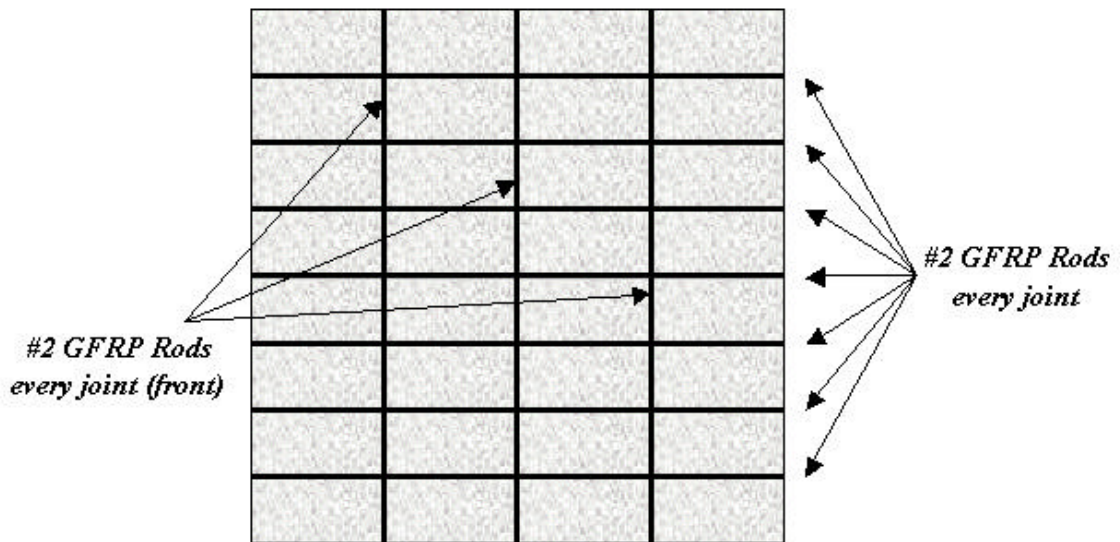


Figure A.1 - 3. Strengthening Scheme for Wall IL3

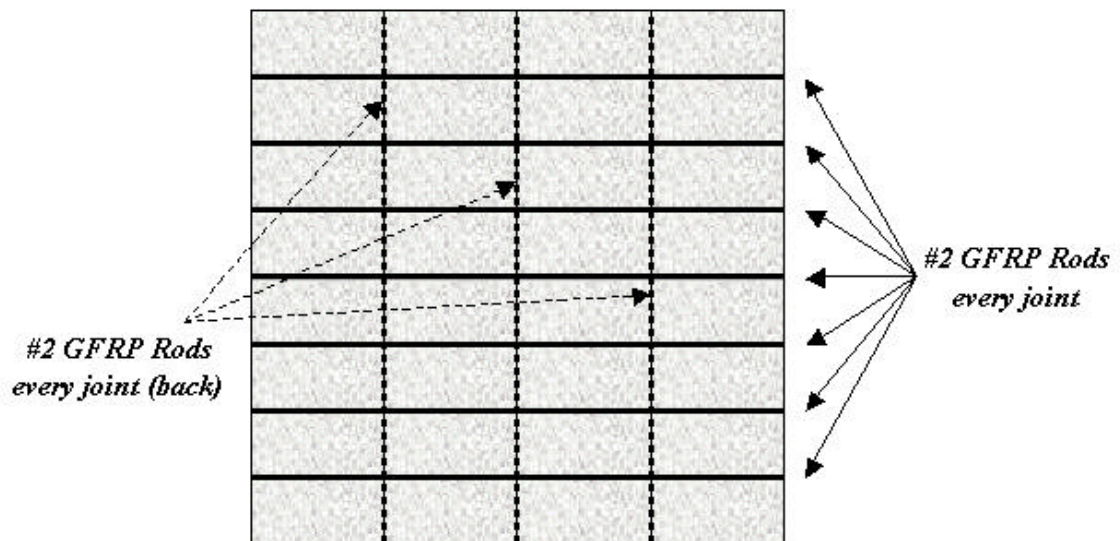


Figure A.1 - 4. Strengthening Scheme for Wall IL4

Appendix A.2: Test Results

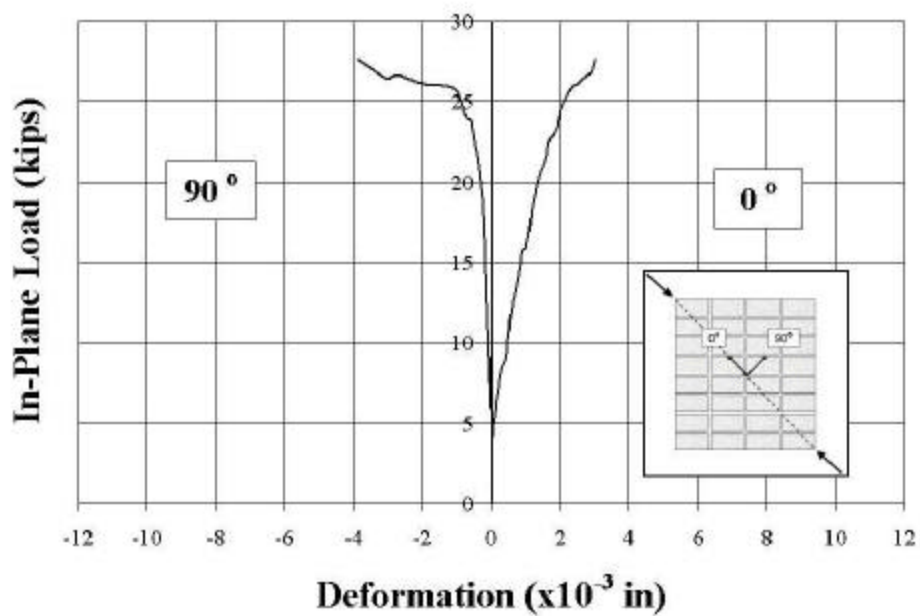


Figure A.2 - 1. In-Plane Load vs. Deformation – Wall IL1-a (Front)

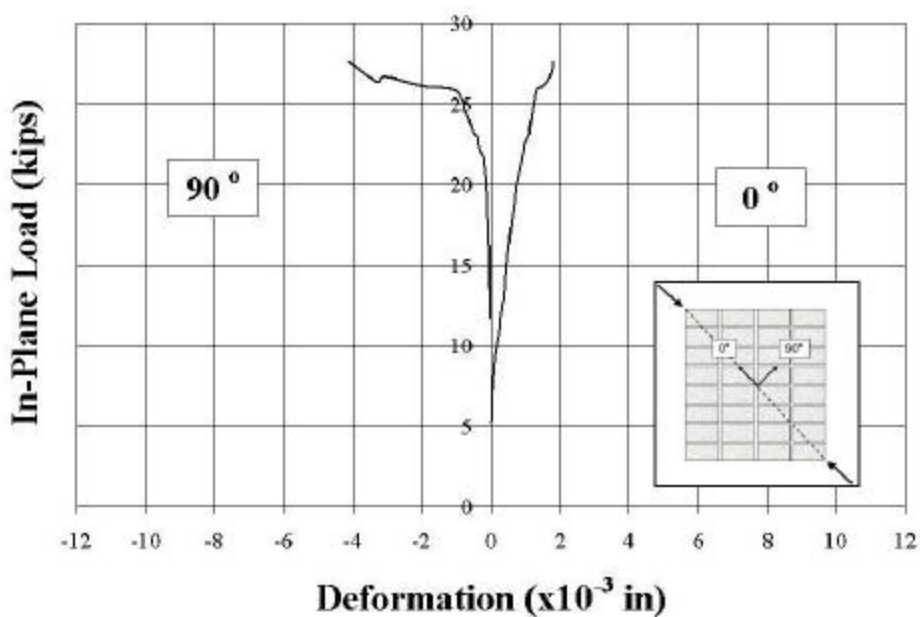


Figure A.2 - 2. In-Plane Load vs. Deformation – Wall IL1-a (Back)

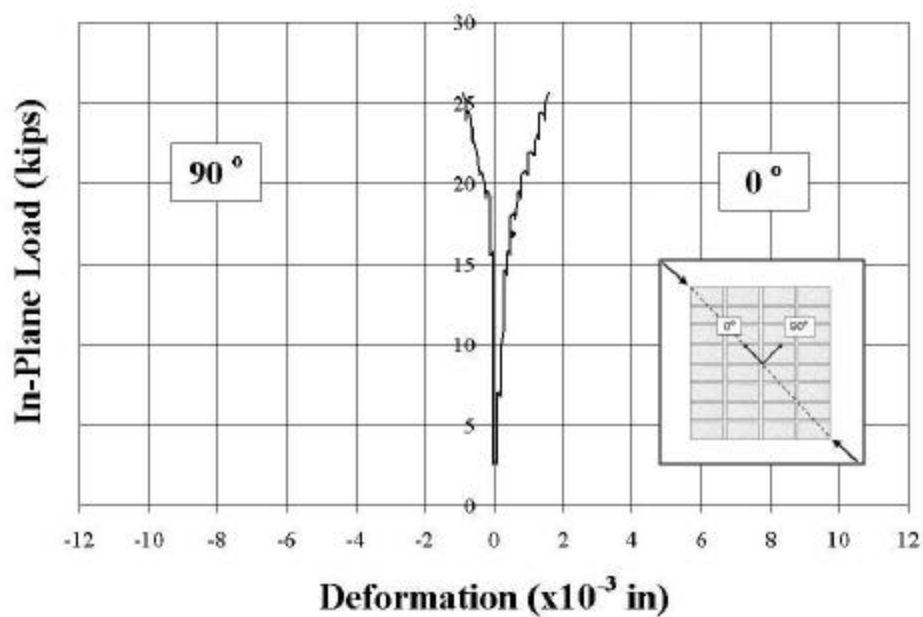


Figure A.2 - 3. In-Plane Load vs. Deformation – Wall IL1-b (Front)

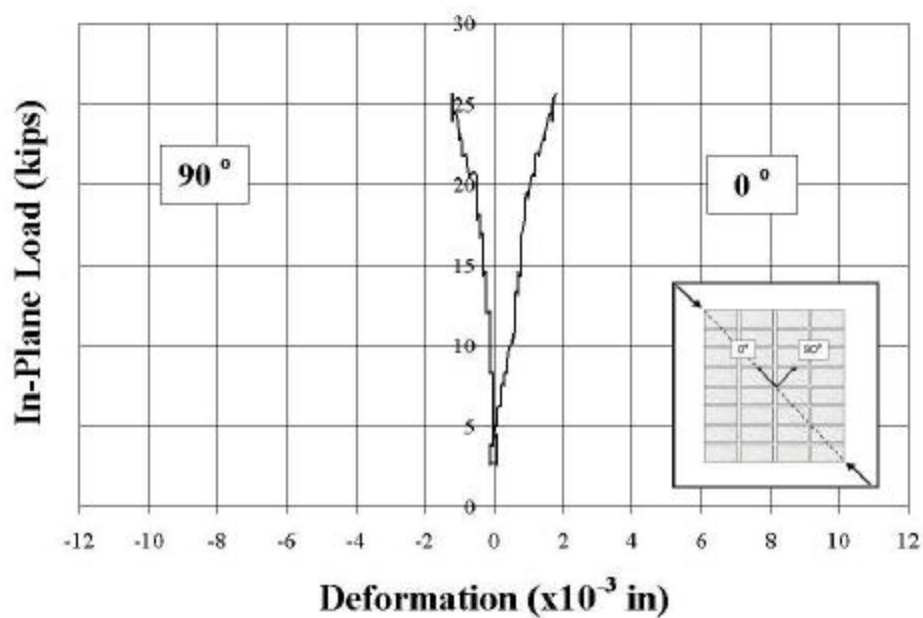


Figure A.2 - 4. In-Plane Load vs. Deformation – Wall IL1-b (Back)

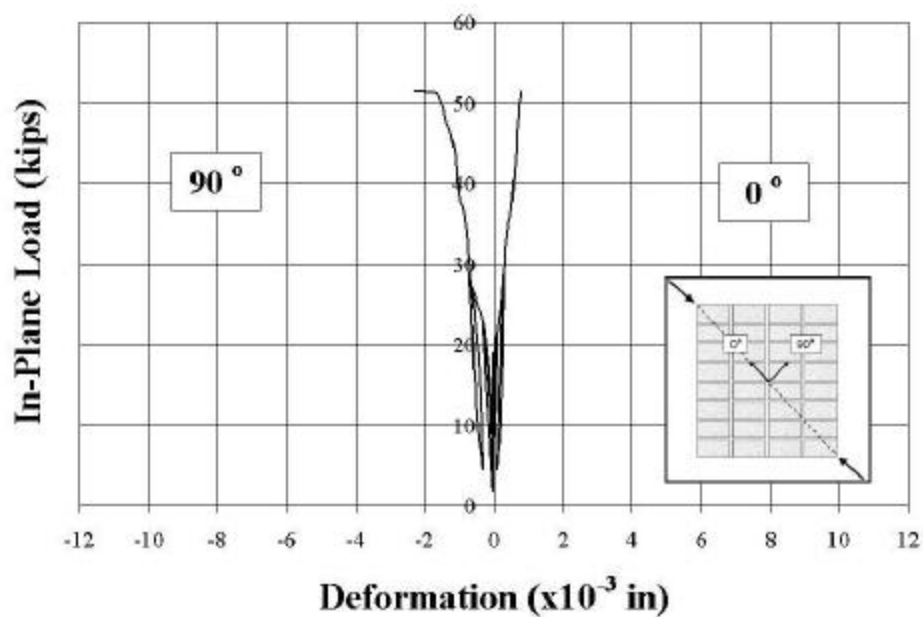


Figure A.2 - 5. In-Plane Load vs. Deformation – Wall IL2 (Front)

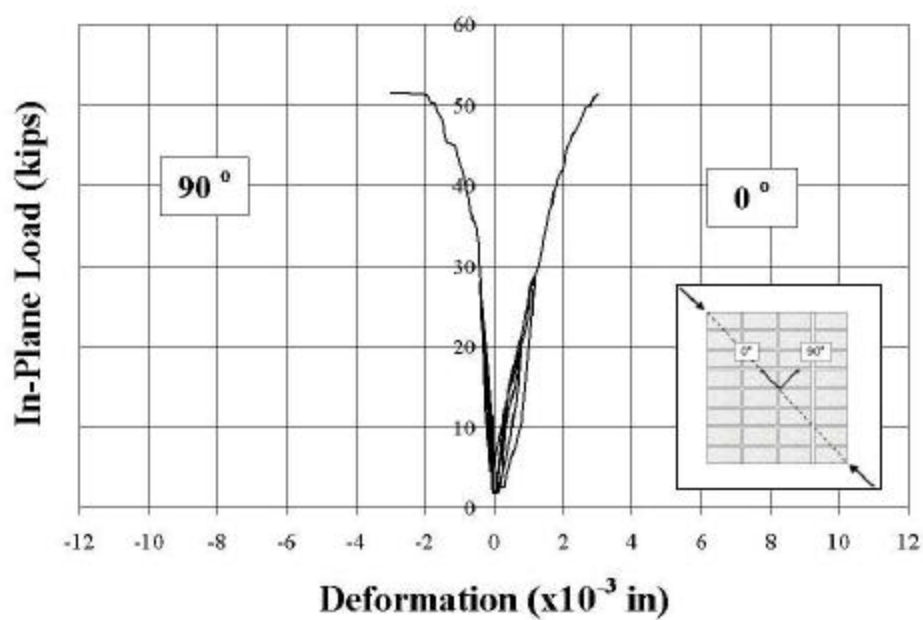


Figure A.2 - 6. In-Plane Load vs. Deformation – Wall IL2 (Back)

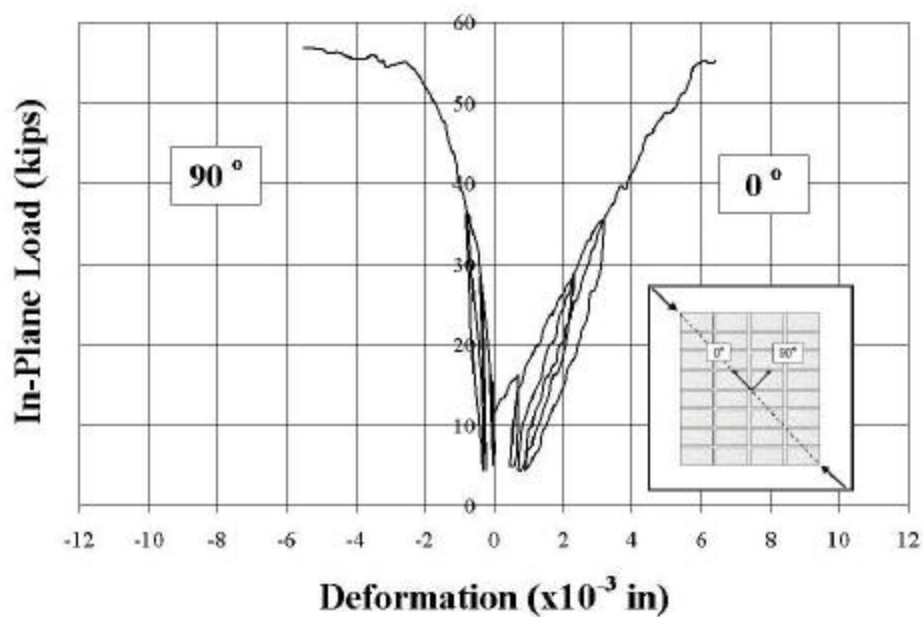


Figure A.2 - 7. In-Plane Load vs. Deformation – Wall IL3 (Front)

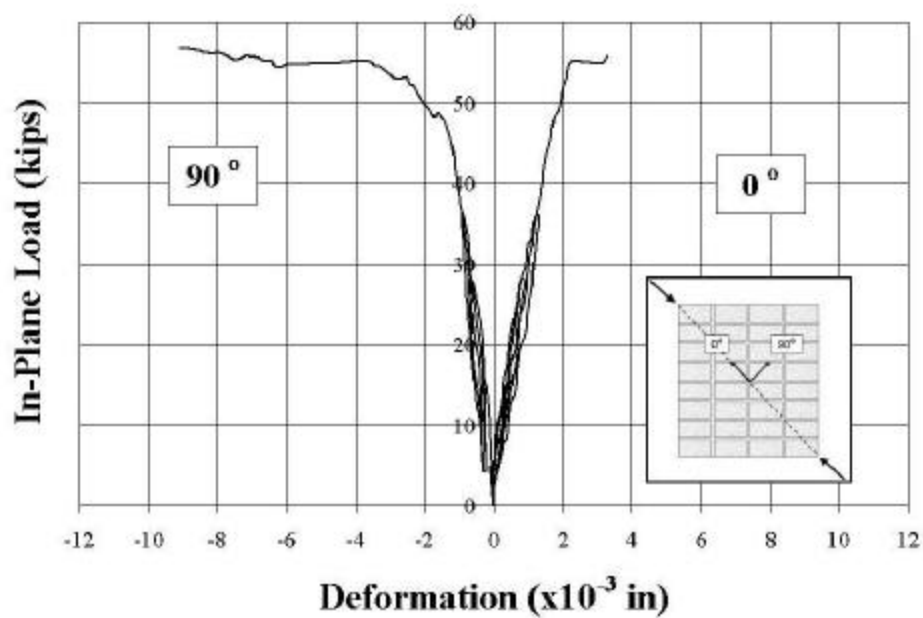


Figure A.2 - 8. In-Plane Load vs. Deformation – Wall IL3 (Back)

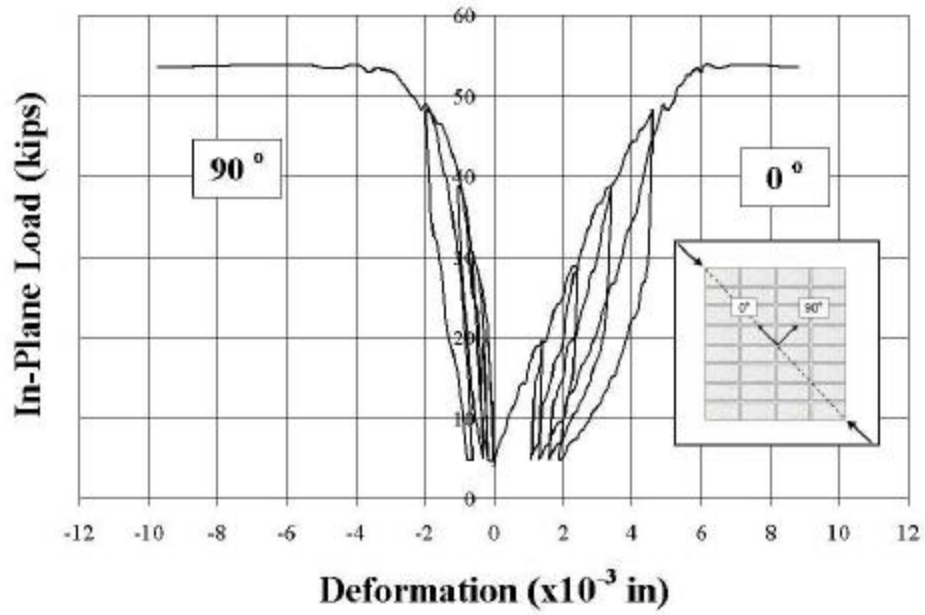


Figure A.2 - 9. In-Plane Load vs. Deformation – Wall IL4 (Front)

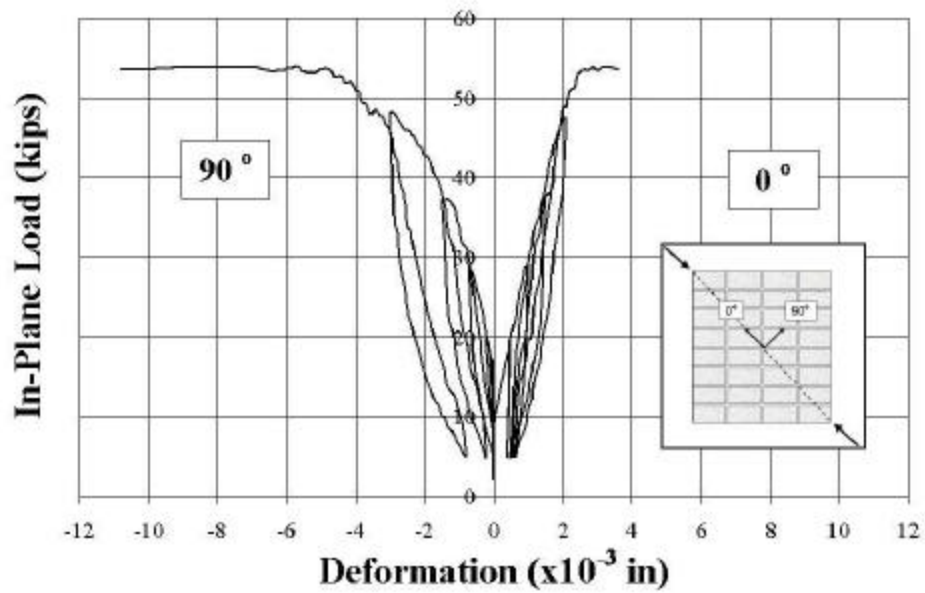


Figure A.2 - 10. In-Plane Load vs. Deformation – Wall IL4 (Back)

Appendix A.3: Cracking Patterns

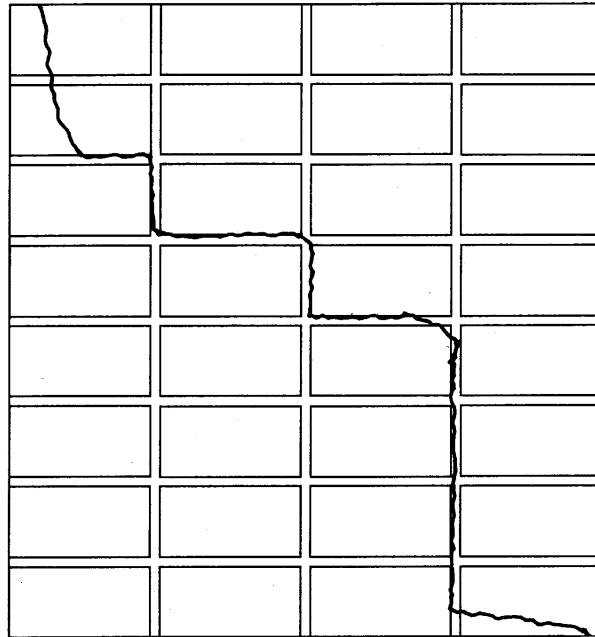


Figure A.3 - 1. Cracking Pattern – Wall IL1-a

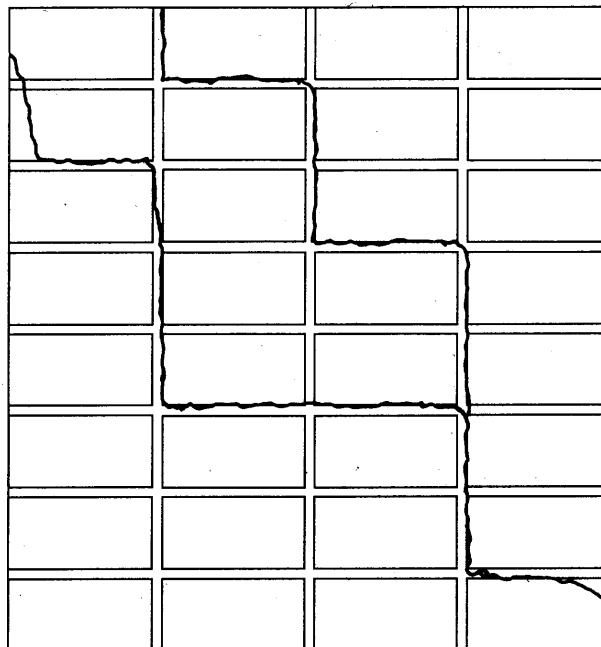


Figure A.3 - 2. Cracking Pattern – Wall IL1-b

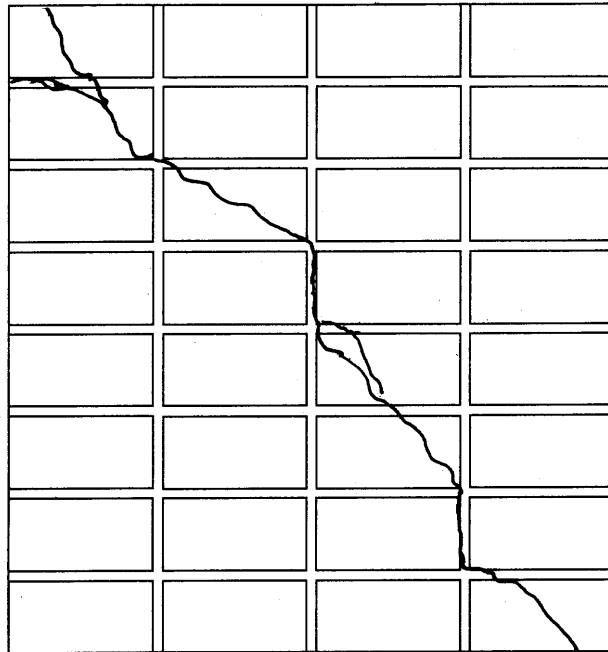


Figure A.3 - 3. Cracking Pattern – Wall IL2 (Front)

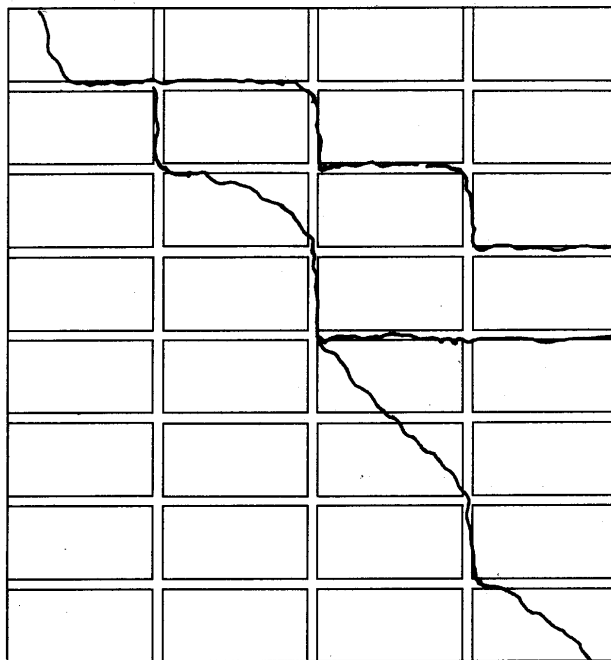


Figure A.3 - 4. Cracking Pattern – Wall IL2 (Back)

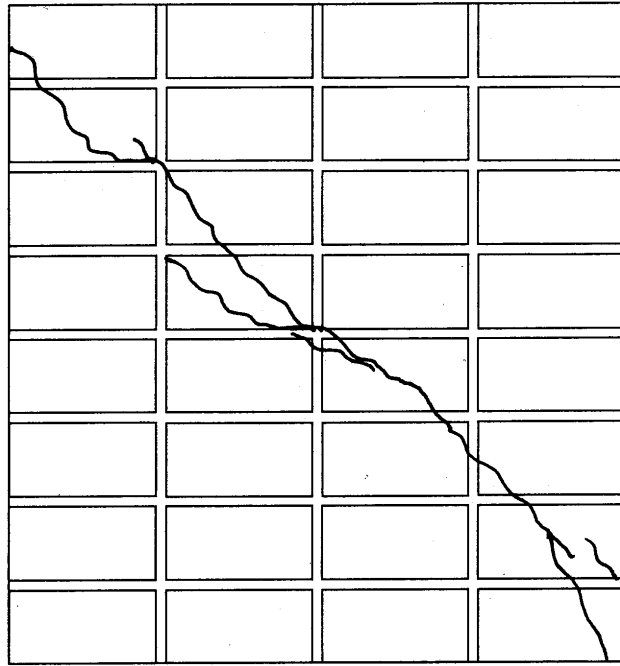


Figure A.3 - 5. Cracking Pattern – Wall IL3 (Front)

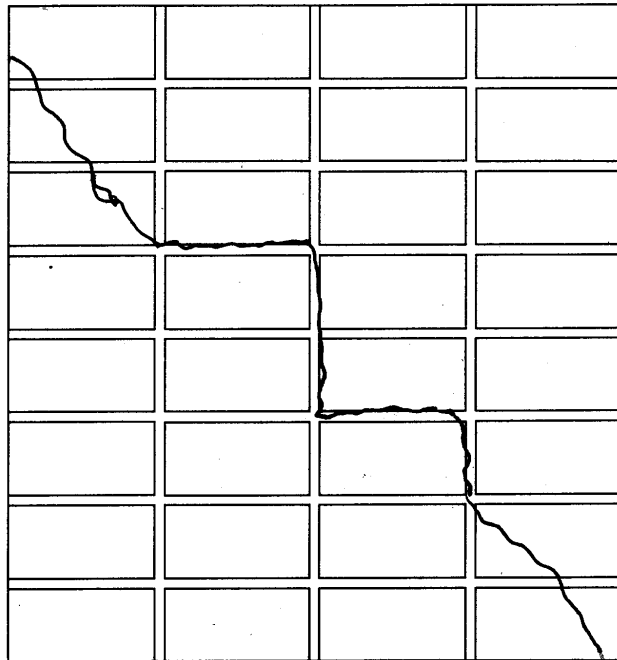


Figure A.3 - 6. Cracking Pattern – Wall IL3 (Back)

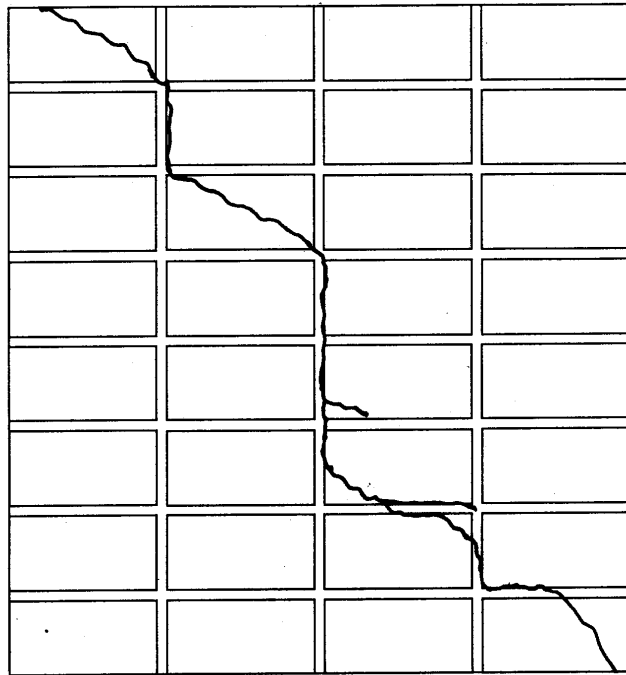


Figure A.3 - 7. Cracking Pattern – Wall IL4 (Front)

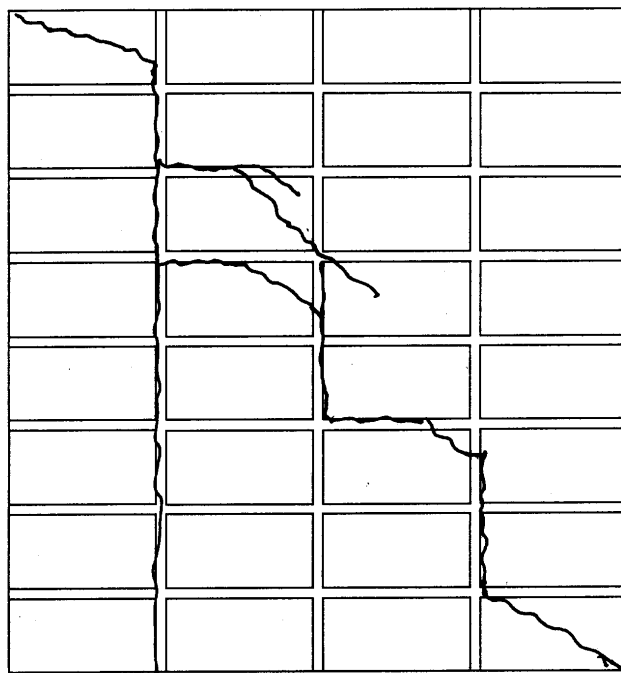


Figure A.3 - 8. Cracking Pattern – Wall IL4 (Back)

Appendix A.4: Photographs



Figure A.4 - 1. Overall View of Test Specimens



Figure A.4 - 2. View of Test Setup



Figure A.4 - 3. View of Hydraulic Jacks



Figure A.4 - 4. Wall IL1-b after collapsing



Figure A.4 - 5. Crack on front side –Wall IL2



Figure A.4 - 6. Crack on back side –Wall IL2



Figure A.4 - 7. Crack on front side –Wall IL3



Figure A.4 - 8. Crack on back side –Wall IL3

APPENDIX B

SERIES IF

Appendix B.1: Strengthening Schemes

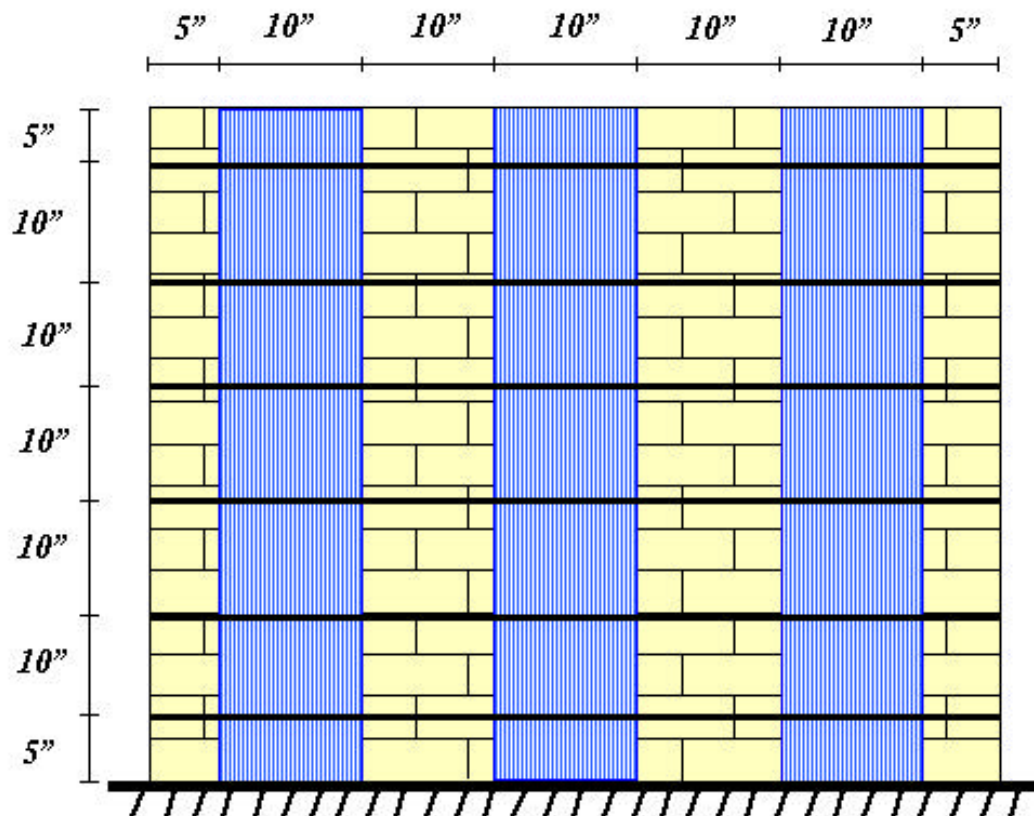
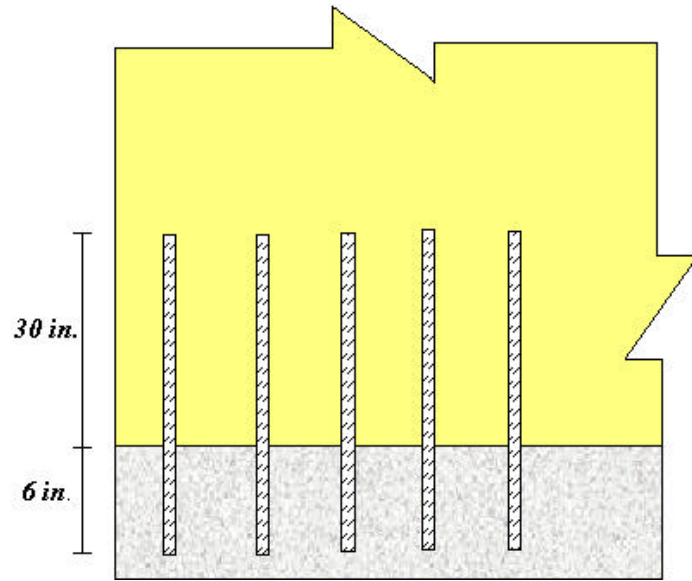


Figure B.1 - 1. Strengthening Scheme for Walls IF2 and IF3



Elevation View

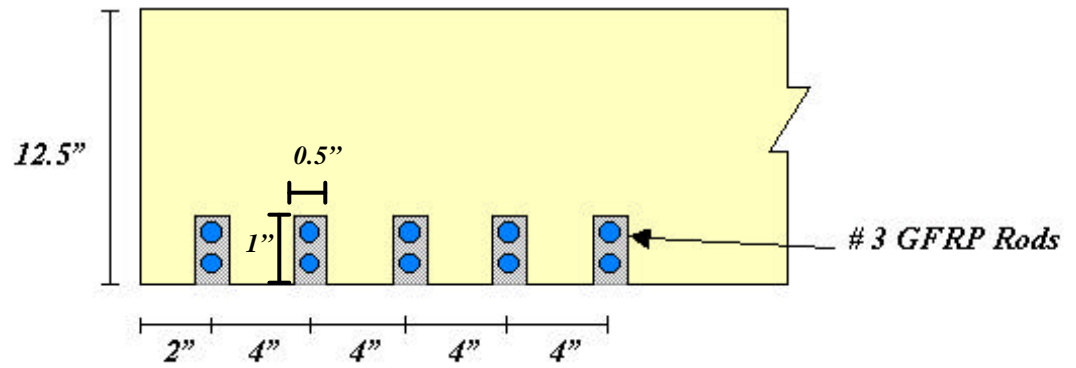


Figure B.1 - 2. #3 GFRP rods in one toe region of Wall IF3

Appendix B.2: Test Results

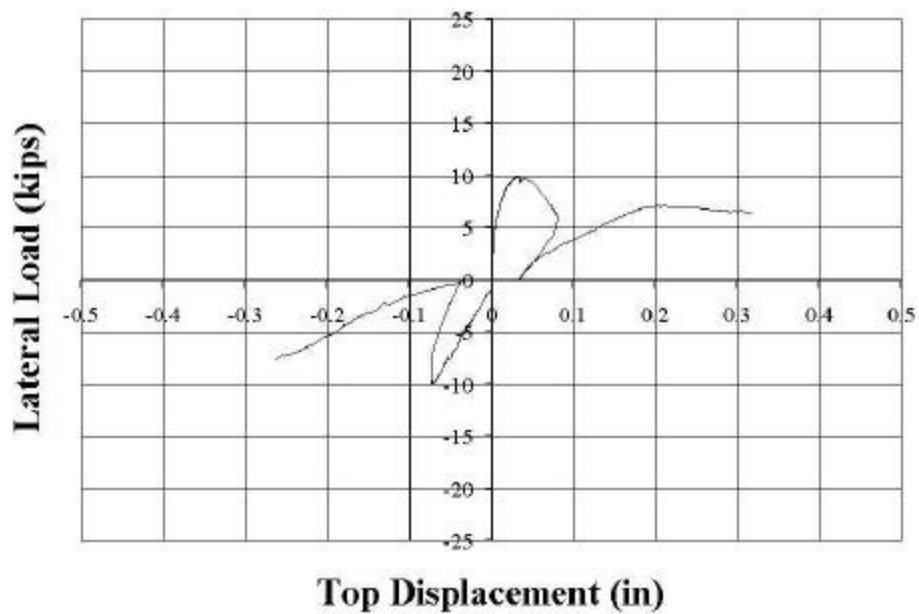


Figure B.2 - 1. Lateral Load vs. Top Displacement – Wall IF1

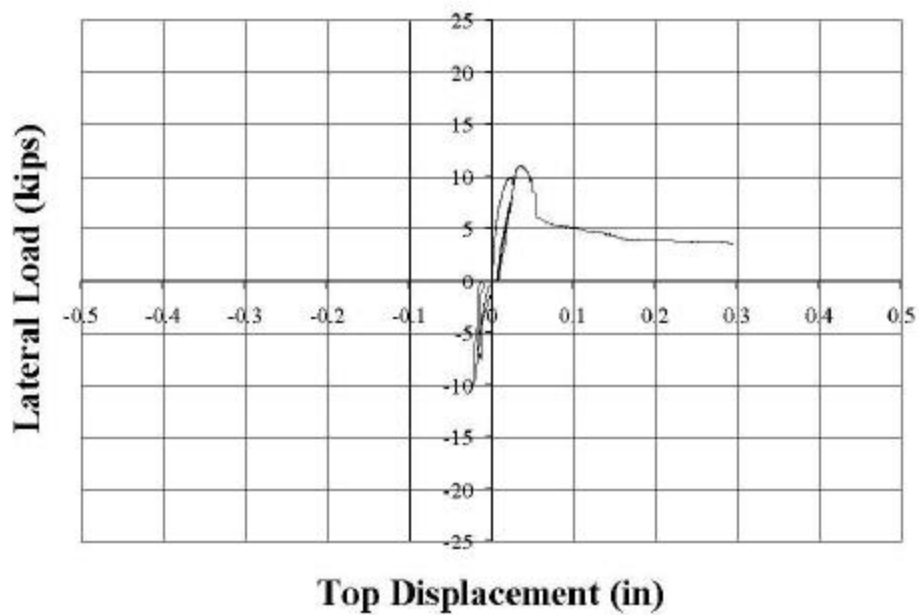


Figure B.2 - 2. Lateral Load vs. Top Displacement – Wall IF2

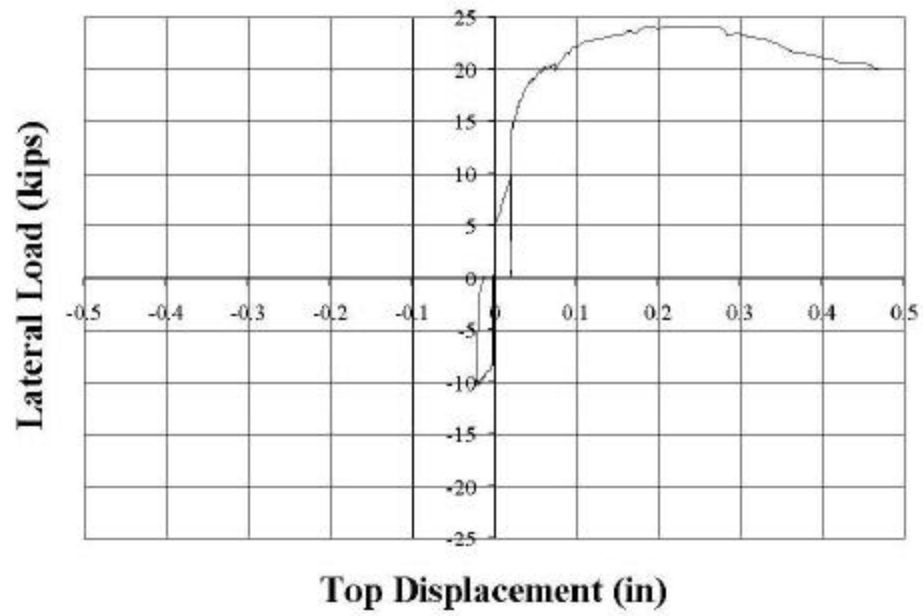
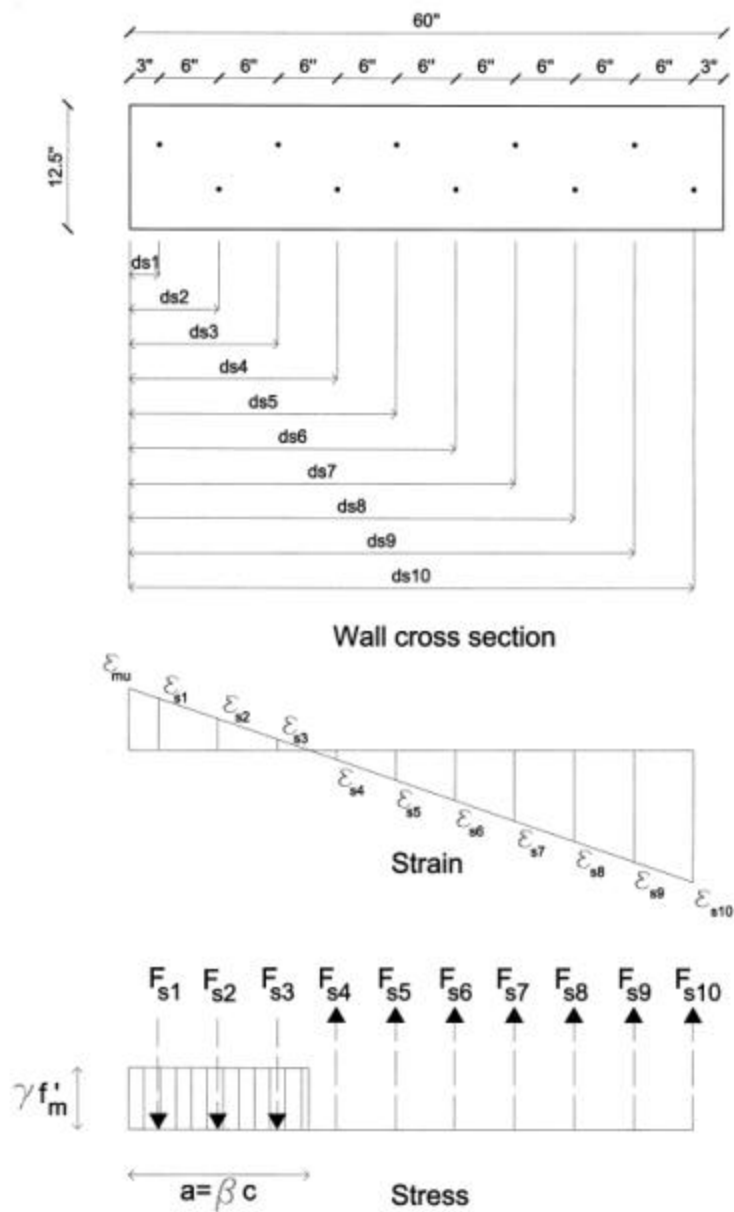


Figure B.2 - 3. Lateral Load vs. Top Displacement – Wall IF3

Appendix B.3: Supporting Calculations

B.3-1: Computation of Flexural Capacity of Wall without Toe Reinforcement



Wall Dimensions

c = 3.9 in
 Length = 60 in
 Height = 60 in

Masonry

ϵ_{mu} = 0.0035 (clay masonry)
 f'_m = 1400 psi
 b = 12.5 in
 $0.72f'_mcb$ = 49.14 kips

Steel

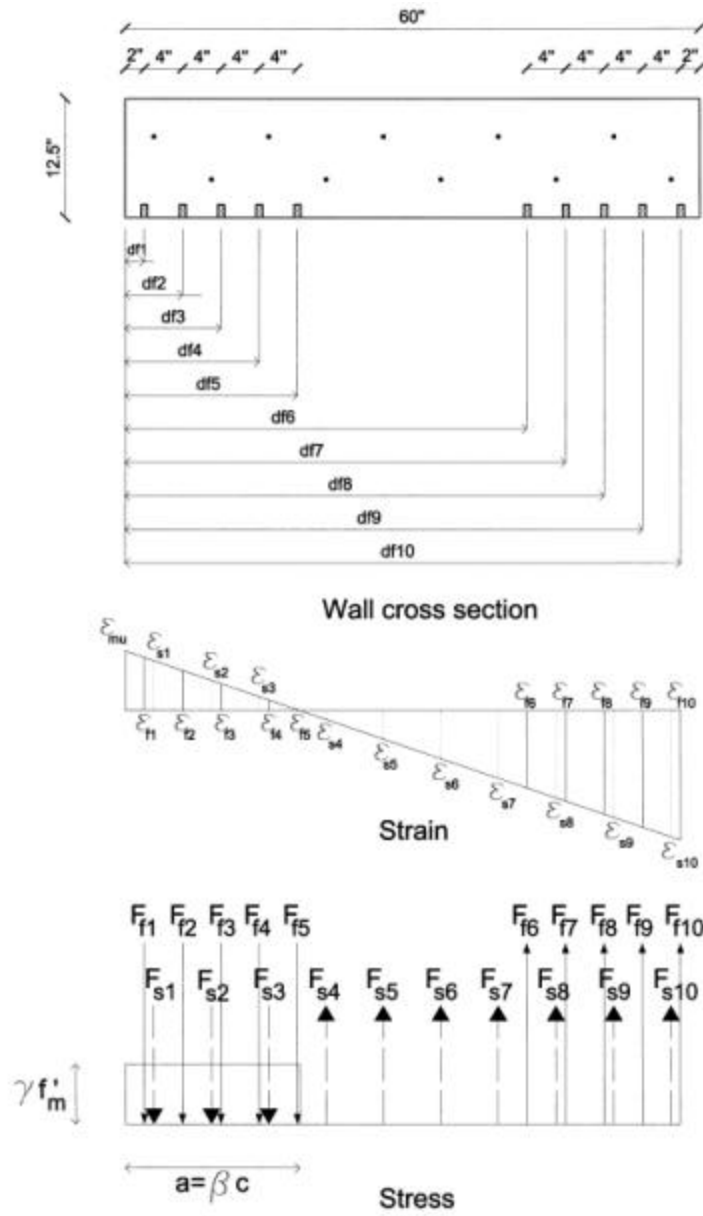
A_s = 0.11 in²
 f_{sy} = 50 ksi
 E_s = 29000 ksi

# Steel	Dist. from Compression Fiber (in)	Stresses (ksi)	Forces (kips)	Arm = di-L/2 (in)	Moment (in-kips)
1	d= 3	fs= -23.4	Fs= -2.6	-27	69.6
2	d= 9	fs= 132.7	Fs= 5.5	-21	-115.5
3	d= 15	fs= 288.9	Fs= 5.5	-15	-82.5
4	d= 21	fs= 445.0	Fs= 5.5	-9	-49.5
5	d= 27	fs= 601.2	Fs= 5.5	-3	-16.5
6	d= 33	fs= 757.3	Fs= 5.5	3	16.5
7	d= 39	fs= 913.5	Fs= 5.5	9	49.5
8	d= 45	fs= 1069.7	Fs= 5.5	15	82.5
9	d= 51	fs= 1225.8	Fs= 5.5	21	115.5
10	d= 57	fs= 1382.0	Fs= 5.5	27	148.5

Ms= 218.1
 Mm= 1392.8

M= 1610.8 in-kips
 V= 26.8 kips

B.3-1: Computation of Flexural Capacity of Wall with Toe Reinforcement



Wall Dimensions

c =	10.6	in
Length =	60	in
Height =	60	in

Masonry

ϵ_{mu} =	0.0035	(clay masonry)
f_m =	1400	psi
b =	12.5	in
$0.72f_mcb$ =	133.56	kips

Steel

A_s =	0.11	in ²
f_{sy} =	50	ksi
E_s =	29000	ksi

FRP

A_f =	0.22	in ²
f_{fu} =	120	ksi
E_f =	6000	ksi

# Steel	Dist. from Compression Fiber (in)	Stresses (ksi)	Forces (kips)	Arm = di-L/2 (in)	Moment (in-kips)
1	d= 3	fs= -72.8	Fs= -5.5	-27	148.5
2	d= 9	fs= -15.3	Fs= -1.7	-21	35.4
3	d= 15	fs= 42.1	Fs= 4.6	-15	-69.5
4	d= 21	fs= 99.6	Fs= 5.5	-9	-49.5
5	d= 27	fs= 157.0	Fs= 5.5	-3	-16.5
6	d= 33	fs= 214.5	Fs= 5.5	3	16.5
7	d= 39	fs= 271.9	Fs= 5.5	9	49.5
8	d= 45	fs= 329.4	Fs= 5.5	15	82.5
9	d= 51	fs= 386.8	Fs= 5.5	21	115.5
10	d= 57	fs= 444.3	Fs= 5.5	27	148.5
Ms=					460.9

# FRP	Dist. from Compression Fiber (in)	Stresses (ksi)	Forces (kips)	Arm = di-L/2 (in)	Moment (in-kisp)
1	d= 2	ff= -17.0	Ff= -3.7	-28	105.0
2	d= 6	ff= -9.1	Ff= -2.0	-24	48.1
3	d= 10	ff= -1.2	Ff= -0.3	-20	5.2
4	d= 14	ff= 6.7	Ff= 1.5	-16	-23.7
5	d= 18	ff= 14.7	Ff= 3.2	-12	-38.7
6	d= 42	ff= 62.2	Ff= 13.7	12	164.2
7	d= 46	ff= 70.1	Ff= 15.4	16	246.9
8	d= 50	ff= 78.1	Ff= 17.2	20	343.4
9	d= 54	ff= 86.0	Ff= 18.9	24	454.0
10	d= 58	ff= 93.9	Ff= 20.7	28	578.5

Mf= 1882.9

Mm= 3405.1

M= 5748.9 in-kips

V= 95.8 kips

Appendix B.4: Photographs



Figure B.4 - 1. Installation of GFRP Laminates



Figure B.4 - 2. Installation of GFRP Rods



Figure B.4 - 3. Preparation of Test Setup

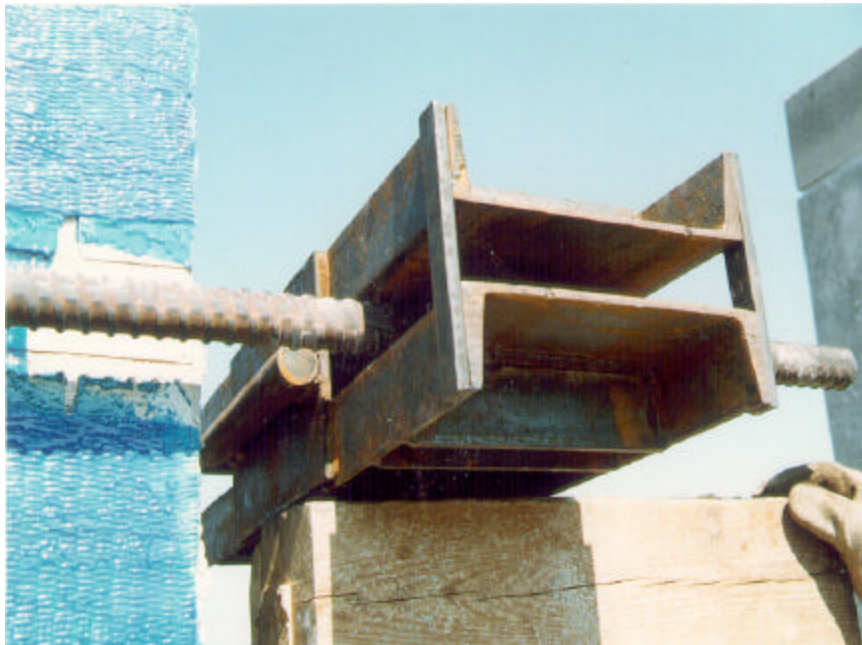


Figure B.4 - 4. Reaction Beam



Figure B.4 - 5. View of the unstrengthened sides



Figure B.4 - 6. Rocking of Wall

APPENDIX C

SERIES OF

Appendix C.1: Strengthening Schemes

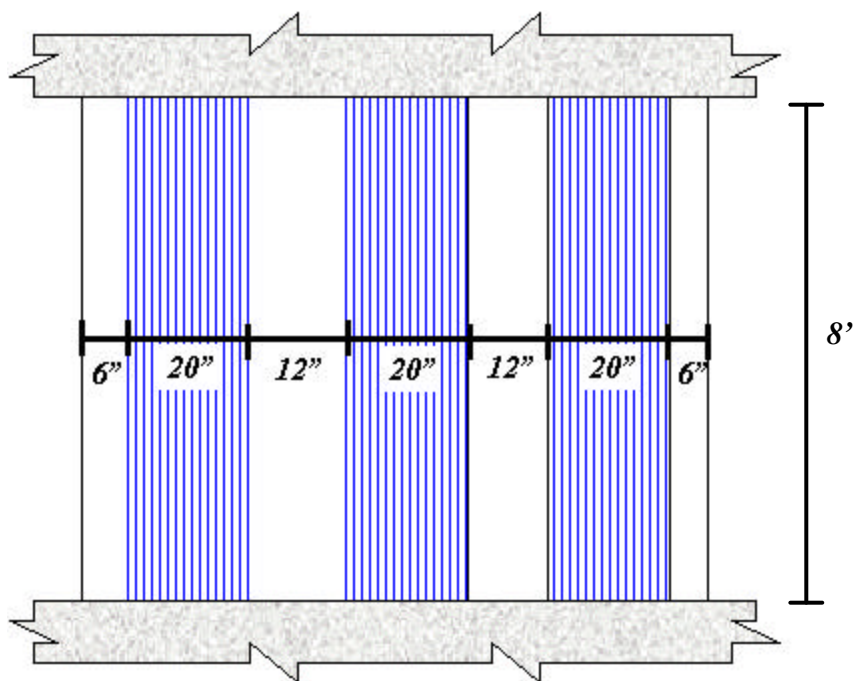


Figure C.1 - 1. Strengthening Scheme for Walls OF3, OF4, OF6 and OF7

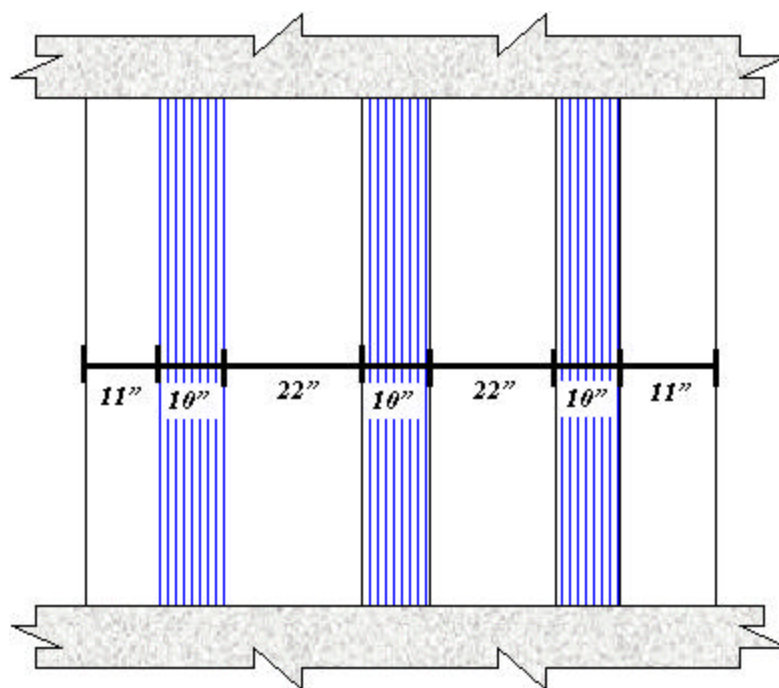


Figure C.1 - 2. Strengthening Scheme for Wall OF5

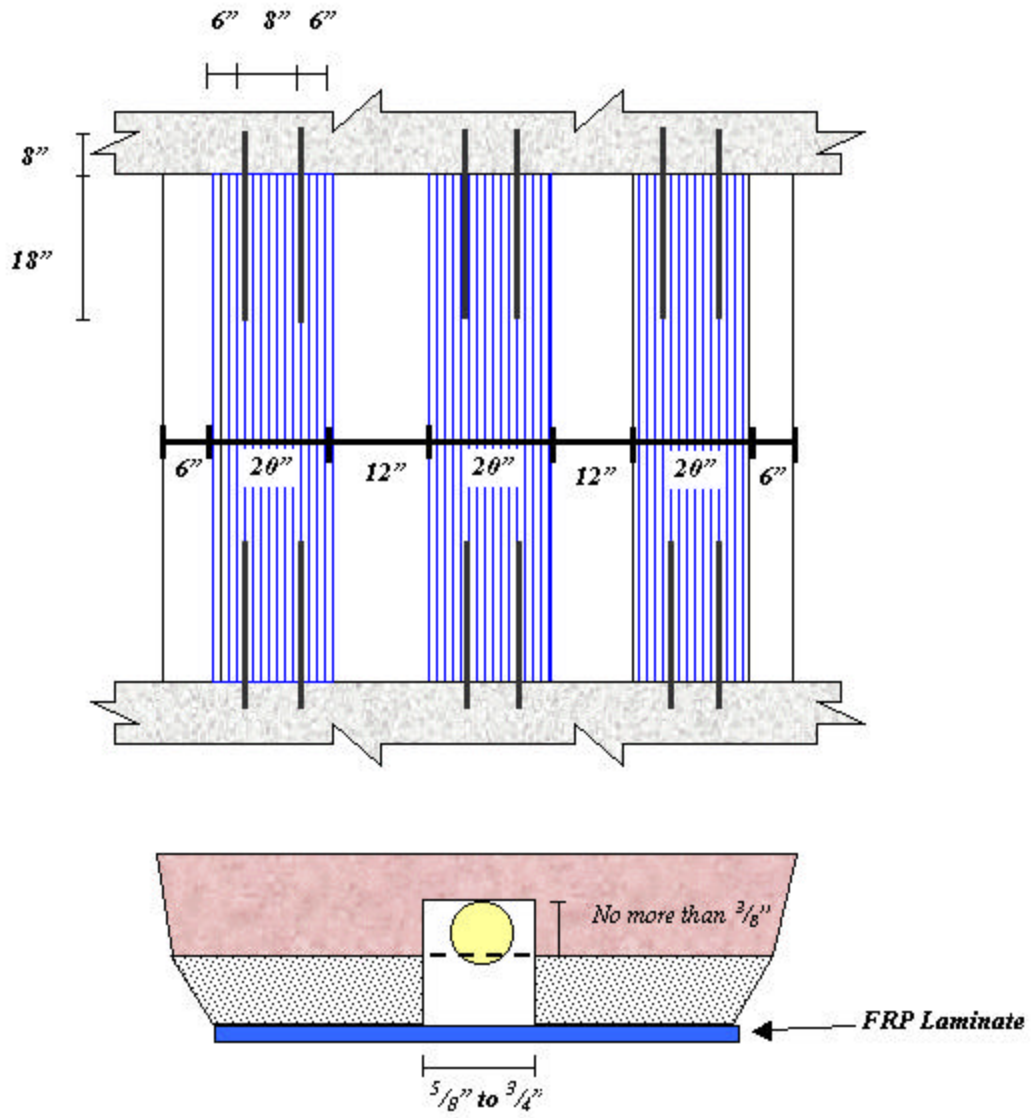


Figure C.1 - 3. Strengthening Scheme for Wall OF8

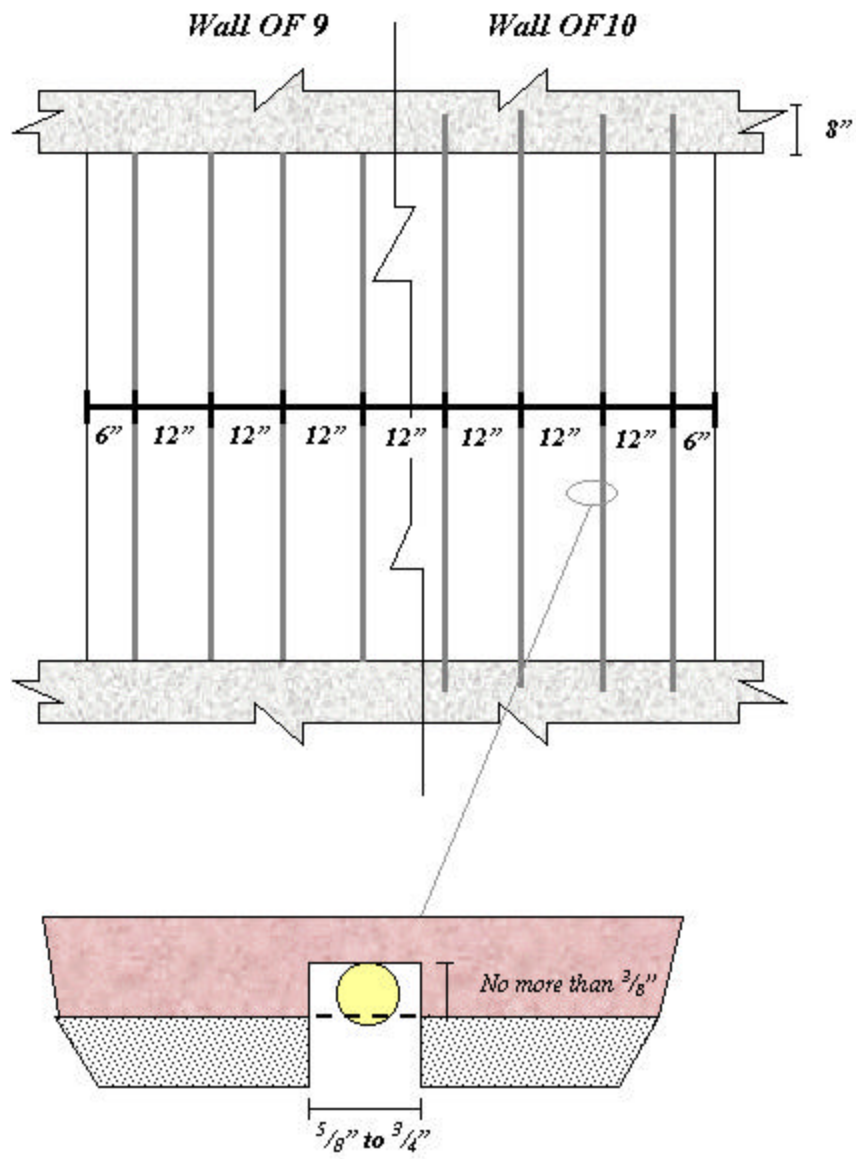


Figure C.1 - 4. Strengthening Scheme for Walls OF9 and OF10

Appendix C.2: Test Results

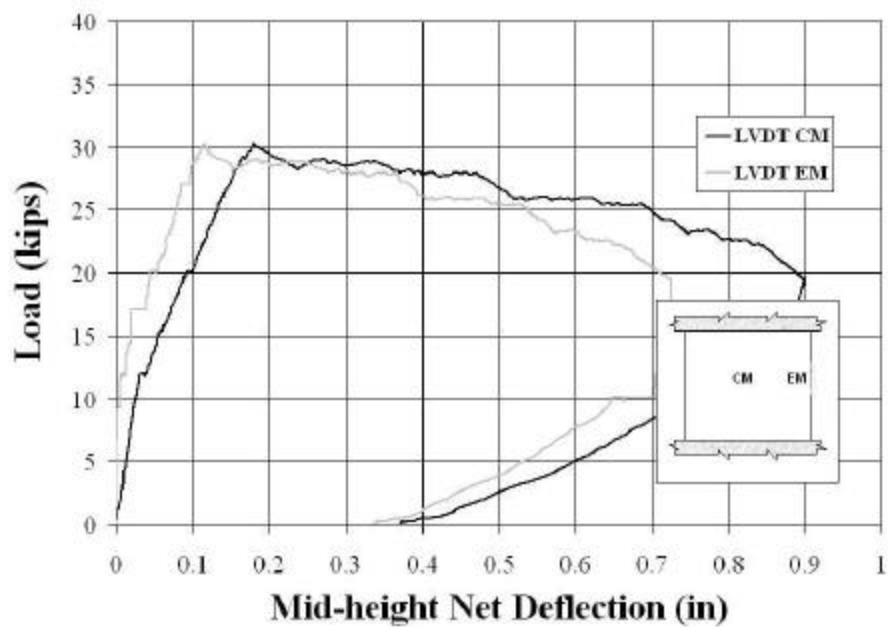


Figure C.2 - 1. Two-way Action – Wall OF1

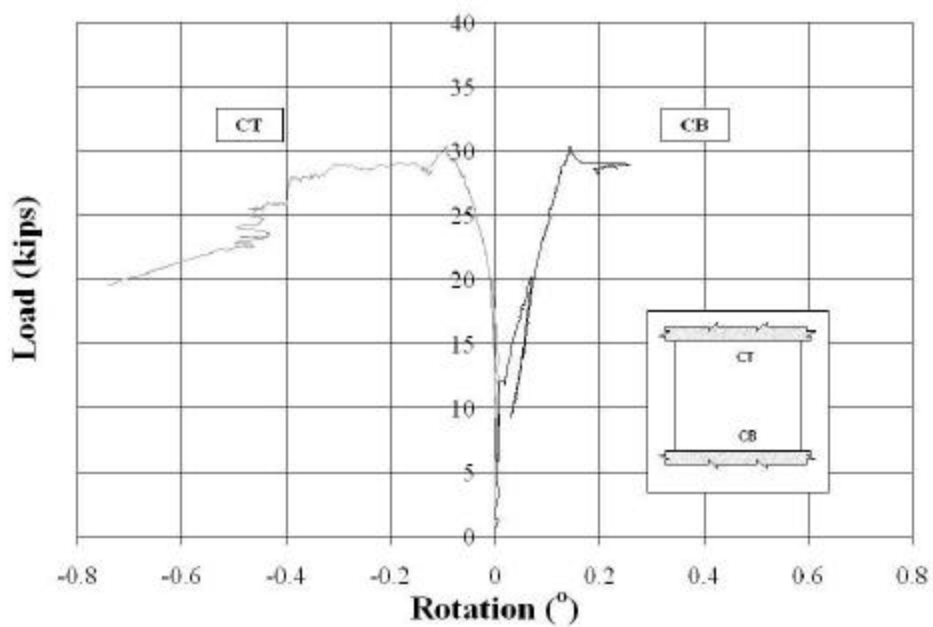


Figure C.2 - 2. Out-of-Plane Load vs. Rotation - Wall OF1

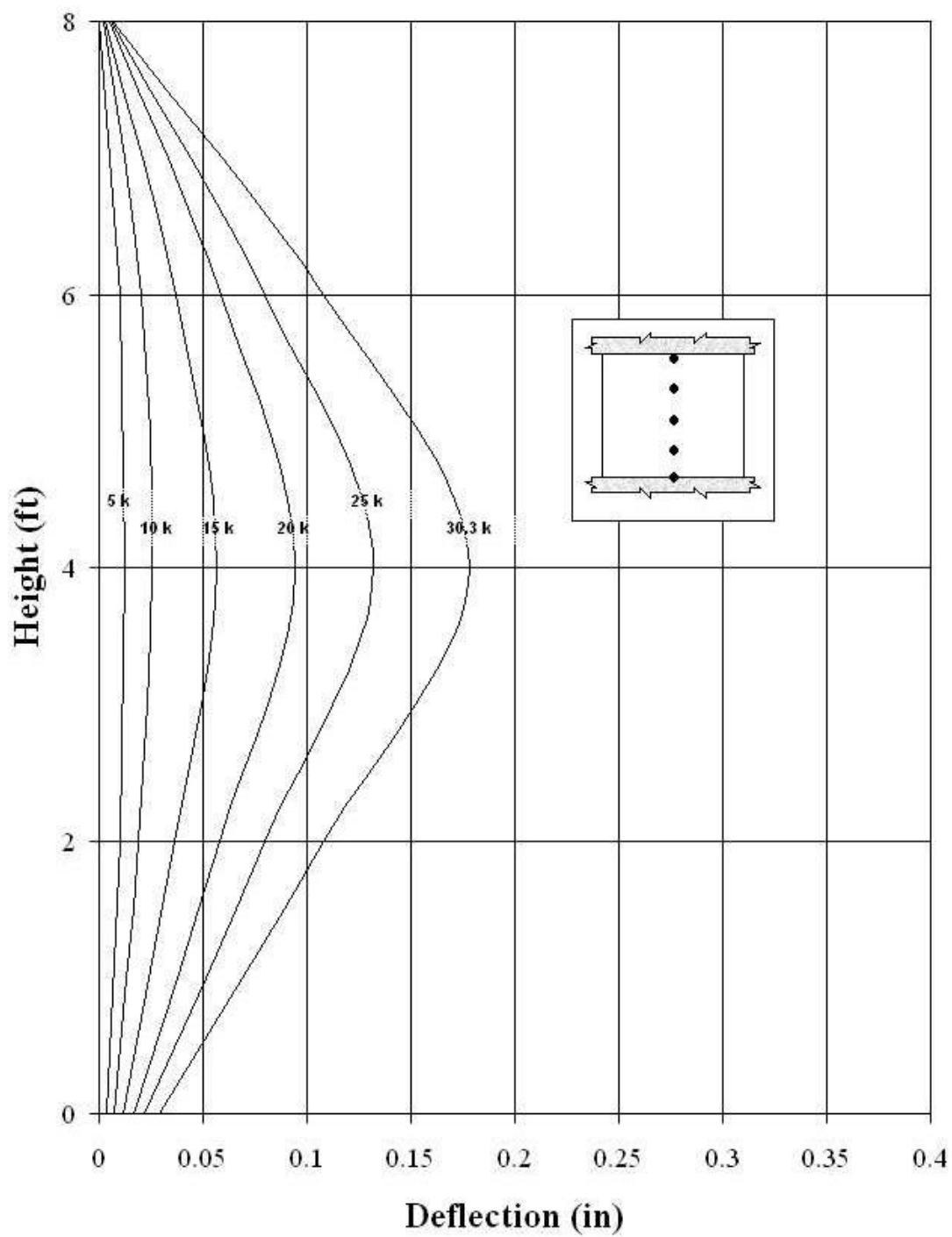


Figure C.2 - 3. Height vs. Deflection – Wall OF1

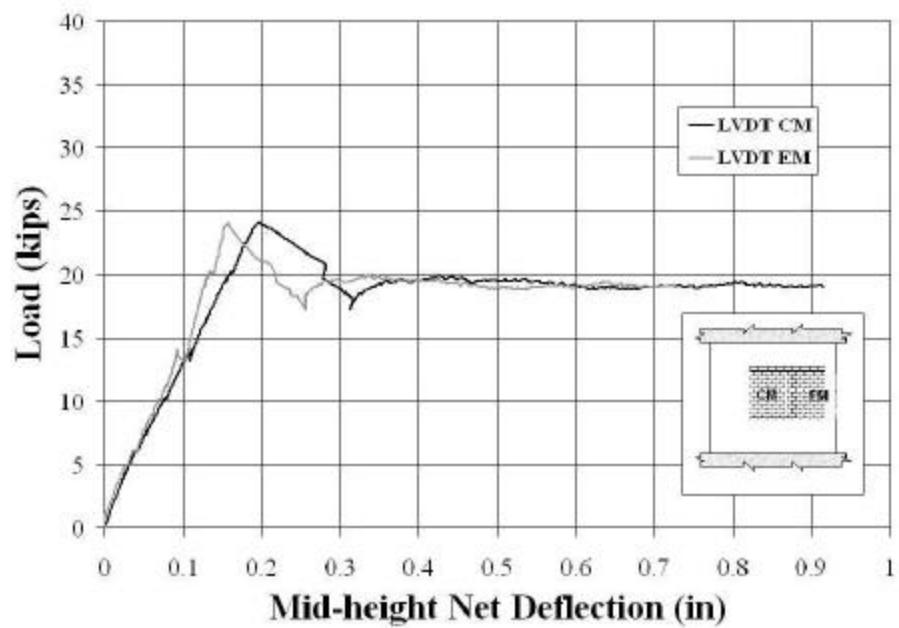


Figure C.2 - 4. Two-way Action – Wall OF2

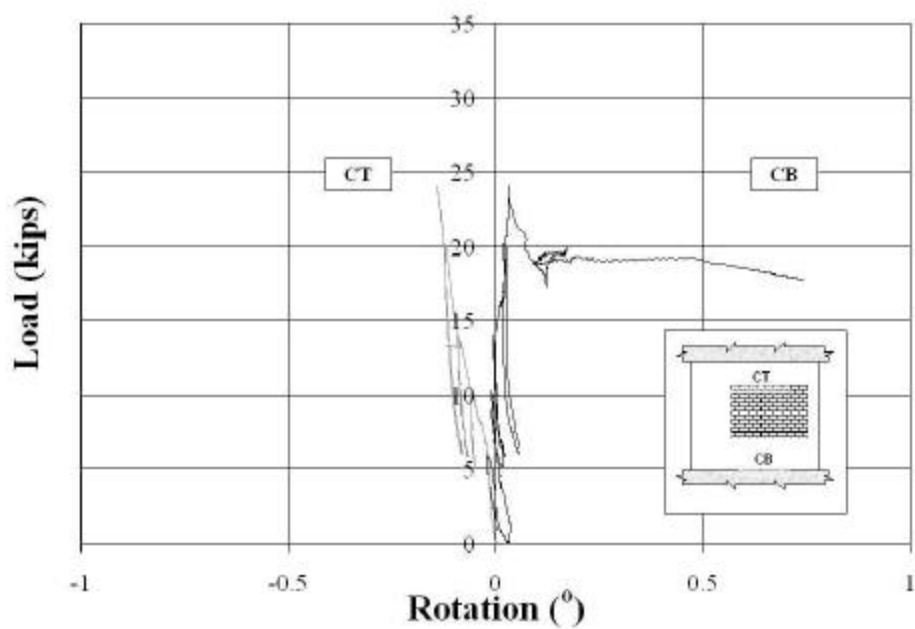


Figure C.2 - 5. Out-of-Plane Load vs. Rotation - Wall OF2

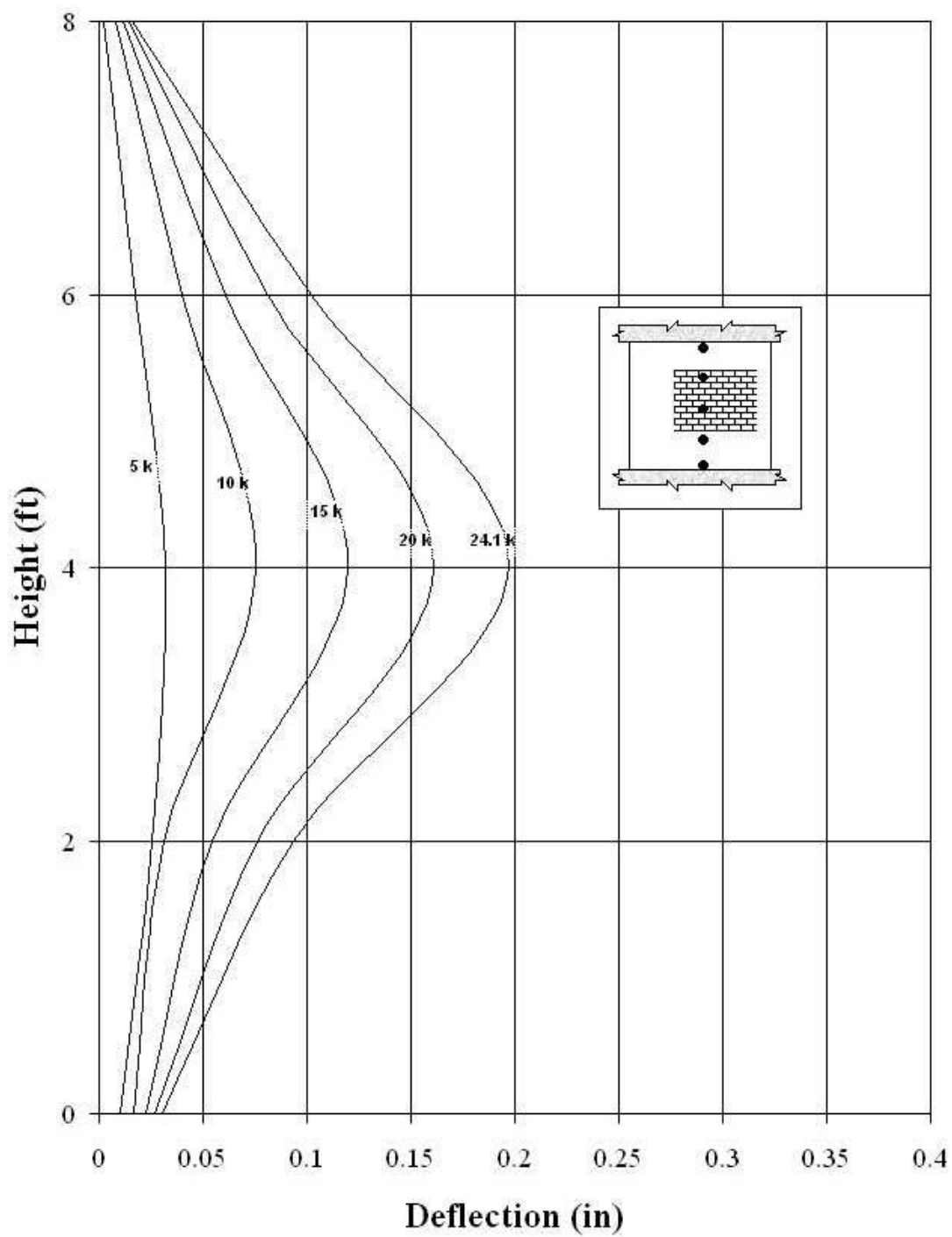


Figure C.2 - 6. Height vs. Deflection – Wall OF2

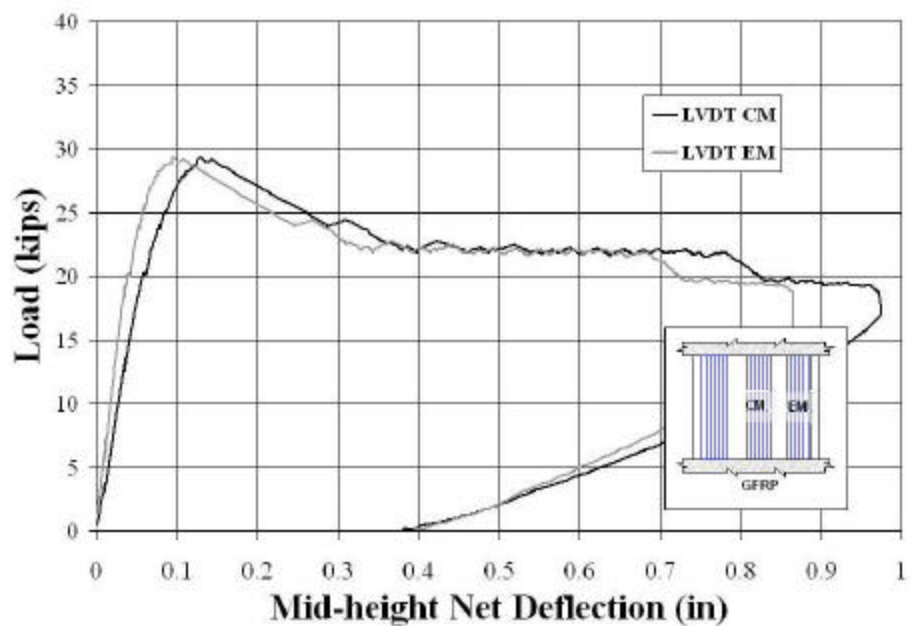


Figure C.2 - 7. Two-way Action – Wall OF3

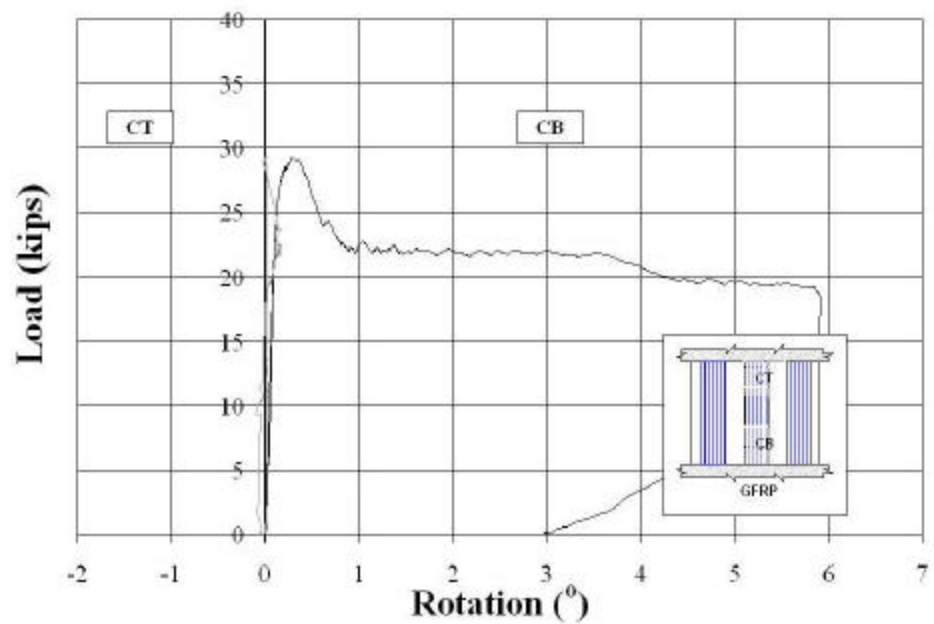


Figure C.2 - 8. Out-of-Plane Load vs. Rotation - Wall OF3

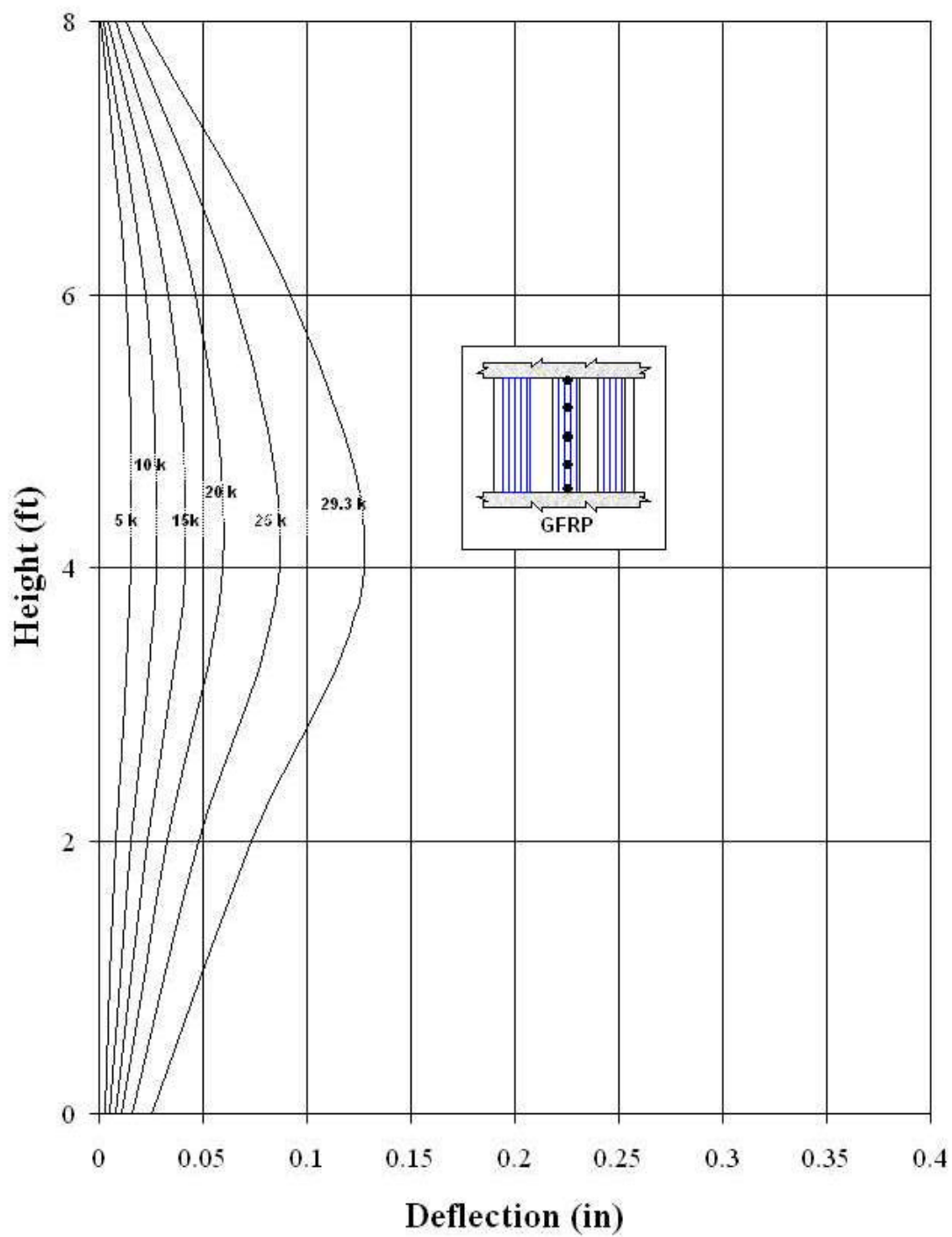


Figure C.2 - 9. Height vs. Deflection – Wall OF3

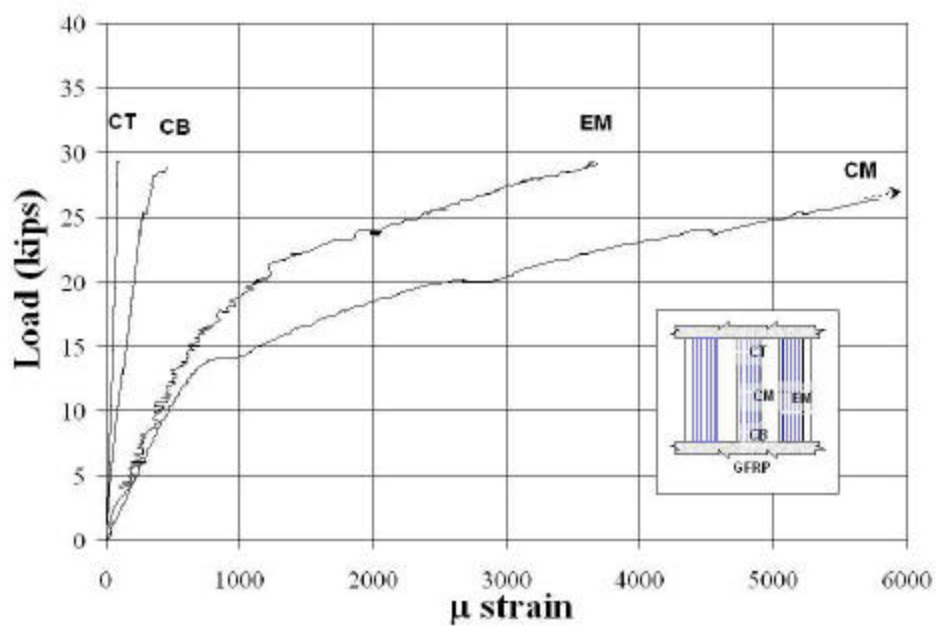


Figure C.2 - 10. Out-of-Plane Load vs. Strains - Wall OF3

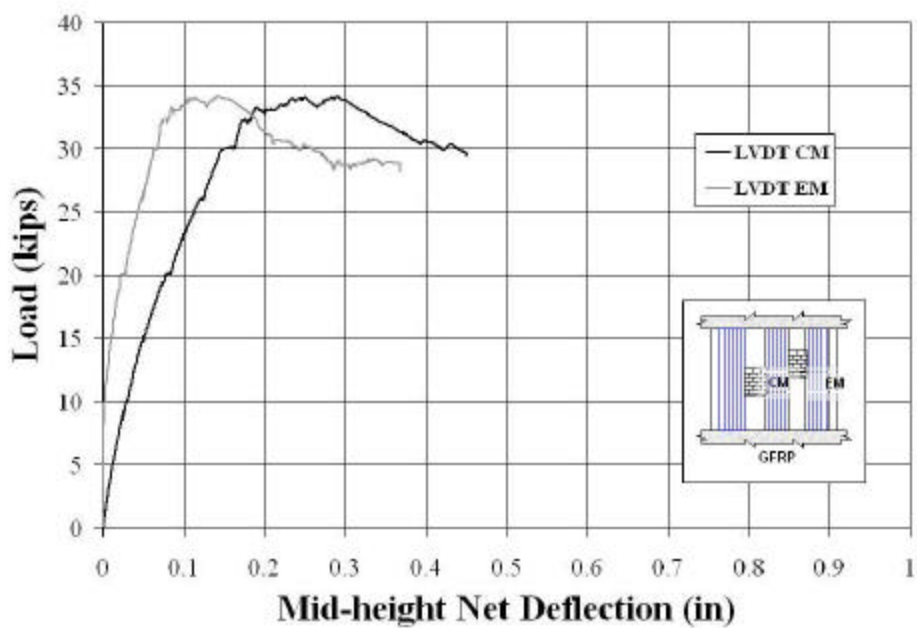


Figure C.2 - 11. Two-way Action - Wall OF4

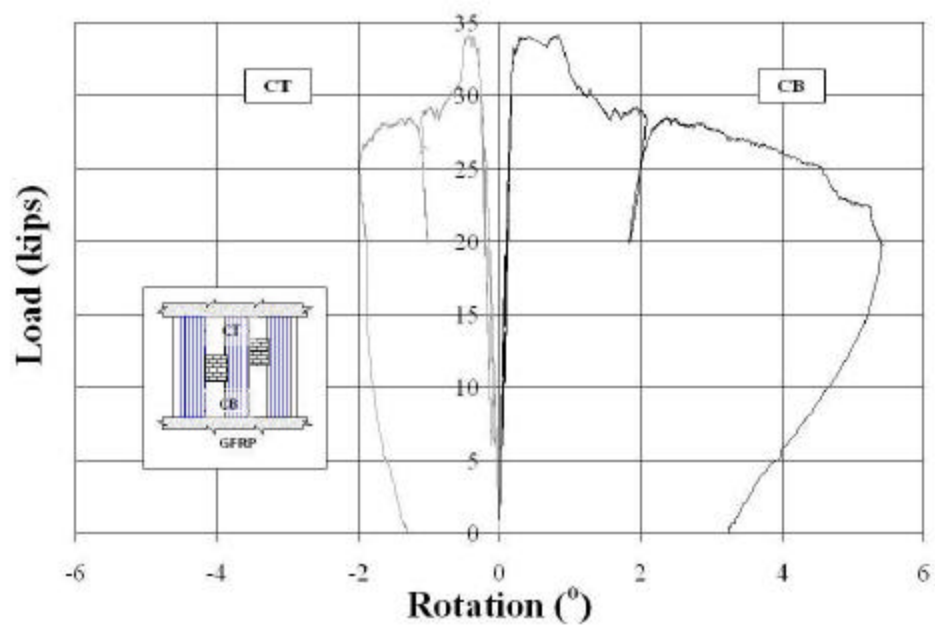


Figure C.2 - 12. Out-of-Plane Load vs. Rotation - Wall OF4

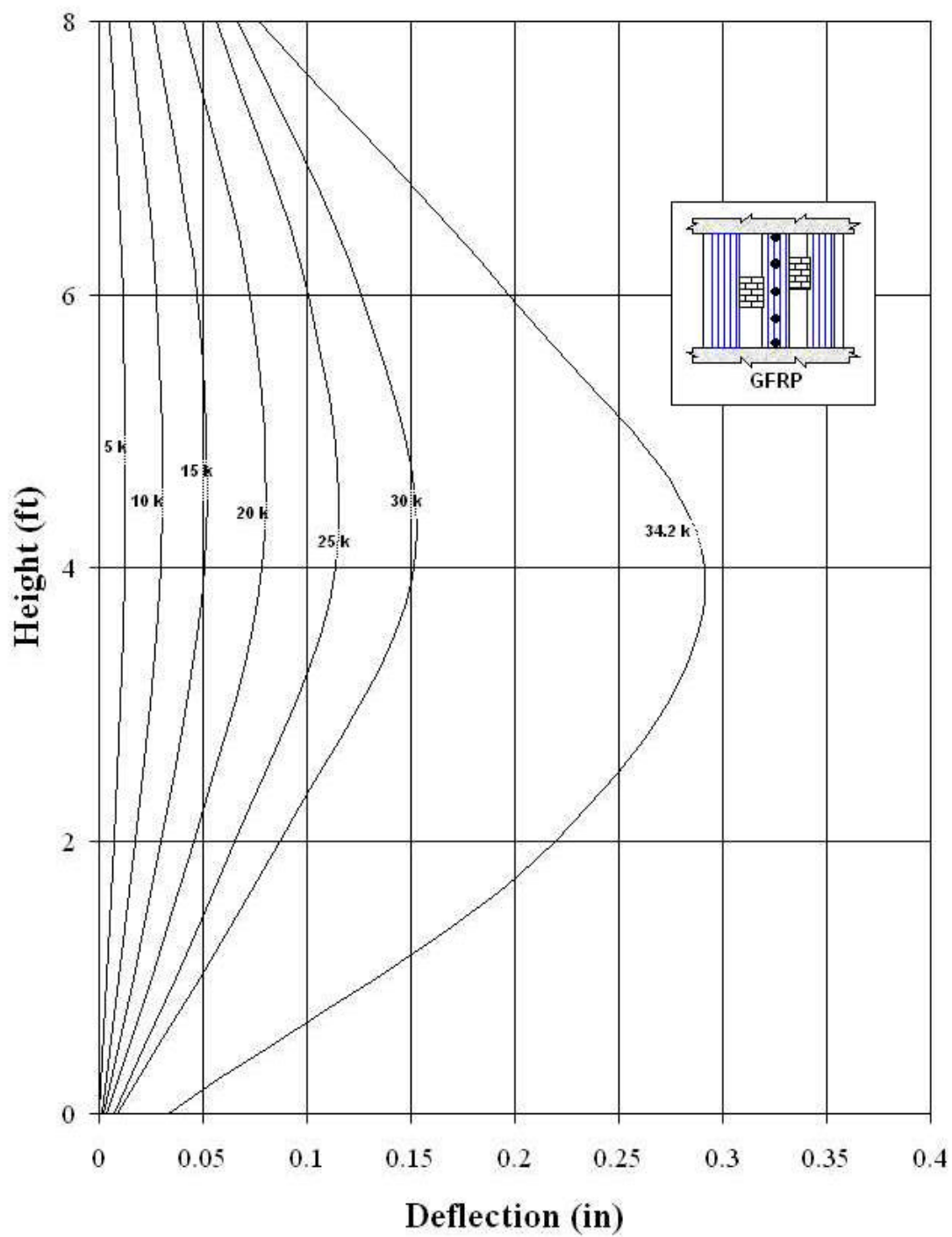


Figure C.2 - 13. Height vs. Deflection– Wall OF4

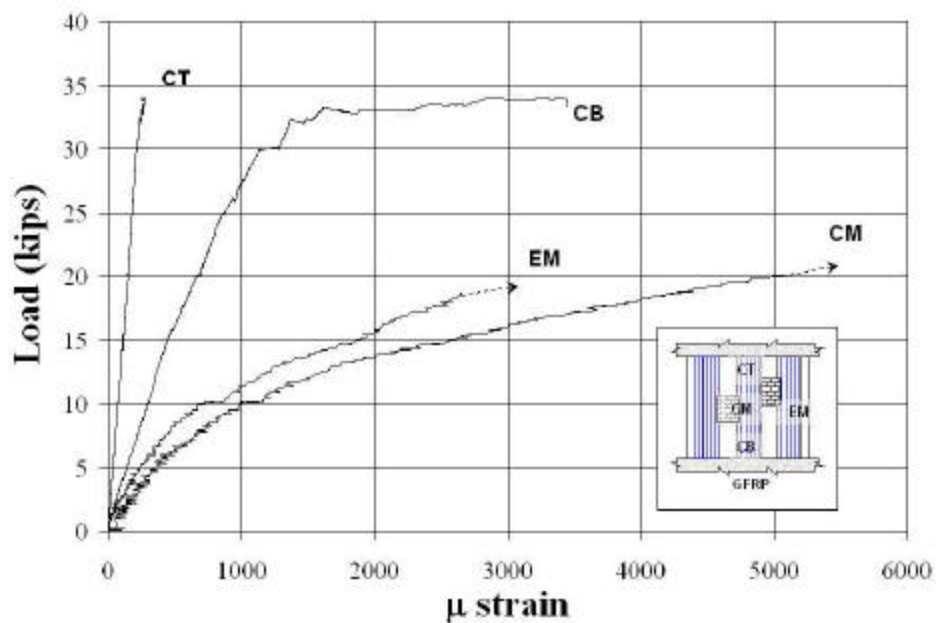


Figure C.2 - 14. Out-of-Plane Load vs. Strains - Wall OF4

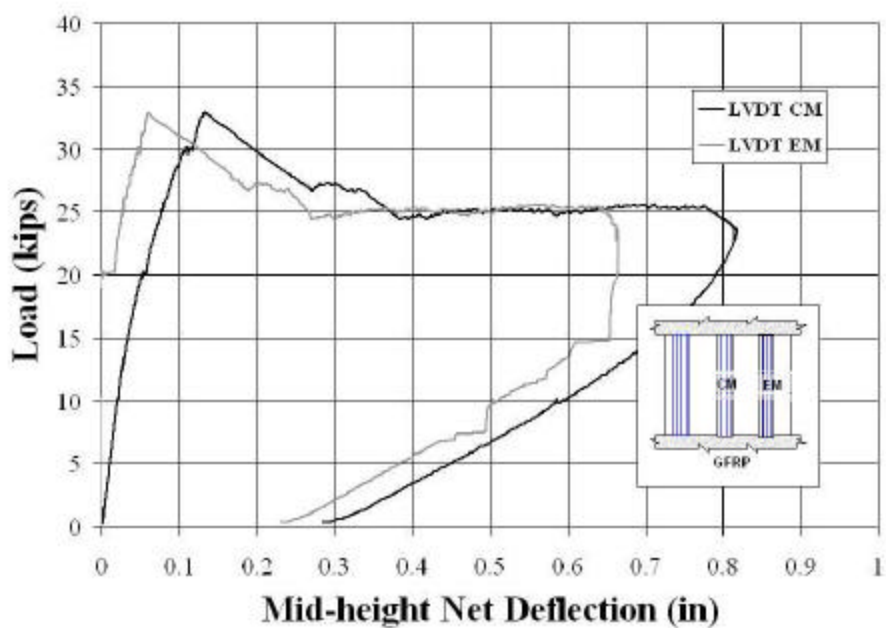


Figure C.2 - 15. Two-way Action – Wall OF5

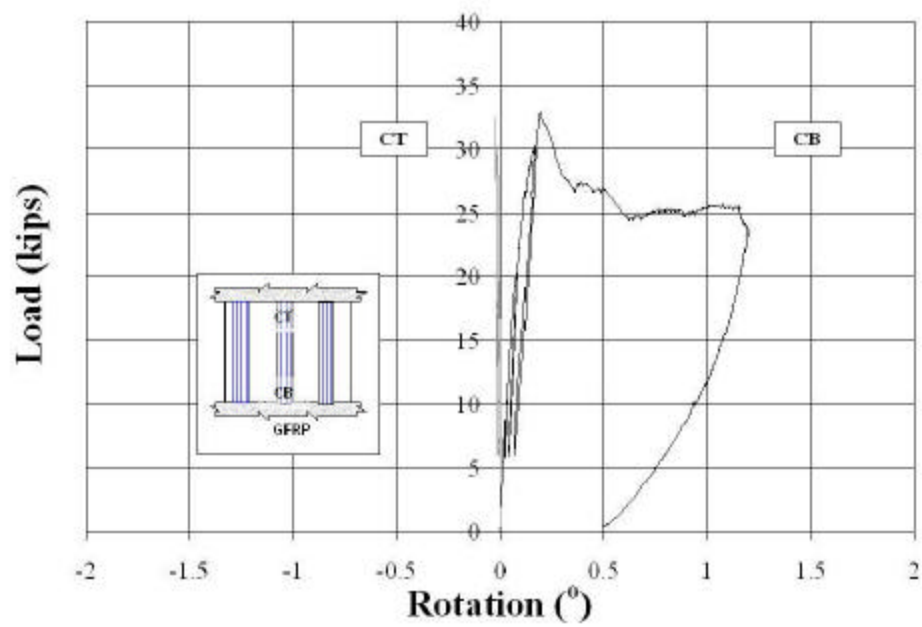


Figure C.2 - 16. Out-of-Plane Load vs. Rotation - Wall OF5

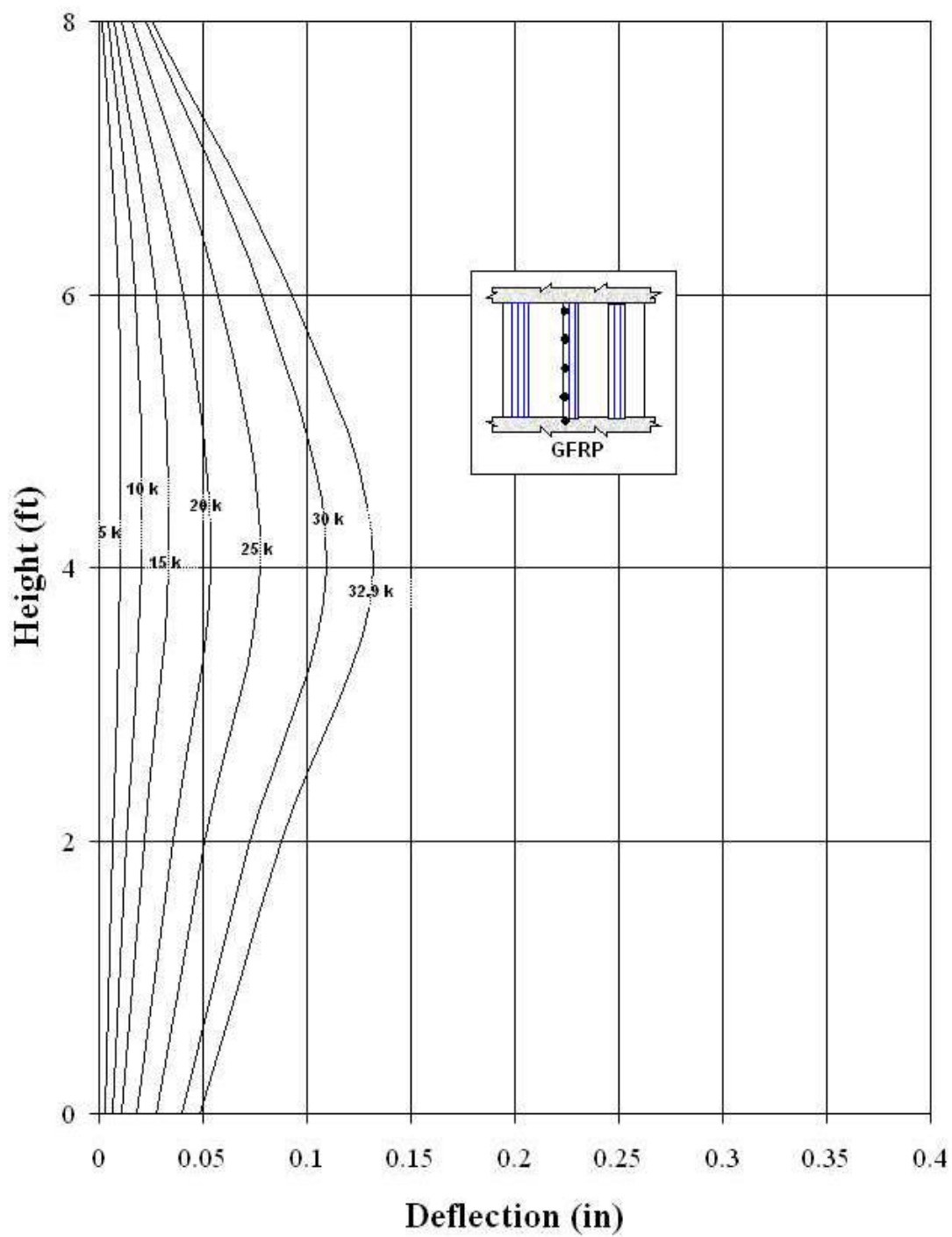


Figure C.2 - 17. Height vs. Deflection – Wall OF5

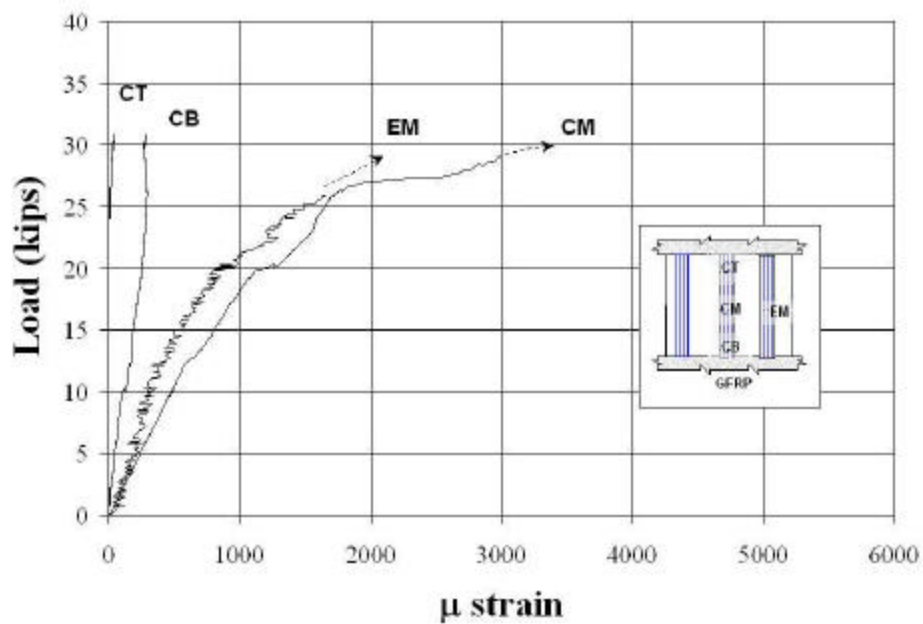


Figure C.2 - 18. Out-of-Plane Load vs. Strains - Wall OF5

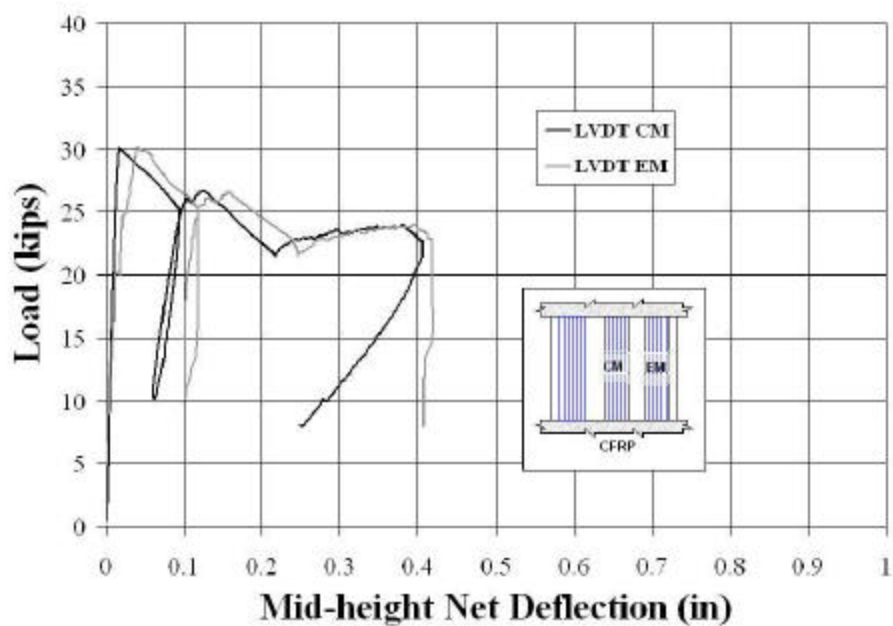


Figure C.2 - 19. Two-way Action - Wall OF6

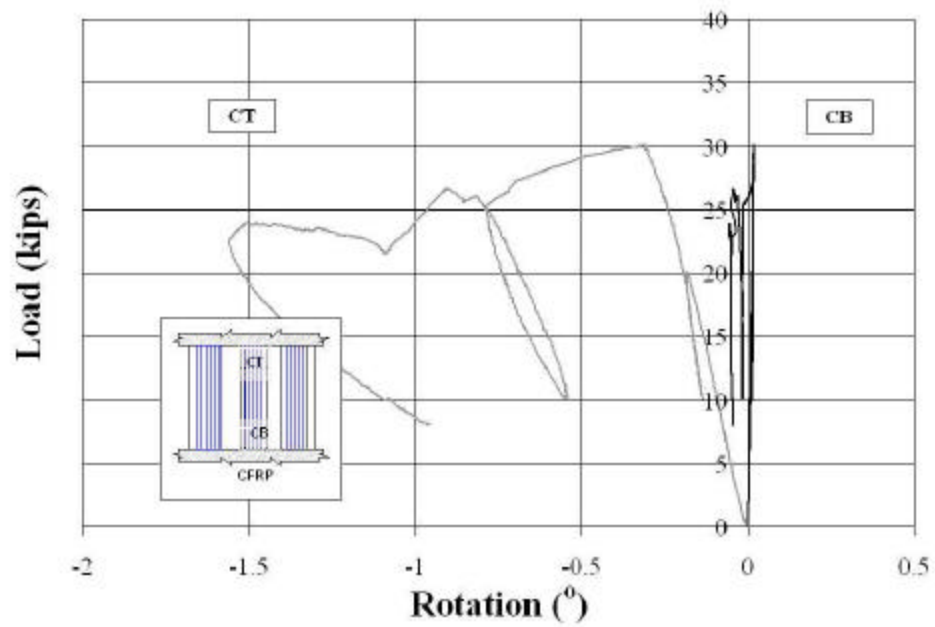


Figure C.2 - 20. Out-of-Plane Load vs. Rotation - Wall OF6

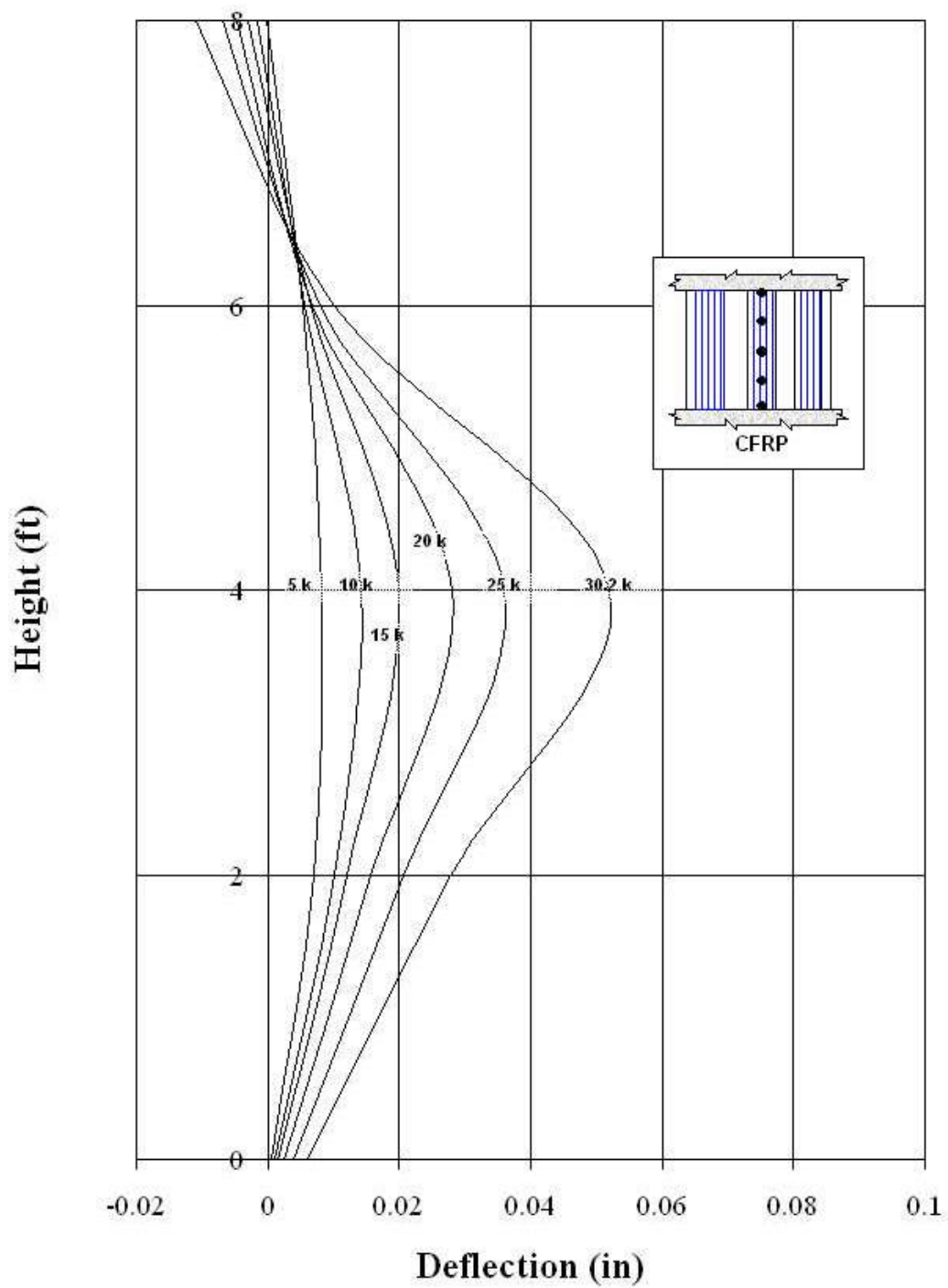


Figure C.2 - 21. Height vs. Deflection – Wall OF6

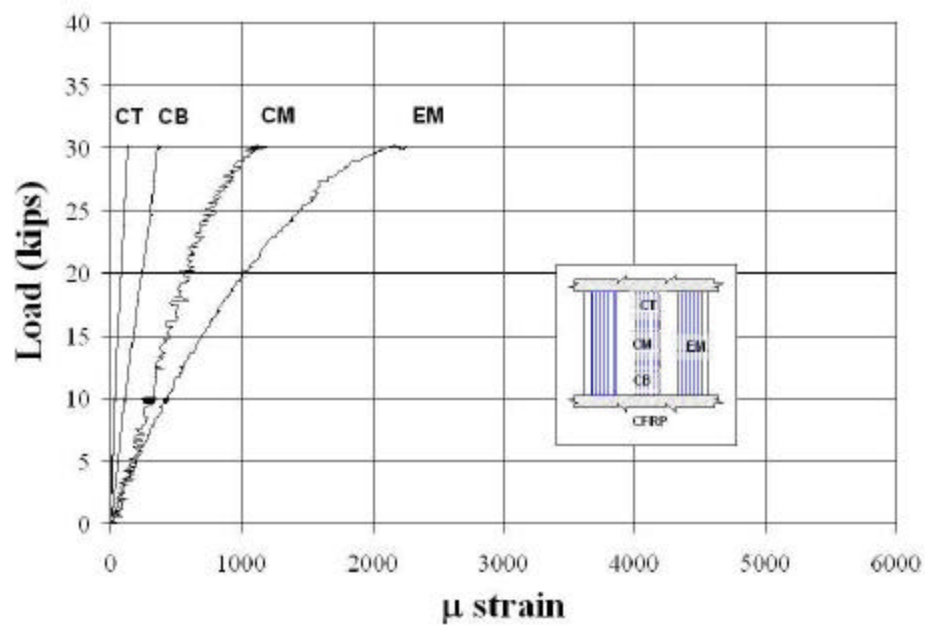


Figure C.2 - 22. Out-of-Plane Load vs. Strains - Wall OF6

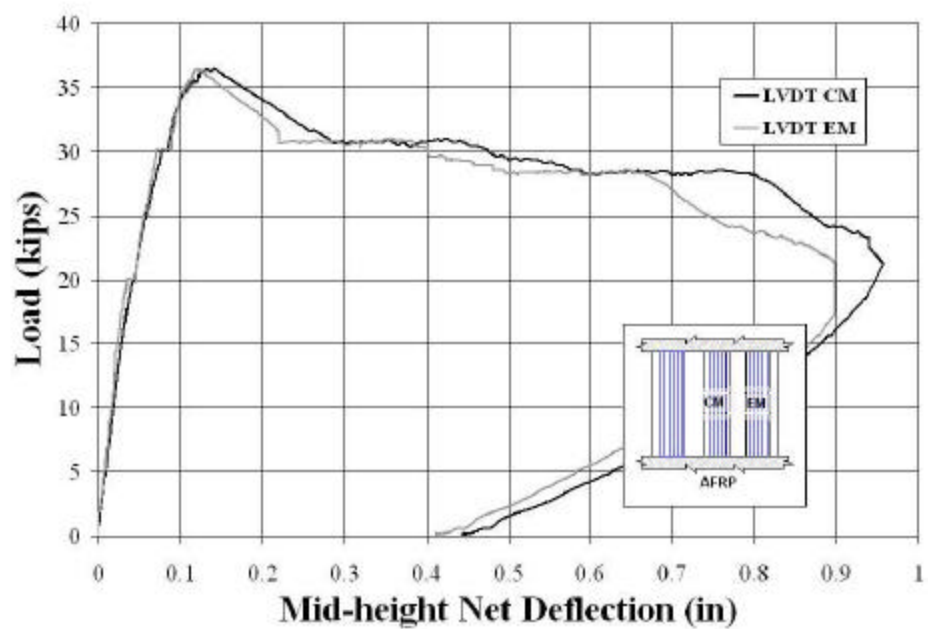


Figure C.2 - 23. Two-way Action - Wall OF7

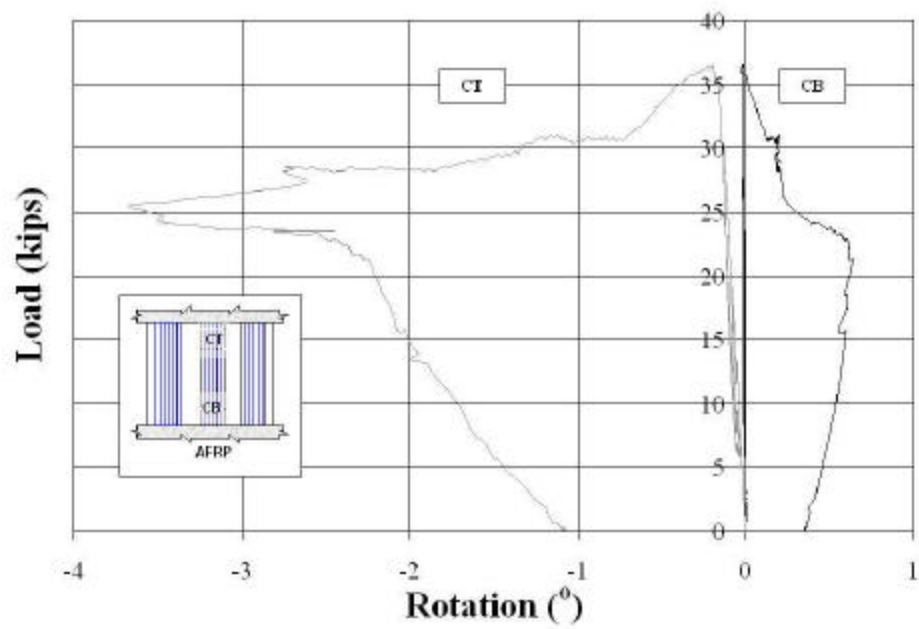


Figure C.2 - 24. Out-of-Plane Load vs. Rotation - Wall OF7

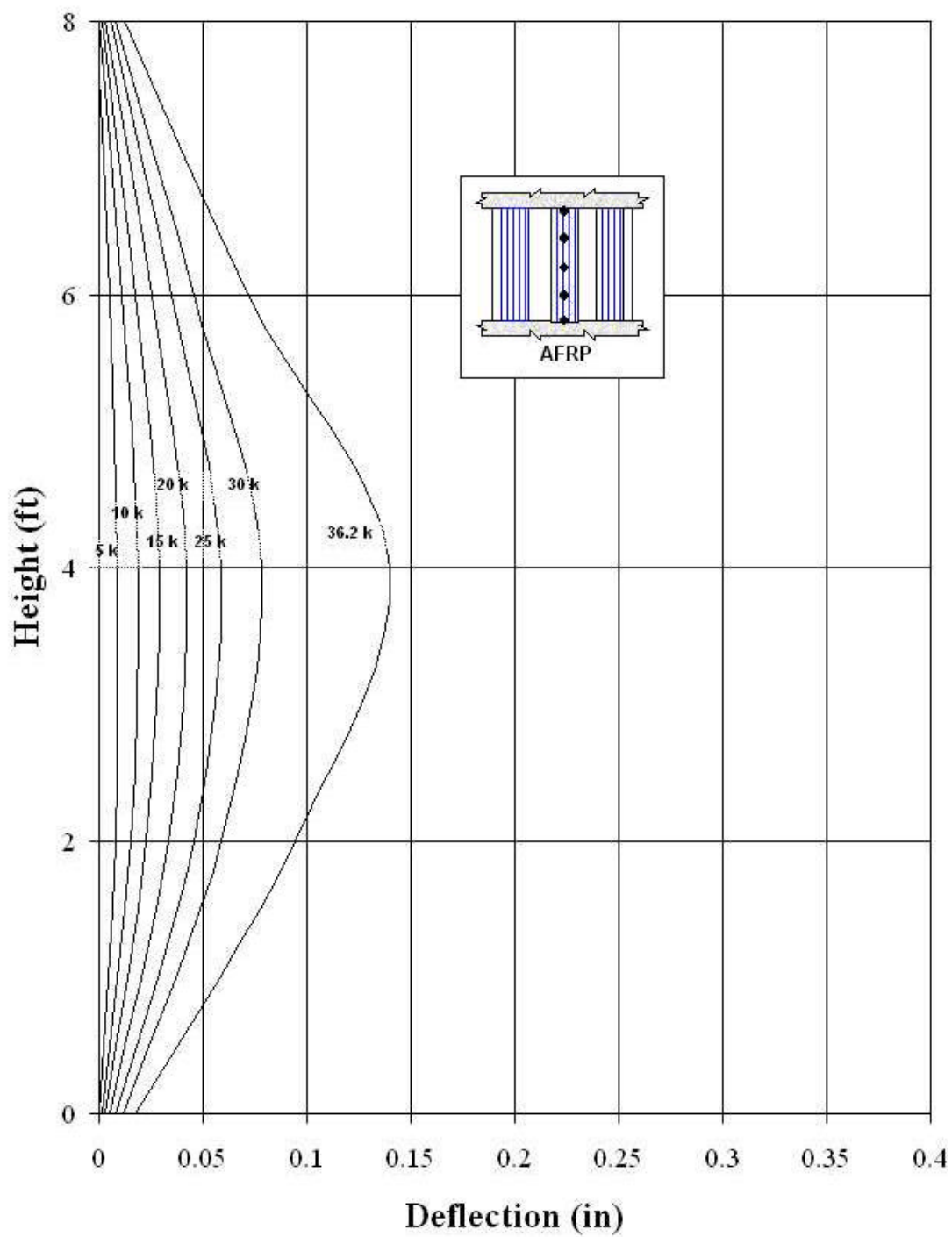


Figure C.2 - 25. Height vs. Deflection – Wall OF7

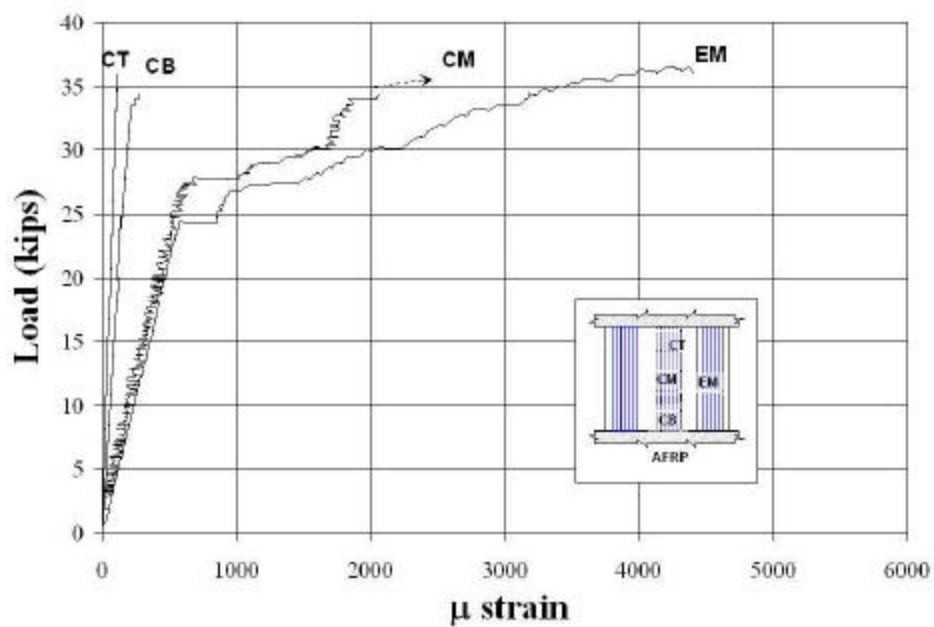


Figure C.2 - 26. Out-of-Plane Load vs. Strains - Wall OF7

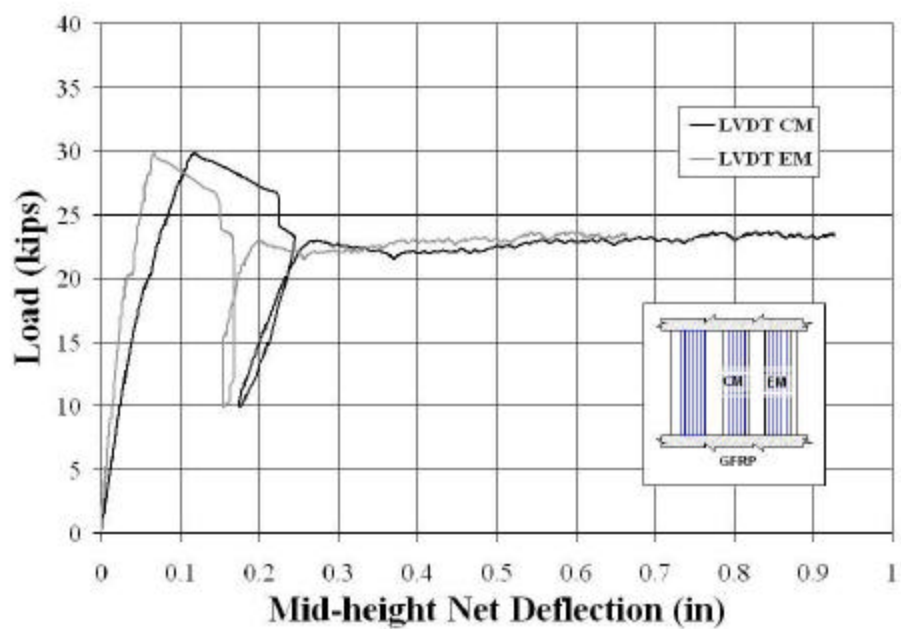


Figure C.2 - 27. Two-way Action - Wall OF8

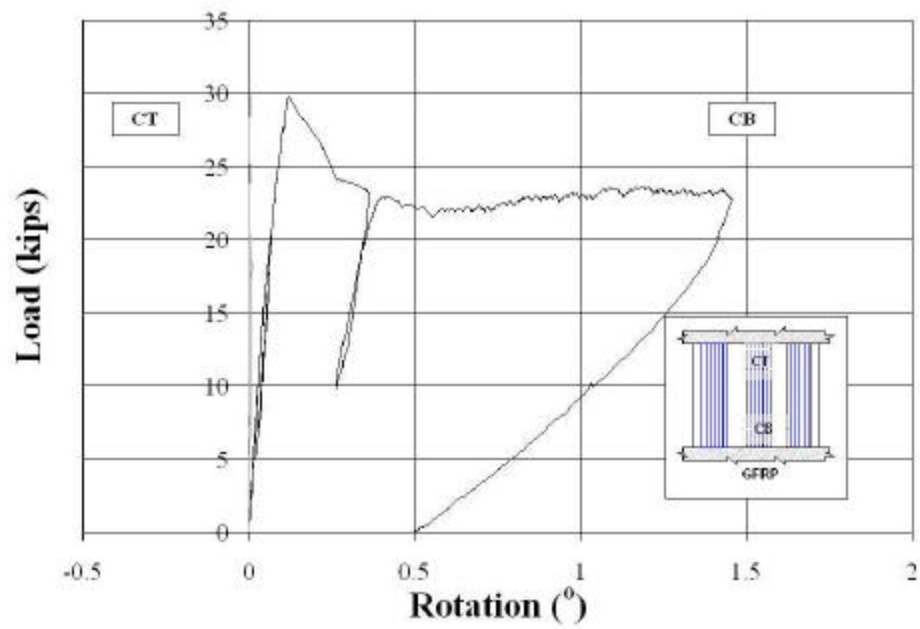


Figure C.2 - 28. Out-of-Plane Load vs. Rotation - Wall OF8

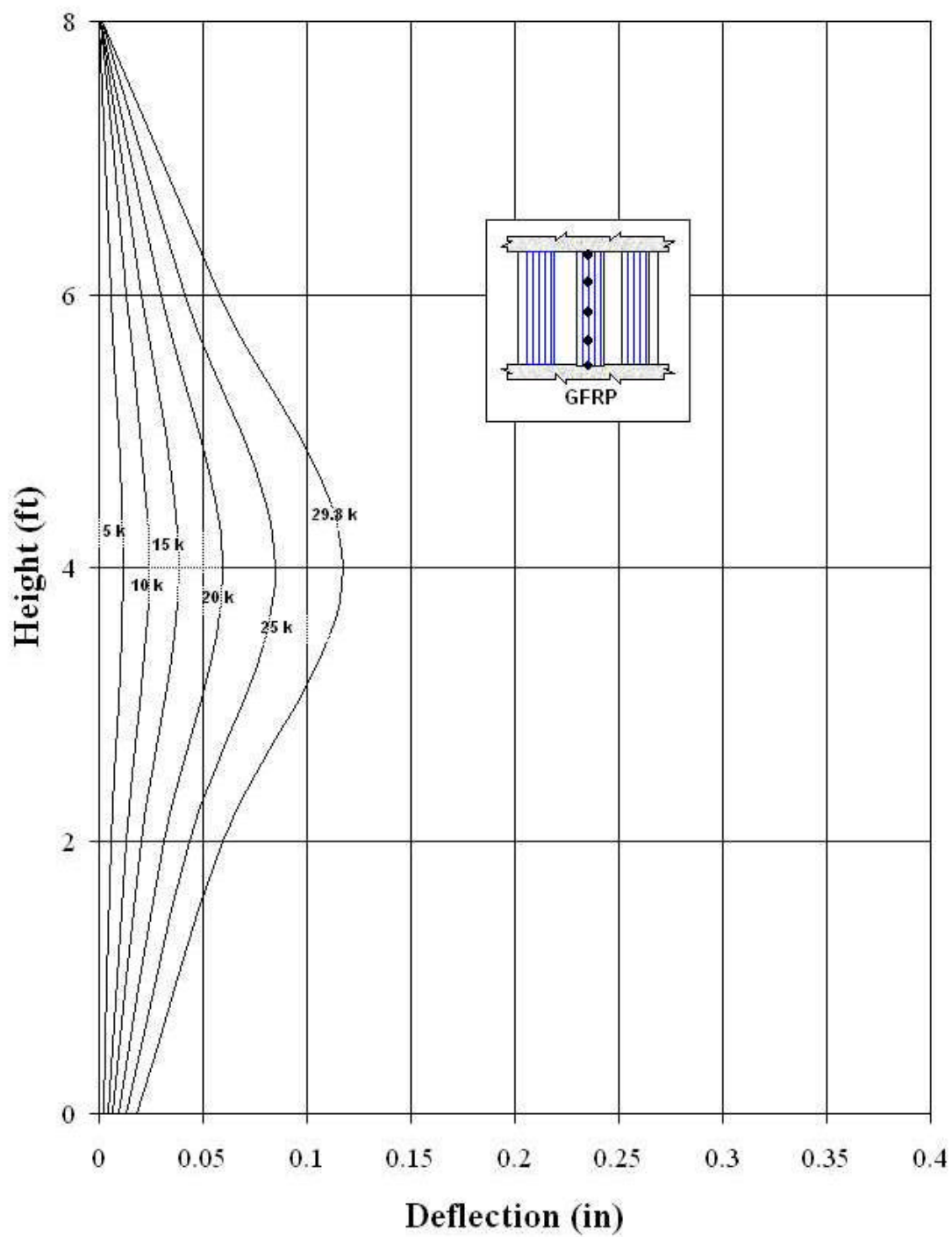


Figure C.2 - 29. Height vs. Deflection – Wall OF8

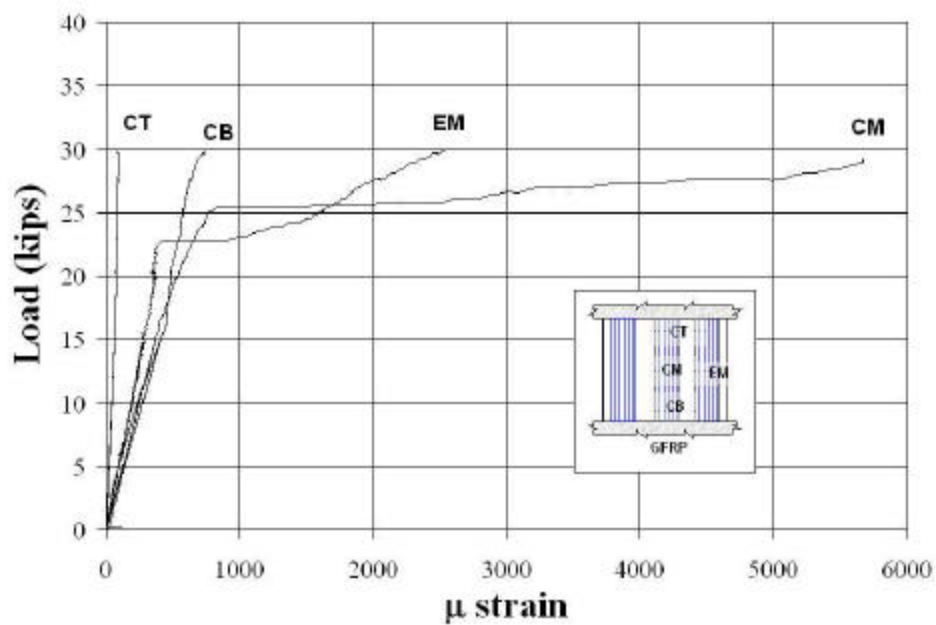


Figure C.2 - 30. Out-of-Plane Load vs. Strains - Wall OF8

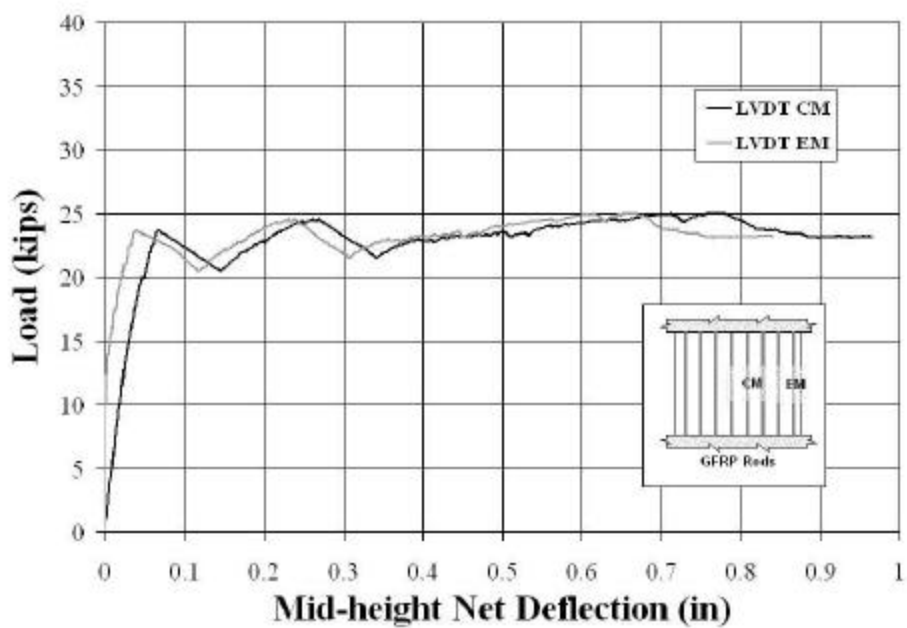


Figure C.2 - 31. Two-way Action - Wall OF9

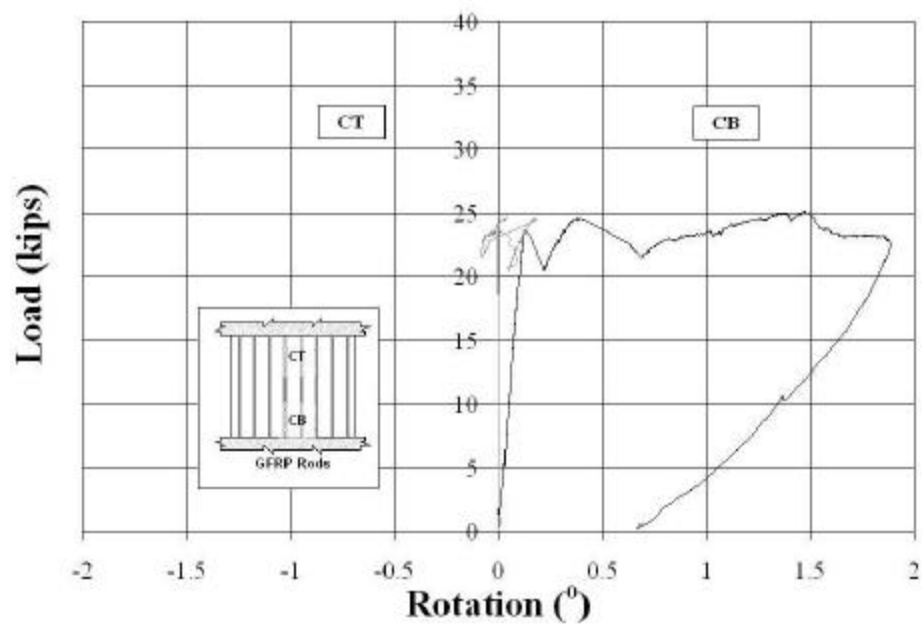


Figure C.2 - 32. Out-of-Plane Load vs. Rotation - Wall OF9

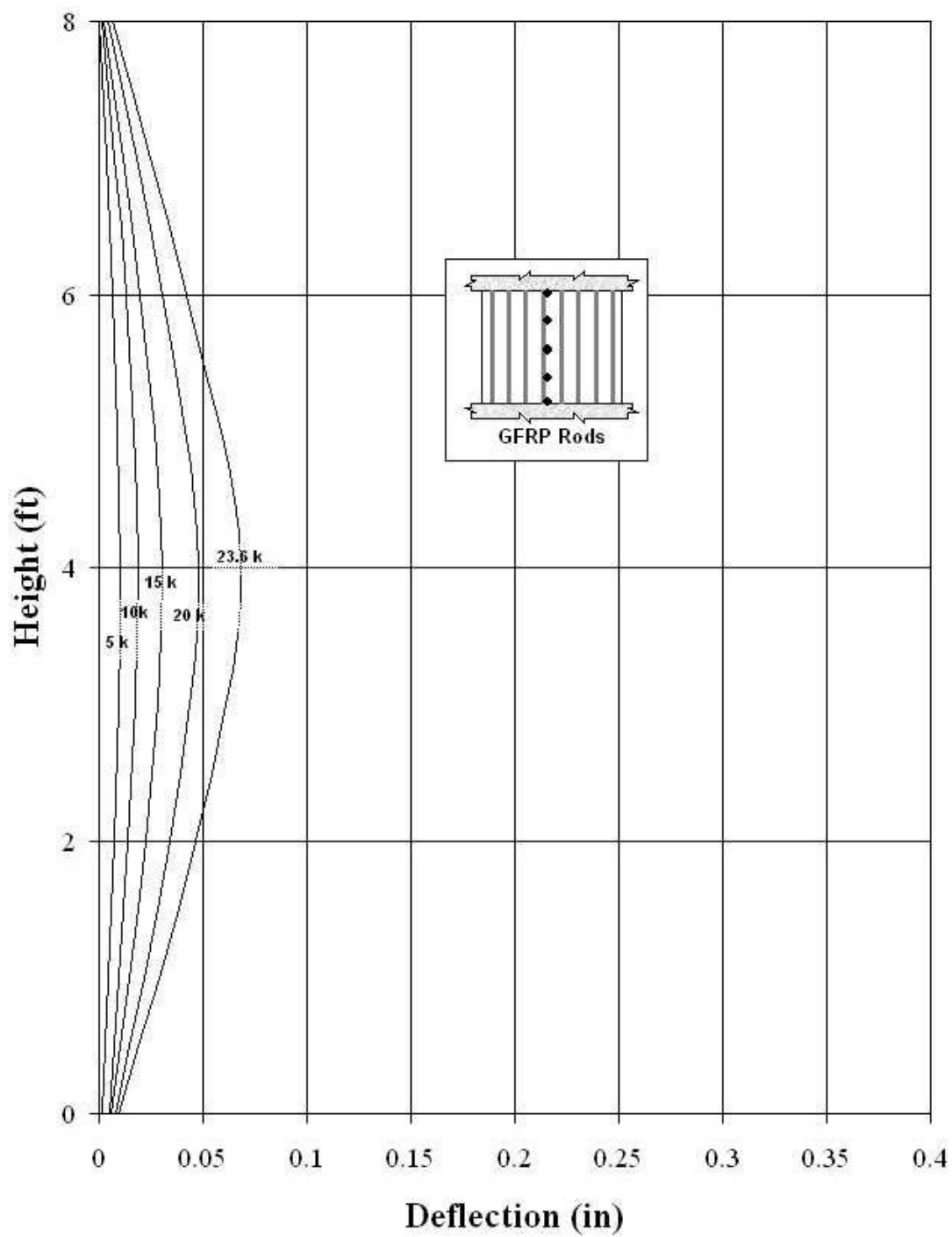


Figure C.2 - 33. Height vs. Deflection – Wall OF9

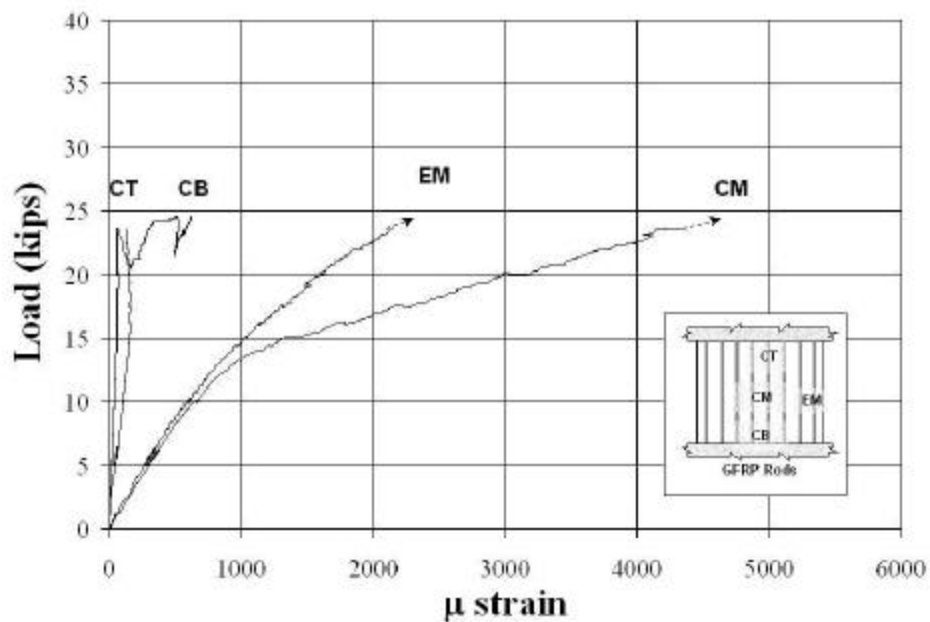


Figure C.2 - 34. Out-of-Plane Load vs. Strains - Wall OF9

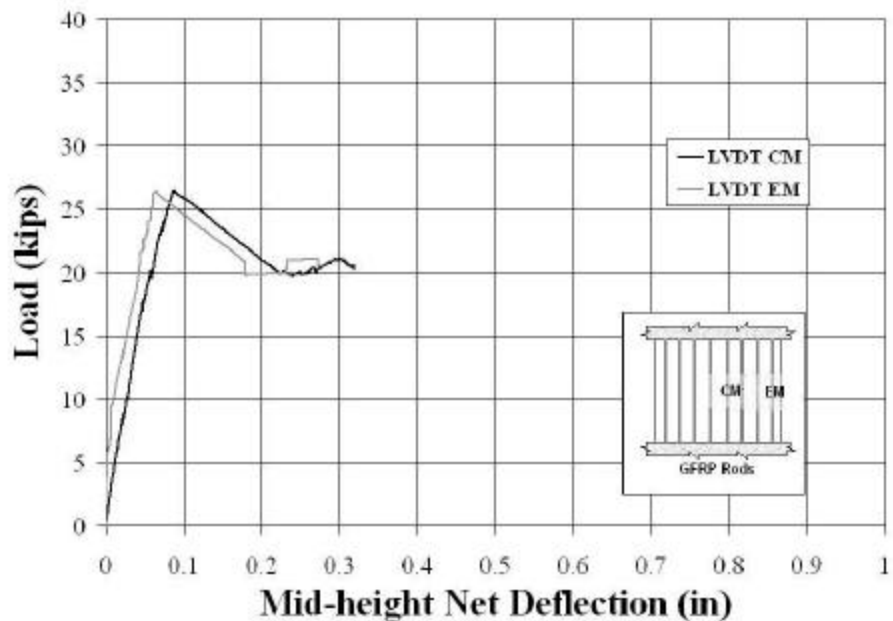


Figure C.2 - 35. Two-way Action - Wall OF10

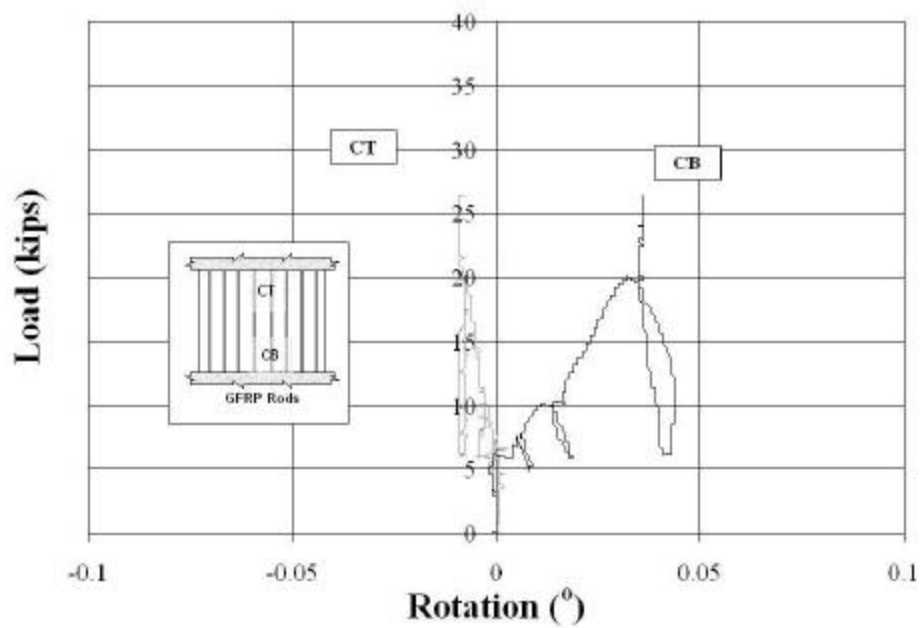


Figure C.2 - 36. Out-of-Plane Load vs. Rotation - Wall OF10

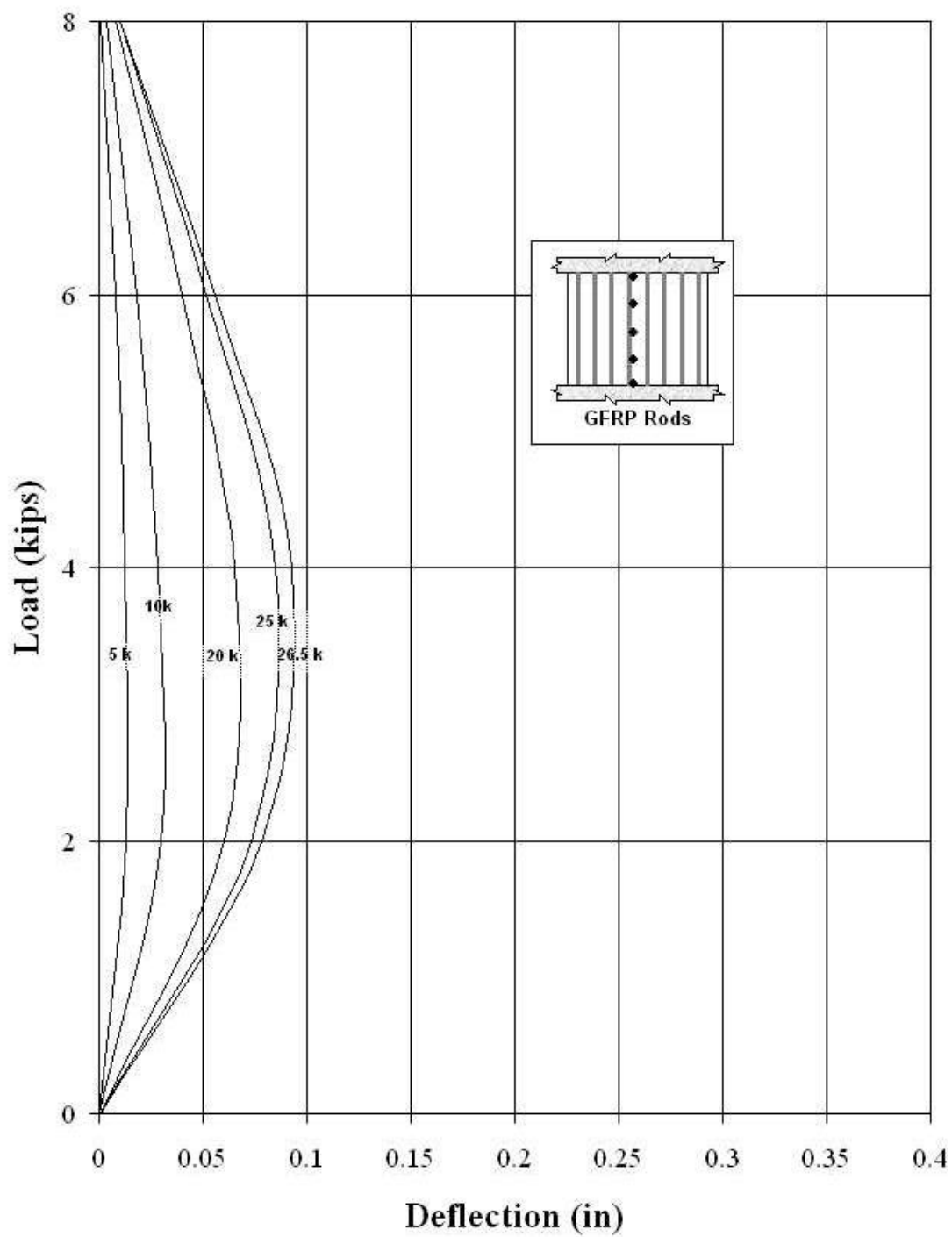


Figure C.2 - 37. Height vs. Deflection – Wall OF10

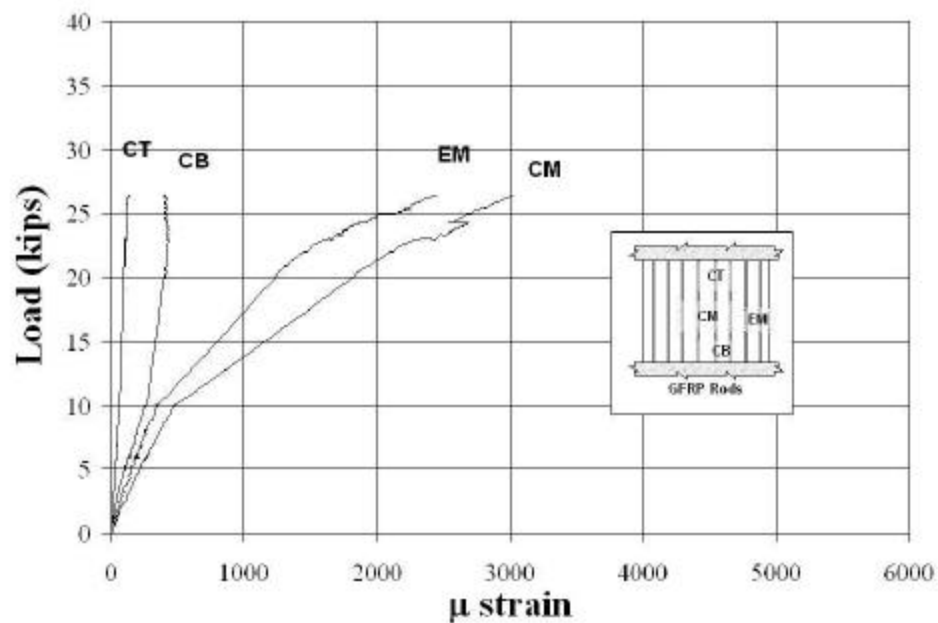


Figure C.2 - 38. Out-of-Plane Load vs. Strains - Wall OF10

Appendix C.3: Supporting Calculations

C.3-1: Calculation of Out-of-Plane Load causing local crushing for example in 5.2.2

Geometric Properties of Masonry Wall

Height=	12	ft
Length=	12	ft
Thickness=	8	in

Engineering Properties

f_m =	2000	psi
ϵ_{max} =	0.0025	in./in.

Width of compressed zone "b"

c=	6.25E-04	
b=	3.54	in
a=	0.70	in

Displacement D_1

Δ_1 =	9.00E-02	in
θ =	2.54E-02	rad
Δ_0 =	1.83	in

Clamping Force T

Assuming triangular distribution

T=	42513	lb/ft
----	-------	-------

Load P

P=	4.5	kips/ft
----	-----	---------

C.3-2: Data used in Figure 5.41

Source	f'_m (ksi)	h/t	t_m (in)	t_r (in)	E_r (ksi)	$\Gamma_r E_r$	$(\Gamma_r E_r) / (f'_m (h/t))$	$M_{exp.}$ (ft-kips)	$M_{the.}$ (ft-kips)	$M_{exp.} / M_{the.}$	Failure
Velazquez	3	14	2	0.074	1500	3.7	0.09	0.59	1.10	0.53	Delamination
Velazquez	3	14	2	0.074	1500	7.4	0.18	1.06	2.20	0.48	Delamination
Velazquez	3	14	2	0.074	855	6.3	0.15	0.94	1.60	0.59	Delamination
Velazquez	3	14	2	0.074	1500	13.8	0.33	1.76	3.90	0.45	Delamination
Velazquez	3	14	2	0.074	1500	4.6	0.11	0.70	1.40	0.5	Delamination
Velazquez	3	28	2	0.074	1500	18.4	0.22	2.66	5.10	0.52	Delamination
Velazquez	3	28	2	0.074	1500	36.8	0.44	4.69	6.80	0.69	Delamination
Velazquez	3	28	2	0.074	1500	9.1	0.11	1.41	2.70	0.52	Delamination
Hamilton	1.8	9	8	0.014	10500	2.1	0.13	1.50	5.60	0.27	Delamination
Hamilton	1.8	9	8	0.014	10500	2.1	0.13	2.08	5.60	0.37	Delamination
Hamilton	1.8	9	8	0.014	10500	2.1	0.13	1.97	5.60	0.35	Delamination-Rupture
Hamilton	1.8	9	8	0.014	10500	2.1	0.13	2.08	5.60	0.37	Delamination-Rupture
UMR	1.8	6	8	0.014	10500	6.8	0.63	8.36	14.40	0.58	Shear
UMR	1.8	6	8	0.011	17000	6.9	0.64	7.45	18.00	0.41	Shear
Velazquez	3	28	2	0.074	1500	55.6	0.66	5.16	8.00	0.64	Shear

Appendix C.4: Photographs



Figure C.4 - 1. Malcolm Bliss Hospital



Figure C.4 - 2. Removal of Plaster Layer



Figure C.4 - 3. Leveling of Masonry Surface



Figure C.4 - 4. Cutting of Fiber Sheets



Figure C.4 - 5. Use of Impregnating Resin as a Primer



Figure C.4 - 6. Installation of Fiber Sheets



Figure C.4 - 7. NSM Rod used as Flexural Reinforcement



Figure C.4 - 8. Drilling of Holes for testing of Walls



Figure C.4 - 9. Overall View of Test Setup



Figure C.4 - 10. Plates used to apply the loads



Figure C.4 - 11. View of Hydraulic Jacks and Reaction Beam



Figure C.4 - 12. Beam on the Reaction Side



Figure C.4 - 13. Wall being tested



Figure C.4 - 14. Delamination of Plaster

BIBLIOGRAPHY

- American Concrete Institute (ACI), Committee 318, "Building Code Requirements for Reinforced Concrete and Commentary," American Concrete Institute, Detroit, Michigan, 1999.
- American Concrete Institute (ACI), Committee 440, "Guide for the Design and Construction of Externally Bonded FRP Systems for Strengthening Concrete Structures," July 2000 (document under review).
- Angel R., Abrams D.P., Shapiro D., Uzarski J., and Webster M, "Behavior of Reinforced Concrete Frames with Masonry Infills," Structural Research Series Report No. 589, Department of Civil Engineering, University of Illinois at Urbana-Champaign, March 1994.
- Annaiah H.R., "Shear Performance of Reinforced Concrete Beams Strengthened in situ with Composites," Master's Thesis, Department of Civil Engineering, The University of Missouri-Rolla, 2000.
- Benett R. M., Boyd K.A., and Flanagan R.D., "Compressive Properties of Structural Clay Tile Prisms," Proceedings of the American Society of Civil Engineers – Journal of Structural Engineering, July 1997, pp. 920-926.
- Binda L., Modena C., Valluzi M.R., and Zago R., "Mechanical Effects of Bed Joint Steel Reinforcement in Historic Brick Masonry Structures," Structural Faults and Repairs 99, 8th International Conference, London, UK, 1999.
- California Seismic Safety Commission, "Status of Unreinforced Masonry Building Law," SSC 2000-02, Sacramento California, 2000.
- Drysdale R., Hamid A., and Baker L., "Masonry Structures – Behavior and Design," The Masonry Society, Boulder, Colorado, 1999.
- Ehsani M.R. and Saadatmanesh H., "Repair and Strengthening of Earthquake-Damaged Concrete and Masonry Walls with Composite Fabrics," First International Conference on Composites in Infrastructure ICCI'96, Tucson, Arizona, January 1996.
- Fricke K.E., Jones W.D., and Huff T.E., "In situ lateral Load Testing of Unreinforced Masonry Hollow Clay Tile Wall," Proceedings of the Sixth Canadian Masonry Symposium, Saskatchewan, Canada, June 1992, pp. 519-530.
- Hamid A.A., "Strengthening of Hollow Block Masonry Basement Walls with Plastic Reinforcing Bars," The Masonry Society Journal, August 1996, pp. 29-33.

- Hamilton H.R. III, Holberg A., Caspersen J., and Dolan C.W, "Strengthening Concrete Masonry with Fiber Reinforced Polymers," Fourth International Symposium on Fiber Reinforced Polymer (FRP) for Reinforced Concrete Structures, Baltimore, Maryland, November 1999, pp. 1103-1115.
- Hartley A., Mullins G., and Sen R., "Repair of Concrete Masonry Block Walls using Carbon Fiber," Advanced Composite Materials in Bridges and Structures, Montreal, Quebec, 1996, pp. 795-802.
- Johnson F.B., and Matthys J. H, " Structural Strength of Hollow Clay Tile Assemblages," Proceedings of the American Society of Civil Engineers – Journal of the Structural Division, February 1973, pp. 259-275.
- Klingner R. E., " A Review of Masonry Construction in the United States of America," Masonry in the Americas, edited by D.P. Abrams, ACI, 1994, pp. 205-237.
- Laursen P.T., Seible F., Hegemier G.A., and Innamorato D, "Seismic Retrofit and Repair of Masonry Walls with Carbon Overlays," Non-Metallic (FRP) Reinforcement for Concrete Structures, edited by L. Taerwe, RILEM, 1995, pp. 616-627.
- Manzouri T., Shing P.B., Schuller M.P, and Atkinson R.H. "Strengthening of Unreinforced Masonry Buildings," Proceedings of the Seventh North American Masonry Conference, South Bend, Indiana, June 1996, pp. 839-852.
- Masonry Standards Joint Committee, "Building Code Requirements for Masonry Structures," ACI-530-99/ASCE 5-99/TMS 402-99, American Concrete Institute, American Society of Civil Engineers, and The Masonry Society, Detroit, New York, and Boulder, 1999.
- Masonry Standards Joint Committee, "Building Code Requirements for Masonry Structures – Working Draft" ACI-530-99/ASCE 5-99/TMS 402-99, American Concrete Institute, American Society of Civil Engineers, and The Masonry Society, Detroit, New York, and Boulder, January, 2001.
- Paulay T., and Priestley M.J.N., "Seismic Design of Reinforced Concrete and Masonry Buildings," John Wiley & Sons, Inc., New York, 1992.
- Prawel S.P., and Reinhorn A.M., "Seismic Retrofit of Structural Masonry Using a Ferrocement Overlay," Proceedings of the Third North American Masonry Conference, Arlington, Texas, June 1985, pp. 50-1 to 50-19.
- Priestley M.J.N., "Seismic Design of Concrete Masonry Shear Walls," ACI Journal, Vol. 83, No. 1, January-February 1986, 58-68.

- Roko K., Boothby T.E., and Bakis C.E., "Failure Modes of Sheet Bonded Fiber Reinforced Polymer Applied to Brick Masonry," Fourth International Symposium on Fiber Reinforced Polymer (FRP) for Reinforced Concrete Structures, Baltimore, Maryland, November 1999, pp. 305-311.
- San Bartolomé A., "Construcciones de Albañilería – Comportamiento Sísmico y Diseño Estructural," Pontificia Universidad Católica del Perú, Fondo Editorial, 1994.
- Sabnis G.M., "Interaction Between Masonry Walls and Frames in Multistory Structures," First Canadian Masonry Symposium, Calgary, Alberta, Canada, 1976, pp. 324-337.
- Schwegler G., "Masonry Construction Strengthened with Fiber Composites in Seismically Endangered Zones," Proceedings of the Tenth European Conference on Earthquake Engineering, Rotterdam, Netherlands, 1995, pp.2299-2303.
- Schwegler G., and Kelterborn P., "Earthquake Resistance of Masonry Structures strengthened with Fiber Composites," Eleventh World Conference on Earthquake Engineering, Acapulco, Mexico, 1996.
- Shing P.B., Schuller M., Hoskere V., and Carter E., "Flexural and Shear Response of Reinforced Masonry Walls," ACI Structural Journal, Vol. 87, No. 6, November-December 1990, pp. 646-656.
- Standard Association of New Zealand, Code of Practice for the Design of Masonry Structures, NZS 4230, Wellington, New Zealand, 1999.
- Taghdi M., Bruneau M., and Saatcioglu M., "Seismic Retrofitting of Low-rise Masonry and Concrete Walls using Steel Strips," ASCE Journal of Structural Engineering, September 2000, pp. 1017-1025.
- Tinazzi D., Arduini, M., Modena C., and Nanni A., "FRP Structural Repointing of Masonry Assemblages," Advanced Composite materials in Bridges and Structures, Ottawa, Ontario, Canada, August 2000, pp.585-592
- TMS, "Performance of Masonry Structures in the Northridge California Earthquake of January 17, 1994," The Masonry Society, Boulder, Colorado, 1994.
- Velazquez-Dimas J.I., "Out-of-Plane Cyclic Behavior of URM Walls Retrofitted with Fiber Composites," Doctoral Dissertation, Department of Civil Engineering and Engineering Mechanics, The University of Arizona, Tucson, Arizona, 1998.
- Velazquez-Dimas J.I, Ehsani, M.R., and Saadatmanesh, H. "Out-of-Plane Behavior of Brick Masonry Walls Strengthened with Fiber Composites," ACI Structural Journal, May-June 2000, pp. 377-387.